

CAMBRIAN HOPF ALGEBRAS

GRÉGORIE CHATEL AND VINCENT PILAUD

ABSTRACT. Cambrian trees are oriented and labeled trees which fulfill local conditions around each node generalizing the conditions for classical binary search trees. Based on the bijective correspondence between signed permutations and leveled Cambrian trees, we define the Cambrian Hopf algebra generalizing J.-L. Loday and M. Ronco's algebra on binary trees. We describe combinatorially the products and coproducts of both the Cambrian algebra and its dual in terms of operations on Cambrian trees. We also define multiplicative bases of the Cambrian algebra and study structural and combinatorial properties of their indecomposable elements. Finally, we extend to the Cambrian setting different algebras connected to binary trees, in particular S. Law and N. Reading's Baxter Hopf algebra on quadrangulations and S. Giraudo's equivalent Hopf algebra on twin binary trees, and F. Chapoton's Hopf algebra on all faces of the associahedron.

CONTENTS

Introduction	2
Part 1. The Cambrian Hopf Algebra	4
1.1. Cambrian trees	4
1.1.1. Cambrian trees and increasing trees	4
1.1.2. Cambrian correspondence	5
1.1.3. Cambrian congruence	7
1.1.4. Cambrian classes and generating trees	8
1.1.5. Rotations and Cambrian lattices	9
1.1.6. Canopy	10
1.1.7. Geometric realizations	10
1.2. Cambrian Hopf Algebra	13
1.2.1. Signed shuffle and convolution products	13
1.2.2. Subalgebra of FQSym_{\pm}	14
1.2.3. Quotient algebra of FQSym_{\pm}^*	17
1.2.4. Duality	19
1.3. Multiplicative bases	19
1.3.1. Multiplicative bases and indecomposable elements	19
1.3.2. Structural properties	20
1.3.3. Enumerative properties	22
Part 2. The Baxter-Cambrian Hopf Algebra	24
2.1. Twin Cambrian trees	24
2.1.1. Twin Cambrian trees	24
2.1.2. Baxter-Cambrian correspondence	25
2.1.3. Baxter-Cambrian congruence	25
2.1.4. Rotations and Baxter-Cambrian lattices	25
2.1.5. Baxter-Cambrian numbers	28
2.1.6. Geometric realizations	36
2.2. Baxter-Cambrian Hopf Algebra	37
2.2.1. Subalgebra of FQSym_{\pm}	37
2.2.2. Quotient algebra of FQSym_{\pm}^*	39

2.3. Cambrian tuples	40
2.3.1. Combinatorics of Cambrian tuples	40
2.3.2. Cambrian tuple Hopf Algebra	43
2.3.3. Dual Cambrian tuple Hopf Algebra	45
Part 3. The Schröder-Cambrian Hopf Algebra	46
3.1. Schröder-Cambrian trees	46
3.1.1. Schröder-Cambrian trees	46
3.1.2. Schröder-Cambrian correspondence	47
3.1.3. Schröder-Cambrian congruence	49
3.1.4. Weak order on ordered partitions and Schröder-Cambrian lattices	49
3.1.5. Canopy	52
3.1.6. Geometric realizations	53
3.2. Schröder-Cambrian Hopf Algebra	54
3.2.1. Shuffle and convolution products on signed ordered partitions	54
3.2.2. Subalgebra of OrdPart_\pm	55
3.2.3. Quotient algebra of OrdPart_\pm^*	57
3.3. Schröder-Cambrian tuples	58
Acknowledgements	59
References	59

INTRODUCTION

The background of this paper is the fascinating interplay between the combinatorial, geometric and algebraic structures of permutations, binary trees and binary sequences (see Table 1):

- ★ **Combinatorially**, the descent map from permutations to binary sequences factors via binary trees through the BST insertion and the canopy map. These maps define lattice homomorphisms from the weak order via the Tamari lattice to the boolean lattice.
- ★ **Geometrically**, the permutahedron is contained in Loday’s associahedron [Lod04] which is in turn contained in the parallelepiped generated by the simple roots. These polytopes are just obtained by deleting inequalities from the facet description of the permutahedron. See Figure 1.
- ★ **Algebraically**, these maps translate to Hopf algebra inclusions from M. Malvenuto and C. Reutenauer’s algebra on permutations [MR95] via J.-L. Loday and M. Ronco’s algebra on binary trees [LR98] to L. Solomon’s descent algebra [Sol76].

Combinatorics	Permutations	Binary trees	Binary sequences
Geometry	Permutahedron $\text{conv}(\mathfrak{S}_n)$	Loday’s associahedron [Lod04]	Parallelepiped gen. by $e_{i+1} - e_i$
Algebra	Malvenuto-Reutenauer Hopf algebra [MR95]	Loday-Ronco Hopf algebra [LR98]	Solomon descent algebra [Sol76]

TABLE 1. Related combinatorial, geometric and algebraic structures.

These structures and their connections have been partially extended in several directions in particular to the Cambrian lattices of N. Reading [Rea06, RS09] and their polytopal realizations by C. Hohlweg, C. Lange, and H. Thomas [HL07, HLT11], to the graph associahedra of M. Carr and S. Devadoss [CD06, Dev09], the nested complexes and their realizations as generalized associahedra by A. Postnikov [Pos09] (see also [PRW08, FS05, Zel06]), or to the m -Tamari lattices of F. Bergeron and L.-F. Prévaille-Ratelle [BPR12] (see also [BMFPR11, BMCPR13]) and the Hopf algebras on these m -structures recently constructed by J.-C. Novelli and J.-Y. Thibon [NT14, Nov14].

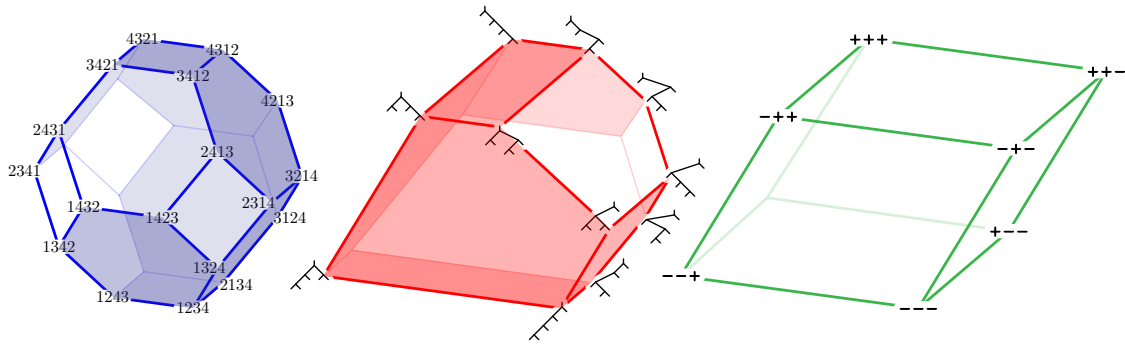


FIGURE 1. The 3-dimensional permutahedron (blue, left), Loday’s associahedron (red, middle), and parallelepiped (green, right). Shaded facets are preserved to get the next polytope.

This paper explores combinatorial and algebraic aspects of Hopf algebras related to the type A Cambrian lattices. N. Reading provides in [Rea06] a procedure to map a signed permutation of \mathfrak{S}_n into a triangulation of a certain convex $(n+3)$ -gon. The dual trees of these triangulations naturally extend rooted binary trees and were introduced and studied as “spines” [LP13] or “mixed cobinary trees” [IO13]. We prefer here the term “Cambrian trees” in reference to N. Reading’s work. The map κ from signed permutations to Cambrian trees is known to encode combinatorial and geometric properties of the Cambrian structures: the Cambrian lattice is the quotient of the weak order under the fibers of κ , each maximal cone of the Cambrian fan is the incidence cone of a Cambrian tree T and is refined by the braid cones of the permutations in the fiber $\kappa^{-1}(T)$, etc.

In this paper, we use this map κ for algebraic purposes. In the first part, we introduce the Cambrian Hopf algebra Camb as a subalgebra of the Hopf algebra FQSym_{\pm} on signed permutations, and the dual Cambrian algebra Camb^* as a quotient algebra of the dual Hopf algebra FQSym_{\pm}^* . Their bases are indexed by all Cambrian trees. Our approach extends that of F. Hivert, J.-C. Novelli and J.-Y. Thibon [HNT05] to construct J.-L. Loday and M. Ronco’s Hopf algebra on binary trees [LR98] as a subalgebra of C. Malvenuto and C. Reutenauer’s Hopf algebra on permutations [MR95]. We also use this map κ to describe both the product and coproduct in the algebras Camb and Camb^* in terms of simple combinatorial operations on Cambrian trees. From the combinatorial description of the product in Camb , we derive multiplicative bases of the Cambrian algebra Camb and study the structural and enumerative properties of their indecomposable elements.

In the second part of this paper, we study Baxter-Cambrian structures, extending in the Cambrian setting the constructions of S. Law and N. Reading on quadrangulations [LR12] and that of S. Giraud on twin binary trees [Gir12]. We define Baxter-Cambrian lattices as quotients of the weak order under the intersections of two opposite Cambrian congruences. Their elements can be labeled by pairs of twin Cambrian trees, *i.e.* Cambrian trees with opposite signatures whose union forms an acyclic graph. We study in detail the number of such pairs of Cambrian trees for arbitrary signatures. Following [LR12], we also observe that the Minkowski sums of opposite associahedra of C. Hohlweg and C. Lange [HL07] provide polytopal realizations of the Baxter-Cambrian lattices. Finally, we introduce the Baxter-Cambrian Hopf algebra BaxCamb as a subalgebra of the Hopf algebra FQSym_{\pm} on signed permutations and its dual BaxCamb^* as a quotient algebra of the dual Hopf algebra FQSym_{\pm}^* . Their bases are indexed by pairs of twin Cambrian trees, and it is also possible to describe both the product and coproduct in the algebras BaxCamb and BaxCamb^* in terms of simple combinatorial operations on Cambrian trees. We also extend our results to arbitrary tuples of Cambrian trees, resulting to the Cambrian tuple algebra.

The last part of the paper is devoted to Schröder-Cambrian structures. We consider Schröder-Cambrian trees which correspond to all faces of all C. Hohlweg and C. Lange’s associahedra [HL07]. We define the Schröder-Cambrian lattice as a quotient of the weak order on ordered partitions defined in [KLN⁺01], thus extending N. Reading’s type A Cambrian lattices [Rea06] to all faces of the associahedron. Finally, we consider the Schröder-Cambrian Hopf algebra SchrCamb , generalizing the algebra defined by F. Chapoton in [Cha00].

Part 1. The Cambrian Hopf Algebra

1.1. CAMBRIAN TREES

In this section, we recall the definition and properties of “Cambrian trees”, generalizing standard binary search trees. They were introduced independently by K. Igusa and J. Ostroff in [IO13] as “mixed cobinary trees” in the context of cluster algebras and quiver representation theory and by C. Lange and V. Pilaud in [LP13] as “spines” (*i.e.* oriented and labeled dual trees) of triangulations of polygons to revisit the multiple realizations of the associahedron of C. Hohlweg and C. Lange [HL07]. Here, we use the term “Cambrian trees” to underline their connection with the type A Cambrian lattices of N. Reading [Rea06]. Although motivating and underlying this paper, these interpretations are not needed for the combinatorial and algebraic constructions presented here, and we only refer to them when they help to get geometric intuition on our statements.

1.1.1. Cambrian trees and increasing trees. Consider a directed tree T on a vertex set V and a vertex $v \in V$. We call *children* (resp. *parents*) of v the sources of the incoming arcs (resp. the targets of the outgoing arcs) at v and *descendants* (resp. *ancestor subtrees*) of v the subtrees attached to them. The main characters of our paper are the following trees, which generalize standard binary search trees. Our definition is adapted from [IO13, LP13].

Definition 1. A **Cambrian tree** is a directed tree T with vertex set V endowed with a bijective vertex labeling $p : V \rightarrow [n]$ such that for each vertex $v \in V$,

- (i) v has either one parent and two children (its descendant subtrees are called **left and right subtrees**) or one child and two parents (its ancestor subtrees are called **left and right subtrees**);
- (ii) all labels are smaller (resp. larger) than $p(v)$ in the left (resp. right) subtree of v .

The **signature** of T is the n -tuple $\varepsilon(T) \in \pm^n$ defined by $\varepsilon(T)_{p(v)} = -$ if v has two children and $\varepsilon(T)_{p(v)} = +$ if v has two parents. Denote by $\text{Camb}(\varepsilon)$ the set of Cambrian trees with signature ε , by $\text{Camb}(n) = \bigsqcup_{\varepsilon \in \pm^n} \text{Camb}(\varepsilon)$ the set of all Cambrian trees on n vertices, and by $\text{Camb} := \bigsqcup_{n \in \mathbb{N}} \text{Camb}(n)$ the set of all Cambrian trees.

Definition 2. An **increasing tree** is a directed tree T with vertex set V endowed with a bijective vertex labeling $q : V \rightarrow [n]$ such that $v \rightarrow w$ in T implies $q(v) < q(w)$.

Definition 3. A **leveled Cambrian tree** is a directed tree T with vertex set V endowed with two bijective vertex labelings $p, q : V \rightarrow [n]$ which respectively define a Cambrian and an increasing tree.

In other words, a leveled Cambrian tree is a Cambrian tree endowed with a linear extension of its transitive closure. Figure 2 provides examples of a Cambrian tree (left), an increasing tree (middle), and a leveled Cambrian tree (right). All edges are oriented bottom-up. Throughout the paper, we represent leveled Cambrian trees on an $(n \times n)$ -grid as follows (see Figure 2):

- (i) each vertex v appears at position $(p(v), q(v))$;

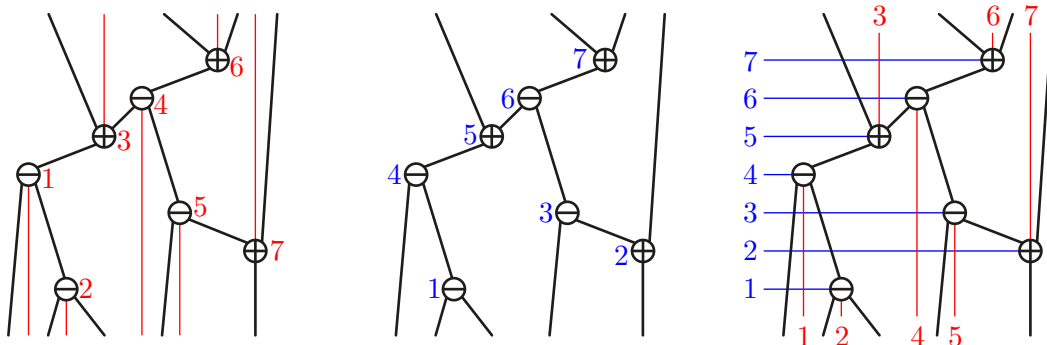


FIGURE 2. A Cambrian tree (left), an increasing tree (middle), and a leveled Cambrian tree (right).

- (ii) negative vertices (with one parent and two children) are represented by \ominus , while positive vertices (with one child and two parents) are represented by \oplus ;
- (iii) we sometimes draw a vertical red wall below the negative vertices and above the positive vertices to mark the separation between the left and right subtrees of each vertex.

Remark 4 (Spines of triangulations). Cambrian trees can be seen as spines (*i.e.* oriented and labeled dual trees) of triangulations of labeled polygons. More precisely, consider an $(n+2)$ -gon P^ε with vertices labeled by $0, \dots, n+1$ from left to right, and where vertex i is located above the diagonal $[0, n+1]$ if $\varepsilon_i = +$ and below it if $\varepsilon_i = -$. We associate with a triangulation σ of P^ε its dual tree having a node labeled by j for each triangle ijk of σ where $i < j < k$, and an edge between any two adjacent triangles oriented from the triangle below to the triangle above their common diagonal. See Figure 3 and refer to [LP13] for details. Throughout the paper, we denote by T^* the triangulation of P^ε dual to the ε -Cambrian tree T , and we use this interpretation to provide the reader with some geometric intuition of definitions and results of this paper.

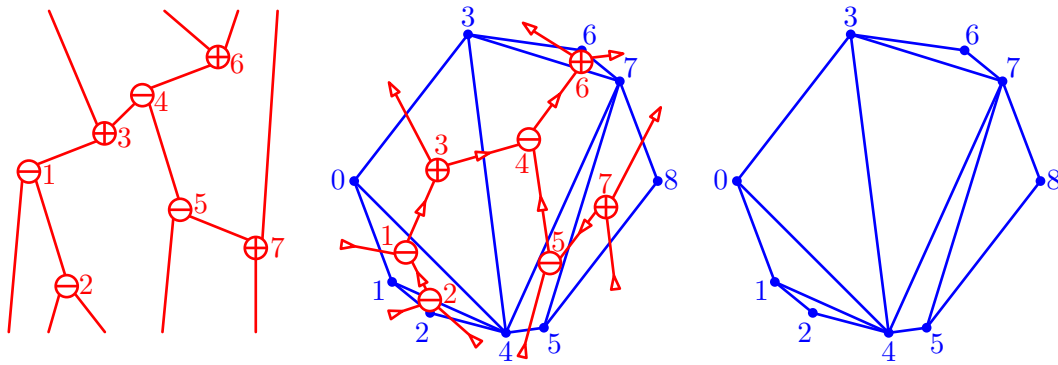


FIGURE 3. Cambrian trees (left) and triangulations (right) are dual to each other (middle).

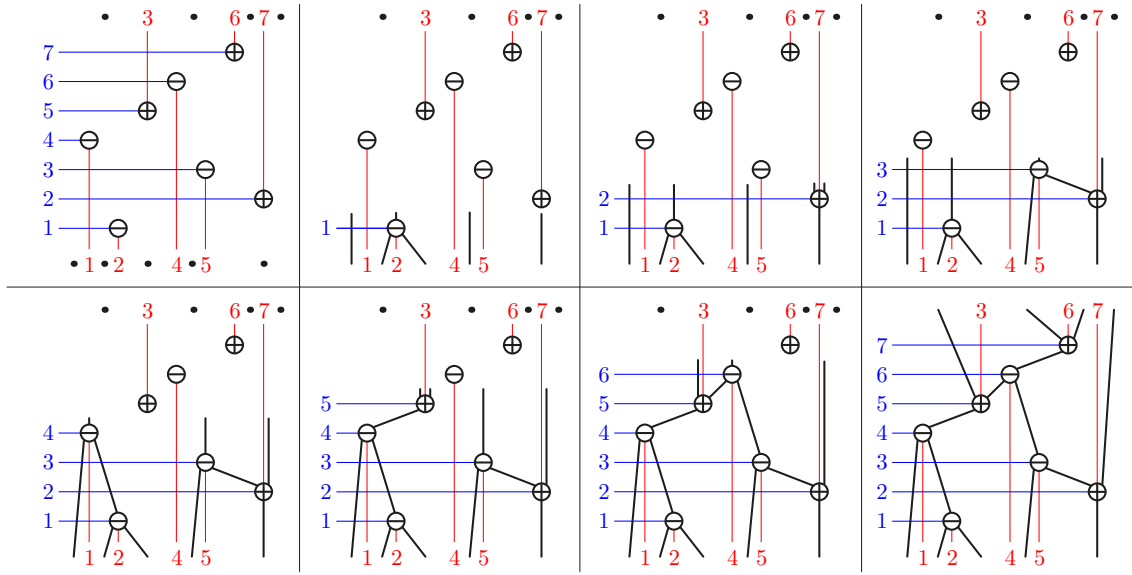
Proposition 5 ([LP13, IO13]). *For any signature $\varepsilon \in \pm^n$, the number of ε -Cambrian trees is the Catalan number $C_n = \frac{1}{n+1} \binom{2n}{n}$. Therefore, $|\text{Camb}(n)| = 2^n C_n$. See [OEIS, A151374].*

There are several ways to prove this statement (to our knowledge, the last two are original):

- (i) From the description of [LP13] given in the previous remark, the number of ε -Cambrian trees is the number of triangulations of a convex $(n+2)$ -gon, counted by the Catalan number.
- (ii) There are natural bijections between ε -Cambrian trees and binary trees. One simple way is to reorient all edges of a Cambrian tree towards an arbitrary leaf to get a binary tree, but the inverse map is more difficult to explain, see [IO13].
- (iii) Cambrian trees are in bijection with certain pattern avoiding signed permutations, see Section 1.1.4. In Proposition 15, we show that the shape of the generating tree for these permutations is independent of ε .
- (iv) In Lemma 38, we give an explicit bijection between ε - and ε' -Cambrian trees, where ε and ε' only differ by swapping two consecutive signs or switching the sign of 1 (or that of n).

1.1.2. Cambrian correspondence. We represent graphically a permutation $\tau \in \mathfrak{S}_n$ by the $(n \times n)$ -table, with rows labeled by positions from bottom to top and columns labeled by values from left to right, and with a dot in row i and column $\tau(i)$ for all $i \in [n]$. (This unusual choice of orientation is necessary to fit later with the existing constructions of [LR98, HNT05].)

A *signed permutation* is a permutation table where each dot receives a $+$ or $-$ sign, see the top left corner of Figure 4. We could equivalently think of a permutation where the positions or the values receive a sign, but it will be useful later to switch the signature from positions to values. The *p -signature* (resp. *v -signature*) of a signed permutation τ is the sequence $\varepsilon_p(\tau)$ (resp. $\varepsilon_v(\tau)$) of signs of τ ordered by positions from bottom to top (resp. by values from left to

FIGURE 4. The insertion algorithm on the signed permutation $\overline{2751346}$.

right). For a signature $\varepsilon \in \pm^n$, we denote by \mathfrak{S}_ε (resp. by \mathfrak{S}^ε) the set of signed permutations τ with p-signature $\varepsilon_p(\tau) = \varepsilon$ (resp. with v-signature $\varepsilon_v(\tau) = \varepsilon$). Finally, we denote by

$$\mathfrak{S}_\pm := \bigsqcup_{\substack{n \in \mathbb{N} \\ \varepsilon \in \pm^n}} \mathfrak{S}_\varepsilon = \bigsqcup_{\substack{n \in \mathbb{N} \\ \varepsilon \in \pm^n}} \mathfrak{S}^\varepsilon$$

the set of all signed permutations.

In concrete examples, we underline negative positions/values while we overline positive positions/values: for example, we write $\overline{2751346}$ for the signed permutation represented on the top left corner of Figure 4, where $\tau = [2, 7, 5, 1, 3, 4, 6]$, $\varepsilon_p = -+---+--+$ and $\varepsilon_v = ---+---++$.

Following [LP13], we now present an algorithm to construct a leveled ε -Cambrian tree $\Theta(\tau)$ from a signed permutation $\tau \in \mathfrak{S}^\varepsilon$. Figure 4 illustrates this algorithm on the permutation $\overline{2751346}$. As a preprocessing, we represent the table of τ (with signed dots in positions $(\tau(i), i)$ for $i \in [n]$) and draw a vertical wall below the negative vertices and above the positive vertices. We then sweep the table from bottom to top (thus reading the permutation τ from left to right) as follows. The procedure starts with an incoming strand in between any two consecutive negative values. A negative dot \ominus connects the two strands immediately to its left and immediately to its right to form a unique outgoing strand. A positive dot \oplus separates the only visible strand (not hidden by a wall) into two outgoing strands. The procedure finishes with an outgoing strand in between any two consecutive positive values. See Figure 4.

Proposition 6 ([LP13]). *The map Θ is a bijection from signed permutations to leveled Cambrian trees.*

Remark 7 (Cambrian correspondence). The *Robinson-Schensted correspondence* is a bijection between permutations and pairs of standard Young tableaux of the same shape. Schensted's algorithm [Sch61] gives an efficient algorithmic way to create the pair of tableaux $(\mathbf{P}(\tau), \mathbf{Q}(\tau))$ corresponding to a given permutation τ by successive insertions: the first tableau $\mathbf{P}(\tau)$ (*insertion tableau*) remembers the inserted elements of τ while the second tableau $\mathbf{Q}(\tau)$ (*recording tableau*) remembers the order in which the elements have been inserted. F. Hivert, J.-C. Novelli and J.-Y. Thibon defined in [HNT05] a similar correspondence, called *sylvester correspondence*, between permutations and pairs of labeled trees of the same shape. In the sylvester correspondence, the first tree (insertion tree) is a standard binary search tree and the second tree (recording tree) is an increasing binary tree. The *Cambrian correspondence* can as well be thought of as a correspondence between signed permutations and pairs of trees of the same shape, where the first

tree (insertion tree) is Cambrian and the second tree (recording tree) is increasing. This analogy motivates the following definition.

Definition 8. Given a signed permutation $\tau \in \mathfrak{S}^\varepsilon$, its **P-symbol** is the insertion Cambrian tree $\mathbf{P}(\tau)$ defined by $\Theta(\tau)$ and its **Q-symbol** is the recording increasing tree $\mathbf{Q}(\tau)$ defined by $\Theta(\tau)$.

The following characterization of the fibers of \mathbf{P} is immediate from the description of the algorithm. We denote by $\mathcal{L}(G)$ the set of linear extensions of a directed graph G .

Proposition 9. The signed permutations $\tau \in \mathfrak{S}^\varepsilon$ such that $\mathbf{P}(\tau) = \mathbf{T}$ are precisely the linear extensions of (the transitive closure of) \mathbf{T} .

Example 10. When $\varepsilon = (+)^n$, the procedure constructs a binary search tree $\mathbf{P}(\tau)$ pointing up by successive insertions from the left. Equivalently, $\mathbf{P}(\tau)$ can be constructed as the increasing tree of τ^{-1} . Here, the *increasing tree* $\text{IT}(\pi)$ of a permutation $\pi = \pi'1\pi''$ is defined inductively by grafting the increasing tree $\text{IT}(\pi')$ on the left and the increasing tree $\text{IT}(\pi'')$ on the right of the bottom root labeled by 1. When $\varepsilon = (-)^n$, this procedure constructs bottom-up a binary search tree $\mathbf{P}(\tau)$ pointing down. This tree would be obtained by successive binary search tree insertions from the right. Equivalently, $\mathbf{P}(\tau)$ can be constructed as the decreasing tree of τ^{-1} . Here, the *decreasing tree* $\text{DT}(\pi)$ of a permutation $\pi = \pi'n\pi''$ is defined inductively by grafting the decreasing tree $\text{DT}(\pi')$ on the left and the decreasing tree $\text{DT}(\pi'')$ on the right of the top root labeled by n . These observations are illustrated on Figure 5.

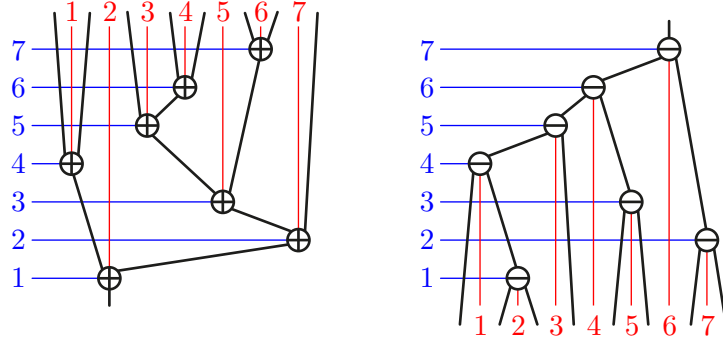


FIGURE 5. The insertion procedure produces binary search trees when the signature is constant positive (left) or constant negative (right).

Remark 11 (Cambrian correspondence on triangulations). N. Reading [Rea06] first described the map \mathbf{P} on the triangulations of the polygon P^ε (remember Remark 4). Namely, the triangulation $\mathbf{P}(\tau)^*$ is the union of the paths π_0, \dots, π_n where π_i is the path between vertices 0 and $n+1$ of P^ε passing through the vertices in the symmetric difference $\varepsilon^{-1}(-) \Delta \tau([i])$.

1.1.3. Cambrian congruence. Following the definition of the sylvester congruence in [HNT05], we now characterize by a congruence relation the signed permutations $\tau \in \mathfrak{S}^\varepsilon$ which have the same \mathbf{P} -symbol $\mathbf{P}(\tau)$. This Cambrian congruence goes back to the original definition of N. Reading [Rea06].

Definition 12 ([Rea06]). For a signature $\varepsilon \in \pm^n$, the ε -Cambrian congruence is the equivalence relation on \mathfrak{S}^ε defined as the transitive closure of the rewriting rules

$$\begin{aligned} UacVbW &\equiv_\varepsilon UcaVbW && \text{if } a < b < c \text{ and } \varepsilon_b = -, \\ UbVacW &\equiv_\varepsilon UbVcaW && \text{if } a < b < c \text{ and } \varepsilon_b = +, \end{aligned}$$

where a, b, c are elements of $[n]$ while U, V, W are words on $[n]$. The **Cambrian congruence** is the equivalence relation on all signed permutations \mathfrak{S}_\pm obtained as the union of all ε -Cambrian congruences:

$$\equiv := \bigsqcup_{\substack{n \in \mathbb{N} \\ \varepsilon \in \pm^n}} \equiv_\varepsilon .$$

Proposition 13. *Two signed permutations $\tau, \tau' \in \mathfrak{S}^\varepsilon$ are ε -Cambrian congruent if and only if they have the same \mathbf{P} -symbol:*

$$\tau \equiv_\varepsilon \tau' \iff \mathbf{P}(\tau) = \mathbf{P}(\tau').$$

Proof. It boils down to observe that two consecutive vertices a, c in a linear extension τ of a ε -Cambrian tree T can be switched while preserving a linear extension τ' of T precisely when they belong to distinct subtrees of a vertex b of T . It follows that the vertices a, c lie on either sides of b so that we have $a < b < c$. If $\varepsilon_b = -$, then a, c appear before b and $\tau = UacVbW$ can be switched to $\tau' = UcaVbW$, while if $\varepsilon_b = +$, then a, c appear after b and $\tau = UbVcaW$ can be switched to $\tau' = UbVcaW$. \square

1.1.4. Cambrian classes and generating trees. We now focus on the equivalence classes of the Cambrian congruence. Remember that the (*right*) *weak order* on \mathfrak{S}^ε is defined as the inclusion order of coinversions, where a *coinversion* of $\tau \in \mathfrak{S}^\varepsilon$ is a pair of values $i < j$ such that $\tau^{-1}(i) > \tau^{-1}(j)$ (no matter the signs on τ). In this paper, we always work with the right weak order, that we simply call weak order for brevity. The following statement is due to N. Reading [Rea06].

Proposition 14 ([Rea06]). *All ε -Cambrian classes are intervals of the weak order on \mathfrak{S}^ε .*

Therefore, the ε -Cambrian trees are in bijection with the weak order maximal permutations of ε -Cambrian classes. Using Definition 12 and Proposition 13, one can prove that these permutations are precisely the permutations in \mathfrak{S}^ε that avoid the signed patterns $b-ac$ with $\varepsilon_b = +$ and $ac-b$ with $\varepsilon_b = -$ (for brevity, we write $\bar{b}-ac$ and $ac-\bar{b}$). It enables us to construct a generating tree \mathcal{T}_ε for these permutations. This tree has n levels, and the nodes at level m are labeled by the permutations of $[m]$ whose values are signed by the restriction of ε to $[m]$ and avoiding the two patterns $\bar{b}-ac$ and $ac-\bar{b}$. The parent of a permutation in \mathcal{T}_ε is obtained by deleting its maximal value. See Figure 6 for examples of such trees. The following statement provides another proof that the number of ε -Cambrian trees on n nodes is always the Catalan number $C_n = \frac{1}{n+1} \binom{2n}{n}$, as well as an explicit bijection between ε - and ε' -Cambrian trees for distinct signatures $\varepsilon, \varepsilon' \in \pm^n$.

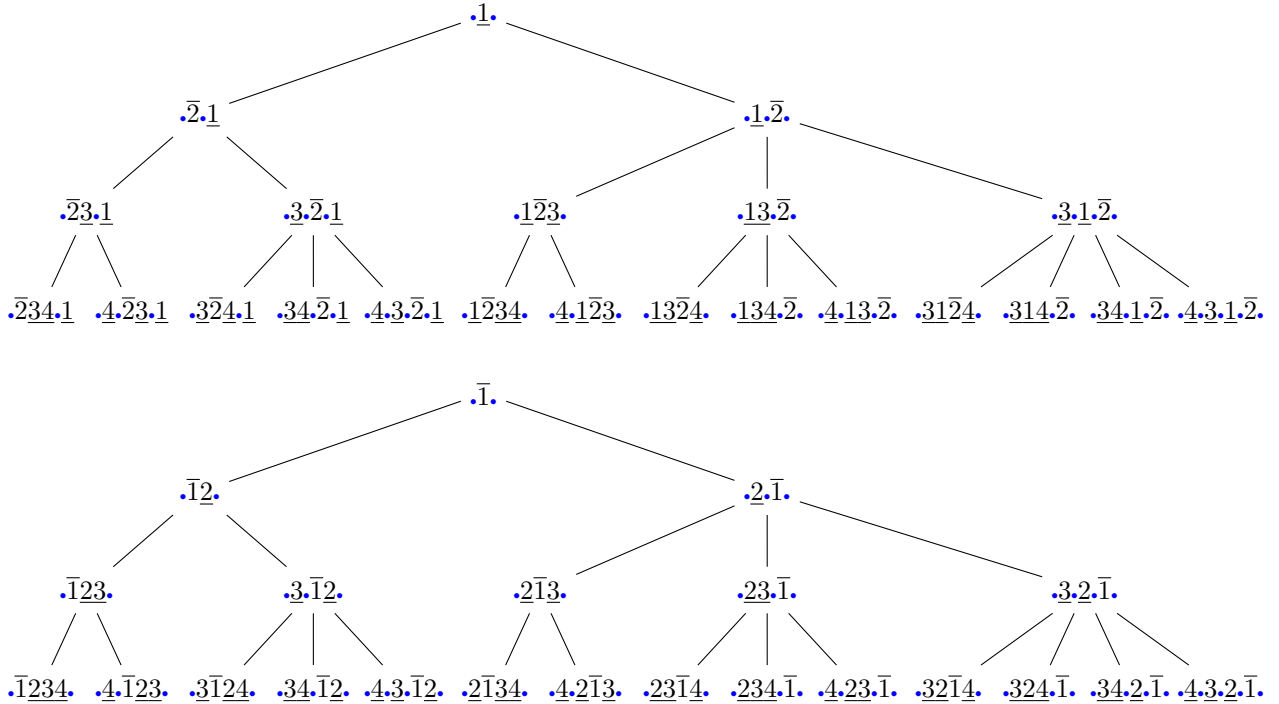


FIGURE 6. The generating trees \mathcal{T}_ε for the signatures $\varepsilon = -+--$ (top) and $\varepsilon = +---$ (bottom). Free gaps are marked with a blue dot.

Proposition 15. *For any signatures $\varepsilon, \varepsilon' \in \pm^n$, the generating trees \mathcal{T}_ε and $\mathcal{T}_{\varepsilon'}$ are isomorphic.*

For the proof, we consider the possible positions of $m + 1$ in the children of a permutation τ at level m in \mathcal{T}_ε . Index by $\{0, \dots, m\}$ from left to right the gaps before the first letter, between two consecutive letters, and after the last letter of τ . We call *free gaps* the gaps in $\{0, \dots, m\}$ where placing $m + 1$ does not create a pattern $ac\bar{b}$ or $\bar{b}ac$. They are marked with a blue point in Figure 6.

Lemma 16. *A permutation with k free gaps has k children in \mathcal{T}_ε , whose numbers of free gaps range from 2 to $k + 1$.*

Proof. Let τ be a permutation at level m in \mathcal{T}_ε with k free gaps. Let σ be the child of τ in \mathcal{T}_ε obtained by inserting $m + 1$ at a free gap $j \in \{0, \dots, m\}$. If ε_{m+1} is negative (resp. positive), then the free gaps of σ are $0, j + 1$ and the free gaps of τ after j (resp. before $j + 1$). The result follows. \square

Proof of Proposition 15. Order the children of a permutation of \mathcal{T}_ε from left to right by increasing number of free gaps as in Figure 6. Lemma 16 shows that the shape of the resulting tree is independent of ε . It ensures that the trees \mathcal{T}_ε and $\mathcal{T}_{\varepsilon'}$ are isomorphic and provides an explicit bijection between the ε -Cambrian trees and ε' -Cambrian trees. \square

1.1.5. Rotations and Cambrian lattices. We now present rotations in Cambrian trees, a local operation which transforms a ε -Cambrian tree into another ε -Cambrian tree where a single oriented cut differs (see Proposition 18).

Definition 17. *Let $i \rightarrow j$ be an edge in a Cambrian tree T , with $i < j$. Let L denote the left subtree of i and B denote the remaining incoming subtree of i , and similarly, let R denote the right subtree of j and A denote the remaining outgoing subtree of j . Let T' be the oriented tree obtained from T just reversing the orientation of $i \rightarrow j$ and attaching the subtrees L and A to i and the subtrees B and R to j . The transformation from T to T' is called *rotation* of the edge $i \rightarrow j$. See Figure 7.*

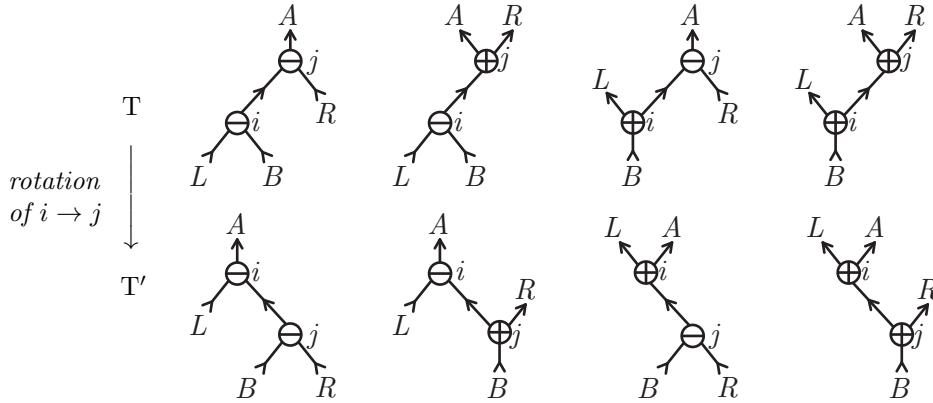


FIGURE 7. Rotations in Cambrian trees: the tree T (top) is transformed into the tree T' (bottom) by rotation of the edge $i \rightarrow j$. The four cases correspond to the possible signs of i and j .

The following proposition states that rotations are compatible with Cambrian trees and their edge cuts. An *edge cut* in a Cambrian tree T is the ordered partition $(X \parallel Y)$ of the vertices of T into the set X of vertices in the source set and the set Y of vertices in the target set of an oriented edge of T .

Proposition 18 ([LP13]). *The result T' of the rotation of an edge $i \rightarrow j$ in a ε -Cambrian tree T is a ε -Cambrian tree. Moreover, T' is the unique ε -Cambrian tree with the same edge cuts as T , except the cut defined by the edge $i \rightarrow j$.*

Remark 19 (Rotations and flips). Rotating an edge e in a ε -Cambrian tree T corresponds to flipping the dual diagonal e^* of the dual triangulation T^* of the polygon P^ε . See [LP13, Lemma 13].

Define the *increasing rotation graph* on $\text{Camb}(\varepsilon)$ to be the graph whose vertices are the ε -Cambrian trees and whose arcs are increasing rotations $T \rightarrow T'$, *i.e.* where the edge $i \rightarrow j$ in T is reversed to the edge $i \leftarrow j$ in T' for $i < j$. See Figure 8 for an illustration. The following statement, adapted from N. Reading's work [Rea06], asserts that this graph is acyclic, that its transitive closure defines a lattice, and that this lattice is closely related to the weak order. See Figure 9.

Proposition 20 ([Rea06]). *The transitive closure of the increasing rotation graph on $\text{Camb}(\varepsilon)$ is a lattice, called ε -Cambrian lattice. The map $\mathbf{P} : \mathfrak{S}^\varepsilon \rightarrow \text{Camb}(\varepsilon)$ defines a lattice homomorphism from the weak order on \mathfrak{S}^ε to the ε -Cambrian lattice on $\text{Camb}(\varepsilon)$.*

Note that the minimal (resp. maximal) ε -Cambrian tree is an oriented path from 1 to n (resp. from n to 1) with an additional incoming leaf at each negative vertex and an additional outgoing leaf at each positive vertex. See Figure 8.

Example 21. When $\varepsilon = (-)^n$, the Cambrian lattice is the classical Tamari lattice [MHPS12]. It can be defined equivalently by left-to-right rotations in planar binary trees, by slope increasing flips in triangulations of $P^{(-)^n}$, or as the quotient of the weak order by the sylvester congruence.

1.1.6. Canopy. The canopy of a binary tree was already used by J.-L. Loday in [LR98, Lod04] but the name was coined by X. Viennot [Vie07]. It was then extended to Cambrian trees (or spines) in [LP13] to define a surjection from the associahedron $\text{Asso}(\varepsilon)$ to the parallelepiped $\text{Para}(n)$ generated by the simple roots. The main observation is that the vertices i and $i + 1$ are always comparable in a Cambrian tree (otherwise, they would be in distinct subtrees of a vertex j which should then lie in between i and $i + 1$).

Definition 22. *The canopy of a Cambrian tree T is the sequence $\mathbf{can}(T) \in \pm^{n-1}$ defined by $\mathbf{can}(T)_i = -$ if i is above $i + 1$ in T and $\mathbf{can}(T)_i = +$ if i is below $i + 1$ in T .*

For example, the canopy of the Cambrian tree of Figure 2 (left) is $-+ + - + -$. The canopy of T behaves nicely with the linear extensions of T and with the Cambrian lattice. To state this, we define for a permutation $\tau \in \mathfrak{S}^\varepsilon$ the sequence $\mathbf{rec}(\tau) \in \pm^{n-1}$, where $\mathbf{rec}(T)_i = -$ if $\tau^{-1}(i) > \tau^{-1}(i + 1)$ and $\mathbf{rec}(T)_i = +$ otherwise. In other words, $\mathbf{rec}(\tau)$ records the *recoils* of the permutation τ , *i.e.* the *descents* of the inverse permutation of τ .

Proposition 23. *The maps \mathbf{P} , \mathbf{can} , and \mathbf{rec} define the following commutative diagram of lattice homomorphisms:*

$$\begin{array}{ccc} \mathfrak{S}^\varepsilon & \xrightarrow{\mathbf{rec}} & \pm^{n-1} \\ & \searrow \mathbf{P} & \nearrow \mathbf{can} \\ & \text{Camb}(\varepsilon) & \end{array}$$

The fibers of these maps on the weak orders of \mathfrak{S}_ε for $\varepsilon = -+---$ and $\varepsilon = +----$ are represented in Figure 9.

1.1.7. Geometric realizations. We close this section with geometric interpretations of the Cambrian trees, Cambrian classes, Cambrian correspondence, and Cambrian lattices. We denote by e_1, \dots, e_n the canonical basis of \mathbb{R}^n and by \mathbb{H} the hyperplane of \mathbb{R}^n orthogonal to $\sum e_i$. Define the *incidence cone* $C(T)$ and the *braid cone* $C^\circ(T)$ of a directed tree T as

$$C(T) := \text{cone} \{e_i - e_j \mid \text{for all } i \rightarrow j \text{ in } T\} \quad \text{and} \quad C^\circ(T) := \{\mathbf{x} \in \mathbb{H} \mid x_i \leq x_j \text{ for all } i \rightarrow j \text{ in } T\}.$$

These two cones lie in the space \mathbb{H} and are polar to each other. For a permutation $\tau \in \mathfrak{S}_n$, we denote by $C(\tau)$ and $C^\circ(\tau)$ the incidence and braid cone of the chain $\tau(1) \rightarrow \dots \rightarrow \tau(n)$. Finally, for a sign vector $\chi \in \pm^{n-1}$, we denote by $C(\chi)$ and $C^\circ(\chi)$ the incidence and braid cone of the oriented path $1 - \dots - n$, where $i \rightarrow i + 1$ if $\chi_i = +$ and $i \leftarrow i + 1$ if $\chi_i = -$.

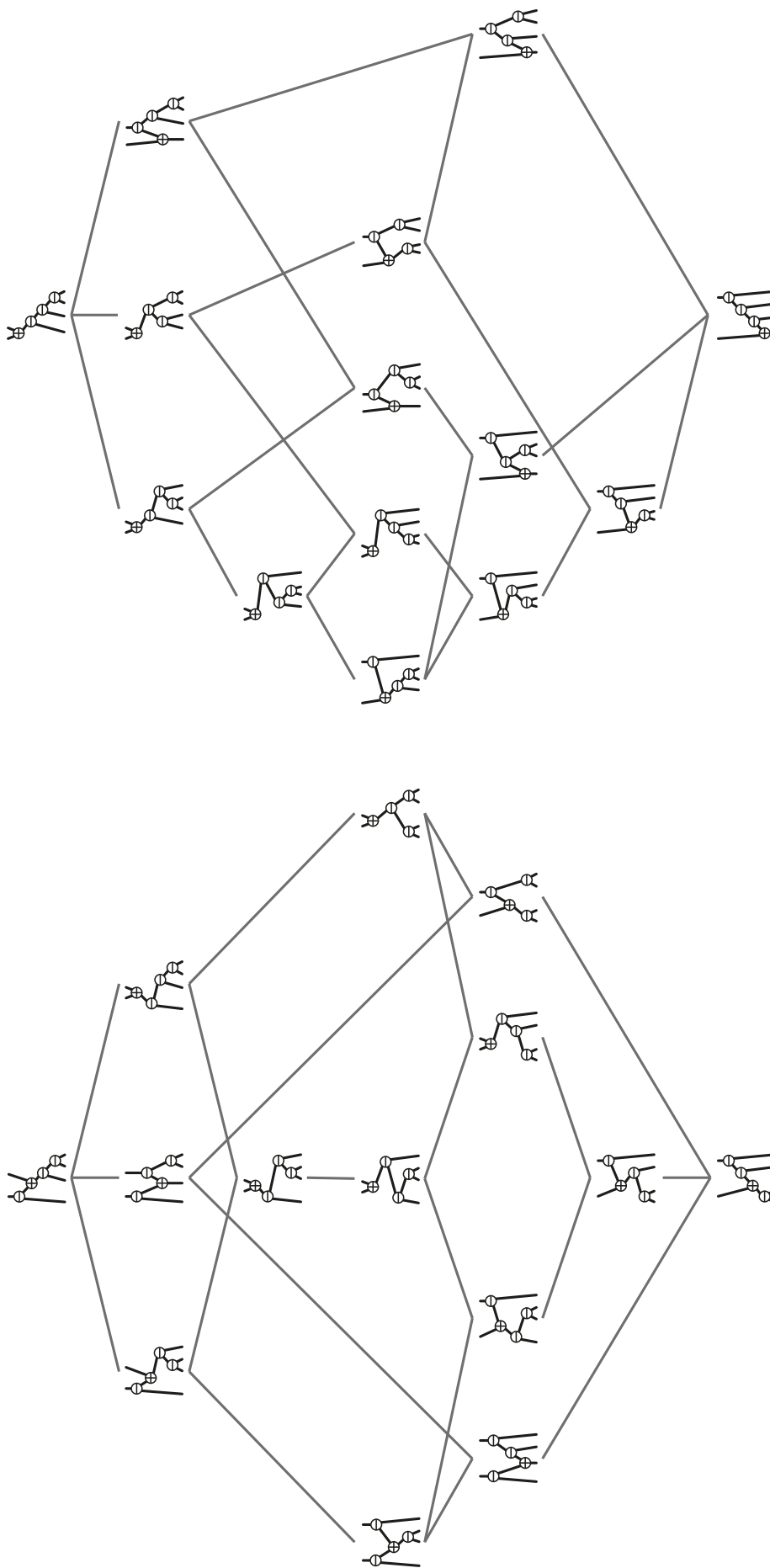


FIGURE 8. The ε -Cambrian lattices on ε -Cambrian trees, for the signatures $\varepsilon = -+----$ (left) and $\varepsilon = +++---$ (right).

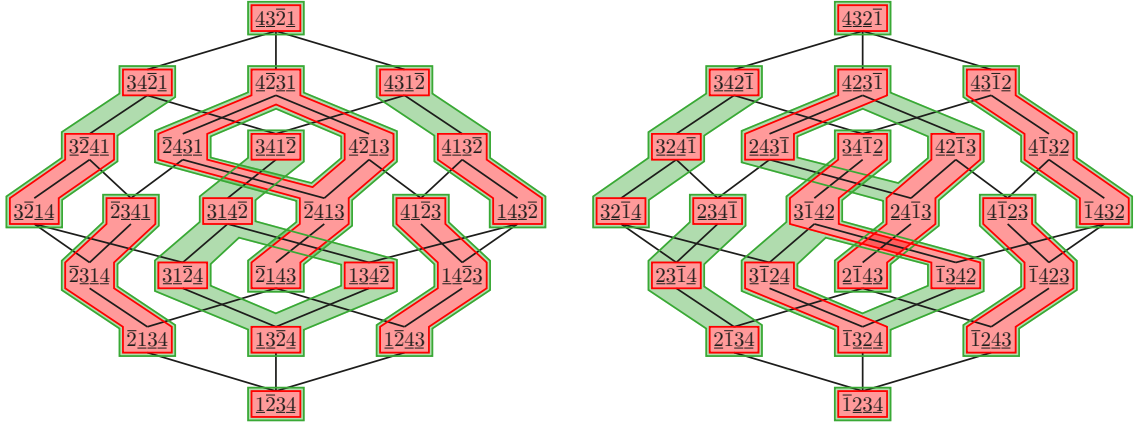


FIGURE 9. The fibers of the maps \mathbf{P} (red) and \mathbf{rec} (green) on the weak orders of \mathfrak{S}_ε for $\varepsilon = -+--$ (left) and $\varepsilon = +- --$ (right).

These cones (together with all their faces) form complete simplicial fans in \mathbb{H} :

- (i) the cones $C^\circ(\tau)$, for all permutations $\tau \in \mathfrak{S}_n$, form the *braid fan*, which is the normal fan of the *permutahedron* $\text{Perm}(n) := \text{conv} \{ \sum_{i \in [n]} \tau(i)e_i \mid \tau \in \mathfrak{S}_n \}$;
- (ii) the cones $C^\circ(T)$, for all ε -Cambrian trees T , form the ε -*Cambrian fan*, which is the normal fan of the ε -*associahedron* $\text{Asso}(\varepsilon)$ of C. Hohlweg and C. Lange [HL07] (see also [LP13]);
- (iii) the cones $C^\circ(\chi)$, for all sign vectors $\chi \in \pm^{n-1}$, form the *boolean fan*, which is the normal fan of the parallelepiped $\text{Para}(n) := \{ \mathbf{x} \in \mathbb{H} \mid i(2n+1-i) \leq 2 \sum_{j \leq i} x_j \leq i(i+1) \text{ for all } i \in [n] \}$.

In fact, $\text{Asso}(\varepsilon)$ is obtained by deleting certain inequalities in the facet description of $\text{Perm}(n)$, and similarly, $\text{Para}(n)$ is obtained by deleting facets of $\text{Asso}(\varepsilon)$. In particular, we have the geometric inclusions $\text{Perm}(n) \subset \text{Asso}(\varepsilon) \subset \text{Para}(n)$. See Figure 10 for 3-dimensional examples.

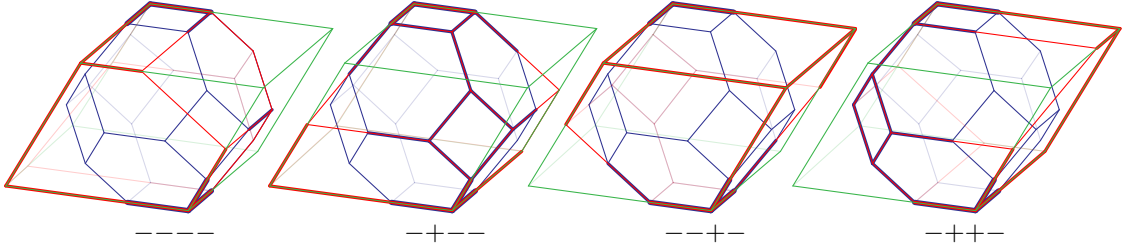


FIGURE 10. The polytope inclusion $\text{Perm}(4) \subset \text{Asso}(\varepsilon) \subset \text{Para}(4)$ for different signatures $\varepsilon \in \pm^4$. The permutahedron $\text{Perm}(4)$ is represented in red, the associahedron $\text{Asso}(\varepsilon)$ in blue, and the parallelepiped $\text{Para}(4)$ in green.

The incidence and braid cones also characterize the maps \mathbf{P} , \mathbf{can} , and \mathbf{rec} as follows

$$\begin{aligned} T = \mathbf{P}(\tau) &\iff C(T) \subseteq C(\tau) \iff C^\circ(T) \supseteq C^\circ(\tau), \\ \chi = \mathbf{can}(T) &\iff C(\chi) \subseteq C(T) \iff C^\circ(\chi) \supseteq C^\circ(T), \\ \chi = \mathbf{rec}(\tau) &\iff C(\chi) \subseteq C(\tau) \iff C^\circ(\chi) \supseteq C^\circ(\tau). \end{aligned}$$

In particular, Cambrian classes are formed by all permutations whose braid cone belong to the same Cambrian cone. Finally, the 1-skeleta of the permutahedron $\text{Perm}(n)$, associahedron $\text{Asso}(\varepsilon)$ and parallelepiped $\text{Para}(n)$, oriented in the direction $(n, \dots, 1) - (1, \dots, n) = \sum_{i \in [n]} (n+1-2i)e_i$ are the Hasse diagrams of the weak order, the Cambrian lattice and the boolean lattice respectively. These geometric properties originally motivated the definition of Cambrian trees in [LP13].

1.2. CAMBRIAN HOPF ALGEBRA

In this section, we introduce the Cambrian Hopf algebra Camb as a subalgebra of the Hopf algebra FQSym_\pm on signed permutations, and the dual Cambrian algebra Camb^* as a quotient algebra of the dual Hopf algebra FQSym_\pm^* . We describe both the product and coproduct in these algebras in terms of combinatorial operations on Cambrian trees. These results extend the approach of F. Hivert, J.-C. Novelli and J.-Y. Thibon [HNT05] to construct the algebra of J.-L. Loday and M. Ronco on binary trees [LR98] as a subalgebra of the algebra of C. Malvenuto and C. Reutenauer on permutations [MR95].

We immediately mention that a different generalization was studied by N. Reading in [Rea05]. His idea was to construct a subalgebra of C. Malvenuto and C. Reutenauer’s algebra FQSym using equivalent classes of a congruence relation defined as the union $\bigcup_{n \in \mathbb{N}} \equiv_{\varepsilon_n}$ of ε_n -Cambrian relation for one fixed signature $\varepsilon_n \in \pm^n$ for each $n \in \mathbb{N}$. In order to obtain a valid Hopf algebra, the choice of $(\varepsilon_n)_{n \in \mathbb{N}}$ has to satisfy certain compatibility relations: N. Reading characterizes the “translational” (resp. “insertional”) families \equiv_n of lattice congruences on \mathfrak{S}_n for which the sums over the elements of the congruence classes of $(\equiv_n)_{n \in \mathbb{N}}$ form the basis of a subalgebra (resp. subcoalgebra) of FQSym . These conditions make the choice of $(\varepsilon_n)_{n \in \mathbb{N}}$ rather constrained. In contrast, by constructing a subalgebra of FQSym_\pm rather than FQSym , we consider simultaneously all Cambrian relations for all signatures. In particular, our Cambrian algebra contains all Hopf algebras of [Rea05] as subalgebras.

1.2.1. **Signed shuffle and convolution products.** For $n, n' \in \mathbb{N}$, let

$$\mathfrak{S}^{(n, n')} := \{\tau \in \mathfrak{S}_{n+n'} \mid \tau(1) < \dots < \tau(n) \text{ and } \tau(n+1) < \dots < \tau(n+n')\}$$

denote the set of permutations of $\mathfrak{S}_{n+n'}$ with at most one descent, at position n . The *shifted concatenation* $\tau\bar{\tau}'$, the *shifted shuffle product* $\tau \sqcup \tau'$, and the *convolution product* $\tau \star \tau'$ of two (unsigned) permutations $\tau \in \mathfrak{S}_n$ and $\tau' \in \mathfrak{S}_{n'}$ are classically defined by

$$\begin{aligned} \tau\bar{\tau}' &:= [\tau(1), \dots, \tau(n), \tau'(1) + n, \dots, \tau'(n') + n] \in \mathfrak{S}_{n+n'}, \\ \tau \sqcup \tau' &:= \{(\tau\bar{\tau}') \circ \pi^{-1} \mid \pi \in \mathfrak{S}^{(n, n')}\} \quad \text{and} \quad \tau \star \tau' := \{\pi \circ (\tau\bar{\tau}') \mid \pi \in \mathfrak{S}^{(n, n')}\}. \end{aligned}$$

For example,

$$\begin{aligned} 12 \sqcup 231 &= \{12453, 14253, 14523, 14532, 41253, 41523, 41532, 45123, 45132, 45312\}, \\ 12 \star 231 &= \{12453, 13452, 14352, 15342, 23451, 24351, 25341, 34251, 35241, 45231\}. \end{aligned}$$

These operations can be visualized graphically on the tables of the permutations τ, τ' . Remember that the table of τ contains a dot at coordinates $(\tau(i), i)$ for each $i \in [n]$. The table of the shifted concatenation $\tau\bar{\tau}'$ contains the table of τ as the bottom left block and the table of τ' as the top right block. The tables in the shifted shuffle product $\tau \sqcup \tau'$ (resp. in the convolution product $\tau \star \tau'$) are then obtained by shuffling the rows (resp. columns) of the table of $\tau\bar{\tau}'$. In particular, we obtain the table of τ if we erase all dots in the n' rightmost columns (resp. topmost rows) of a table in the shifted shuffle product $\tau \sqcup \tau'$ (resp. in the convolution product $\tau \star \tau'$). See Figure 11.

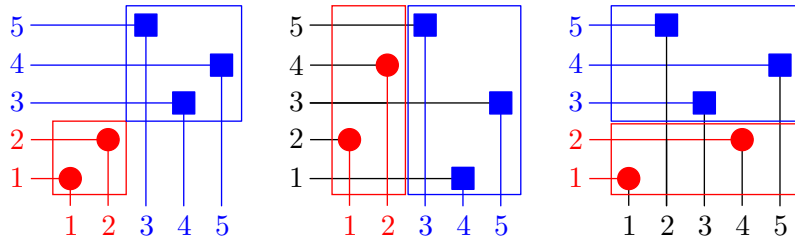


FIGURE 11. The table of the shifted concatenation $\tau\bar{\tau}'$ (left) has two blocks containing the tables of the permutations $\tau = 12$ and $\tau' = 231$. Elements of the shifted shuffle product $\tau \sqcup \tau'$ (middle) and of the convolution product $\tau \star \tau'$ (right) are obtained by shuffling respectively the rows and columns of the table of $\tau\bar{\tau}'$.

η -congruent to σ and in the convolution product $\tilde{\tau} \star \tilde{\tau}'$. It follows that $\mathbb{F}_{\tilde{\tau}} \otimes \mathbb{F}_{\tilde{\tau}'}$ also appears in the coproduct $\Delta(\mathbb{P}_T)$. The proofs for the other rewriting rule on τ , as well as for both rewriting rules on τ' , are symmetric, and the general case for $\tau \equiv_{\varepsilon} \tilde{\tau}$ and $\tau' \equiv_{\varepsilon'} \tilde{\tau}'$ follows by transitivity. \square

Another proof of this statement would be to show that the Cambrian congruence yields a φ -good monoïd [Pri13]. In the remaining of this section, we provide direct descriptions of the product and coproduct of \mathbb{P} -basis elements of **Camb** in terms of combinatorial operations on Cambrian trees.

PRODUCT The product in the Cambrian algebra can be described in terms of intervals in Cambrian lattices. Given two Cambrian trees T, T' , we denote by $T \nearrow \bar{T}'$ the tree obtained by grafting the rightmost outgoing leaf of T on the leftmost incoming leaf of T' and shifting all labels of T' . Note that the resulting tree is $\varepsilon\varepsilon'$ -Cambrian, where $\varepsilon\varepsilon'$ is the concatenation of the signatures $\varepsilon = \varepsilon(T)$ and $\varepsilon' = \varepsilon(T')$. We define similarly $T \nwarrow \bar{T}'$. Examples are given in Figure 12.

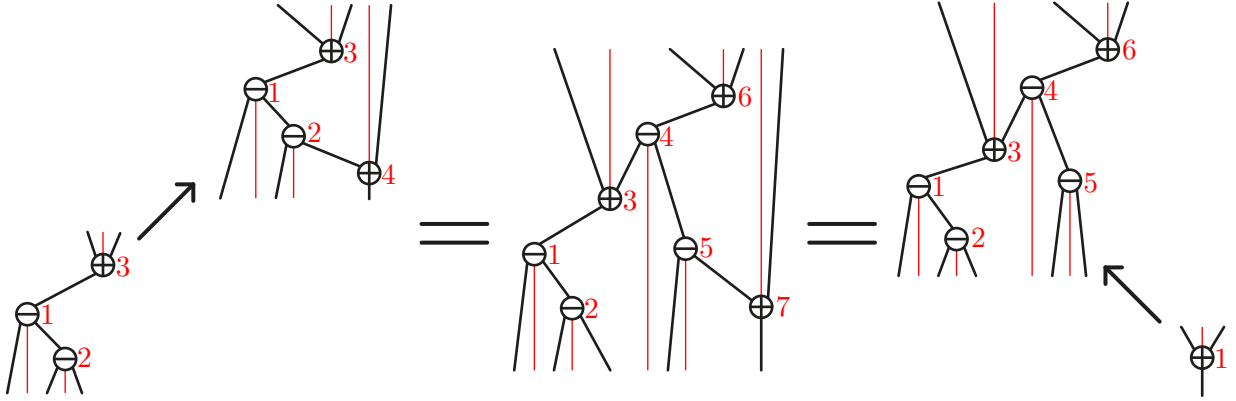


FIGURE 12. Grafting Cambrian trees.

Proposition 25. *For any Cambrian trees T, T' , the product $\mathbb{P}_T \cdot \mathbb{P}_{T'}$ is given by*

$$\mathbb{P}_T \cdot \mathbb{P}_{T'} = \sum_S \mathbb{P}_S,$$

where S runs over the interval between $T \nearrow \bar{T}'$ and $T \nwarrow \bar{T}'$ in the $\varepsilon(T)\varepsilon(T')$ -Cambrian lattice.

Proof. For any Cambrian tree T , the linear extensions $\mathcal{L}(T)$ form an interval of the weak order [Rea06]. Moreover, the shuffle product of two intervals of the weak order is an interval of the weak order. Therefore, the product $\mathbb{P}_T \cdot \mathbb{P}_{T'}$ is a sum of \mathbb{P}_S where S runs over an interval of the Cambrian lattice. It remains to characterize the minimal and maximal elements of this interval.

Let μ_T and ω_T denote respectively the smallest and the greatest linear extension of T in weak order. The product $\mathbb{P}_T \cdot \mathbb{P}_{T'}$ is the sum of \mathbb{P}_S over the interval

$$[\mu_T, \omega_T] \sqcup [\mu_{T'}, \omega_{T'}] = [\mu_T \bar{\mu}_{T'}, \bar{\omega}_{T'} \omega_T],$$

where $\bar{\cdot}$ denotes as usual the shifting operator on permutations. The result thus follows from the fact that

$$\mathbf{P}(\mu_T \bar{\mu}_{T'}) = T \nearrow \bar{T}' \quad \text{and} \quad \mathbf{P}(\bar{\omega}_{T'} \omega_T) = T \nwarrow \bar{T}'. \quad \square$$

For example, we can compute the product

$$\begin{aligned} \mathbb{P}_{\begin{array}{c} \text{---} \\ \diagup \quad \diagdown \\ \text{---} \end{array}} \cdot \mathbb{P}_{\begin{array}{c} \text{---} \\ \diagdown \quad \diagup \\ \text{---} \end{array}} &= \mathbb{F}_{1\bar{2}} \cdot (\mathbb{F}_{\bar{2}1\bar{3}} + \mathbb{F}_{\bar{2}3\bar{1}}) \\ &= \left(\begin{array}{l} \mathbb{F}_{1\bar{2}4\bar{3}5} + \mathbb{F}_{1\bar{2}4\bar{5}3} + \mathbb{F}_{1\bar{4}2\bar{3}5} \\ + \mathbb{F}_{1\bar{4}2\bar{5}3} + \mathbb{F}_{1\bar{4}5\bar{2}3} + \mathbb{F}_{4\bar{1}2\bar{3}5} \\ + \mathbb{F}_{4\bar{1}2\bar{5}3} + \mathbb{F}_{4\bar{1}5\bar{2}3} + \mathbb{F}_{4\bar{5}1\bar{2}3} \end{array} \right) + \left(\begin{array}{l} \mathbb{F}_{1\bar{4}3\bar{2}5} + \mathbb{F}_{1\bar{4}3\bar{5}2} \\ + \mathbb{F}_{1\bar{4}5\bar{3}2} + \mathbb{F}_{4\bar{1}3\bar{2}5} \\ + \mathbb{F}_{4\bar{1}3\bar{5}2} + \mathbb{F}_{4\bar{1}5\bar{3}2} \\ + \mathbb{F}_{4\bar{5}1\bar{3}2} \end{array} \right) + \left(\begin{array}{l} \mathbb{F}_{4\bar{3}1\bar{2}5} + \mathbb{F}_{4\bar{3}1\bar{5}2} \\ + \mathbb{F}_{4\bar{3}5\bar{1}2} + \mathbb{F}_{4\bar{5}3\bar{1}2} \end{array} \right) \\ &= \mathbb{P}_{\begin{array}{c} \text{---} \\ \diagup \quad \diagdown \\ \text{---} \end{array}} + \mathbb{P}_{\begin{array}{c} \text{---} \\ \diagdown \quad \diagup \\ \text{---} \end{array}} + \mathbb{P}_{\begin{array}{c} \text{---} \\ \diagup \quad \diagdown \\ \text{---} \end{array}}. \end{aligned}$$

The first equality is obtained by computing the linear extensions of the two factors, the second by computing the shuffle product and grouping terms according to their \mathbf{P} -symbol, displayed in the last line. Proposition 25 enables us to shortcut the computation by avoiding to resort to the \mathbb{F} -basis.

COPRODUCT The coproduct in the Cambrian algebra can also be described in combinatorial terms. Define a *cut* of a Cambrian tree S to be a set γ of edges such that any geodesic vertical path in S from a down leaf to an up leaf contains precisely one edge of γ . Such a cut separates the tree T into two forests, one above γ and one below γ , denoted $A(S, \gamma)$ and $B(S, \gamma)$, respectively. An example is given in Figure 13.

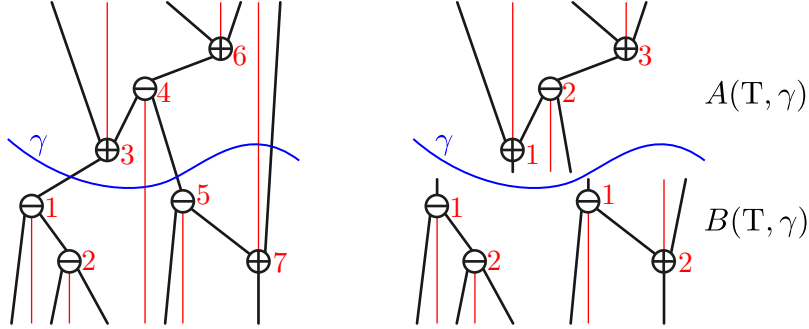


FIGURE 13. A cut γ of a Cambrian tree T defines two forests $A(T, \gamma)$ and $B(T, \gamma)$.

Proposition 26. *For any Cambrian tree S , the coproduct $\Delta\mathbb{P}_S$ is given by*

$$\Delta\mathbb{P}_S = \sum_{\gamma} \left(\prod_{T \in B(S, \gamma)} \mathbb{P}_T \right) \otimes \left(\prod_{T' \in A(S, \gamma)} \mathbb{P}_{T'} \right),$$

where γ runs over all cuts of S .

Proof. Let σ be a linear extension of S and $\tau, \tau' \in \mathfrak{S}_{\pm}$ such that $\sigma \in \tau \star \tau'$. As discussed in Section 1.2.1, the tables of τ and τ' respectively appear in the bottom and top rows of the table of σ . We can therefore associate a cut of S to each element which appears in the coproduct $\Delta\mathbb{P}_S$.

Reciprocally, given a cut γ of S , we are interested in the linear extensions of S where all indices below γ appear before all indices above γ . These linear extensions are precisely the permutations formed by a linear extension of $B(T, \gamma)$ followed by a linear extension of $A(T, \gamma)$. But the linear extensions of a forest are obtained by shuffling the linear extensions of its connected components. The result immediately follows since the product $\mathbb{P}_T \cdot \mathbb{P}_{T'}$ precisely involves the shuffle of the linear extensions of T with the linear extensions of T' . \square

For example, we can compute the coproduct

$$\begin{aligned} \Delta\mathbb{P}_{\begin{array}{c} \circ \\ \diagup \quad \diagdown \\ \circ \quad \circ \end{array}} &= \Delta(\mathbb{F}_{\bar{2}1\bar{3}} + \mathbb{F}_{\bar{2}\bar{3}1}) \\ &= 1 \otimes (\mathbb{F}_{\bar{2}1\bar{3}} + \mathbb{F}_{\bar{2}\bar{3}1}) + \mathbb{F}_{\bar{1}} \otimes \mathbb{F}_{1\bar{2}} + \mathbb{F}_{\bar{1}} \otimes \mathbb{F}_{2\bar{1}} + \mathbb{F}_{\bar{2}\bar{1}} \otimes \mathbb{F}_{\bar{1}} + \mathbb{F}_{\bar{1}\bar{2}} \otimes \mathbb{F}_{\bar{1}} + (\mathbb{F}_{\bar{2}1\bar{3}} + \mathbb{F}_{\bar{2}\bar{3}1}) \otimes 1 \\ &= 1 \otimes \mathbb{P}_{\begin{array}{c} \circ \\ \diagup \quad \diagdown \\ \circ \quad \circ \end{array}} + \mathbb{P}_{\begin{array}{c} \circ \\ \diagup \\ \circ \end{array}} \otimes \mathbb{P}_{\begin{array}{c} \circ \\ \diagdown \\ \circ \end{array}} + \mathbb{P}_{\begin{array}{c} \circ \\ \diagdown \\ \circ \end{array}} \otimes \mathbb{P}_{\begin{array}{c} \circ \\ \diagup \\ \circ \end{array}} + \mathbb{P}_{\begin{array}{c} \circ \\ \diagup \quad \diagdown \\ \circ \quad \circ \end{array}} \otimes \mathbb{P}_{\begin{array}{c} \circ \\ \diagup \\ \circ \end{array}} + \mathbb{P}_{\begin{array}{c} \circ \\ \diagdown \\ \circ \end{array}} \otimes \mathbb{P}_{\begin{array}{c} \circ \\ \diagdown \\ \circ \end{array}} + \mathbb{P}_{\begin{array}{c} \circ \\ \diagup \quad \diagdown \\ \circ \quad \circ \end{array}} \otimes 1 \\ &= 1 \otimes \mathbb{P}_{\begin{array}{c} \circ \\ \diagup \quad \diagdown \\ \circ \quad \circ \end{array}} + \mathbb{P}_{\begin{array}{c} \circ \\ \diagup \\ \circ \end{array}} \otimes (\mathbb{P}_{\begin{array}{c} \circ \\ \diagdown \\ \circ \end{array}} \cdot \mathbb{P}_{\begin{array}{c} \circ \\ \diagdown \\ \circ \end{array}}) + \mathbb{P}_{\begin{array}{c} \circ \\ \diagdown \\ \circ \end{array}} \otimes \mathbb{P}_{\begin{array}{c} \circ \\ \diagup \\ \circ \end{array}} + \mathbb{P}_{\begin{array}{c} \circ \\ \diagup \quad \diagdown \\ \circ \quad \circ \end{array}} \otimes \mathbb{P}_{\begin{array}{c} \circ \\ \diagdown \\ \circ \end{array}} + \mathbb{P}_{\begin{array}{c} \circ \\ \diagdown \\ \circ \end{array}} \otimes 1. \end{aligned}$$

Proposition 26 enables us to shortcut the computation by avoiding to resort to the \mathbb{F} -basis. We compute directly the last line, which corresponds to the five possible cuts of the Cambrian tree $\begin{array}{c} \circ \\ \diagup \quad \diagdown \\ \circ \quad \circ \end{array}$.

MATRIOCHKA ALGEBRAS To conclude, we connect the Cambrian algebra to the recoils algebra Rec , defined as the Hopf subalgebra of FQSym_\pm generated by the elements

$$\mathbb{X}_\chi := \sum_{\substack{\tau \in \mathfrak{S}_\pm \\ \text{rec}(\tau) = \chi}} \mathbb{F}_\tau$$

for all sign vectors $\chi \in \pm^{n-1}$. The commutative diagram of Proposition 23 ensures that

$$\mathbb{X}_\chi = \sum_{\substack{T \in \text{Camb} \\ \text{can}(T) = \chi}} \mathbb{P}_T,$$

and thus that Rec is a subalgebra of Camb . In other words, the Cambrian algebra is sandwiched between the signed permutation algebra and the recoils algebra $\text{Rec} \subset \text{Camb} \subset \text{FQSym}_\pm$. This property has to be compared with the polytope inclusions discussed in Section 1.1.7.

1.2.3. Quotient algebra of FQSym_\pm^* . We switch to the dual Hopf algebra FQSym_\pm^* with basis $(\mathbb{G}_\tau)_{\tau \in \mathfrak{S}_\pm}$ and whose product and coproduct are defined by

$$\mathbb{G}_\tau \cdot \mathbb{G}_{\tau'} = \sum_{\sigma \in \tau \star \tau'} \mathbb{G}_\sigma \quad \text{and} \quad \Delta \mathbb{G}_\sigma = \sum_{\sigma \in \tau \sqcup \tau'} \mathbb{G}_\tau \otimes \mathbb{G}_{\tau'}.$$

The following statement is automatic from Theorem 24.

Theorem 27. *The graded dual Camb^* of the Cambrian algebra is isomorphic to the image of FQSym_\pm^* under the canonical projection*

$$\pi : \mathbb{C}\langle A \rangle \longrightarrow \mathbb{C}\langle A \rangle / \equiv,$$

where \equiv denotes the Cambrian congruence. The dual basis \mathbb{Q}_T of \mathbb{P}_T is expressed as $\mathbb{Q}_T = \pi(\mathbb{G}_\tau)$, where τ is any linear extension of T .

Similarly as in the previous section, we can describe combinatorially the product and coproduct of \mathbb{Q} -basis elements of Camb^* in terms of operations on Cambrian trees.

PRODUCT Call *gaps* the $n + 1$ positions between two consecutive integers of $[n]$, including the position before 1 and the position after n . A gap γ defines a *geodesic vertical path* $\lambda(T, \gamma)$ in a Cambrian tree T from the bottom leaf which lies in the same interval of consecutive negative labels as γ to the top leaf which lies in the same interval of consecutive positive labels as γ . See Figure 15. A multiset Γ of gaps therefore defines a *lamination* $\lambda(T, \Gamma)$ of T , *i.e.* a multiset of pairwise non-crossing geodesic vertical paths in T from down leaves to up leaves. When cut along the paths of a lamination, the Cambrian tree T splits into a forest.

Consider two Cambrian trees T and T' on $[n]$ and $[n']$ respectively. For any shuffle s of their signatures ε and ε' , consider the multiset Γ of gaps of $[n]$ given by the positions of the negative signs of ε' in s and the multiset Γ' of gaps of $[n']$ given by the positions of the positive signs of ε in s . We denote by $T_s \setminus T'$ the Cambrian tree obtained by connecting the up leaves of the forest defined by the lamination $\lambda(T, \Gamma)$ to the down leaves of the forest defined by the lamination $\lambda(T', \Gamma')$.

Example 28. Consider the Cambrian trees T° and T^\square of Figure 14. To distinguish signs in T° and T^\square , we circle the signs in $\varepsilon(T^\circ) = \ominus\ominus\oplus$ and square the signs in $\varepsilon(T^\square) = \boxminus\boxplus\boxplus$. Consider now an arbitrary shuffle $s = \boxminus\ominus\oplus\boxplus\oplus\boxplus$ of these two signatures. The resulting laminations of T° and T^\square , as well as the Cambrian tree $T^\circ \setminus_s T^\square$ are represented in Figure 14.

Proposition 29. *For any Cambrian trees T, T' , the product $\mathbb{Q}_T \cdot \mathbb{Q}_{T'}$ is given by*

$$\mathbb{Q}_T \cdot \mathbb{Q}_{T'} = \sum_s \mathbb{Q}_{T_s \setminus T'},$$

where s runs over all shuffles of the signatures of T and T' .

Proof. Let τ and τ' be linear extensions of T and T' respectively, let $\sigma \in \tau \star \tau'$ and let $S = \mathbf{P}(\sigma)$. As discussed in Section 1.2.1, the convolution $\tau \star \tau'$ shuffles the columns of the tables of τ and τ' while preserving the order of their rows. According to the description of the insertion algorithm Θ , the tree S thus consists in T below and T' above, except that the vertical walls falling from the negative nodes of T' split T and similarly the vertical walls rising from the positive nodes of T

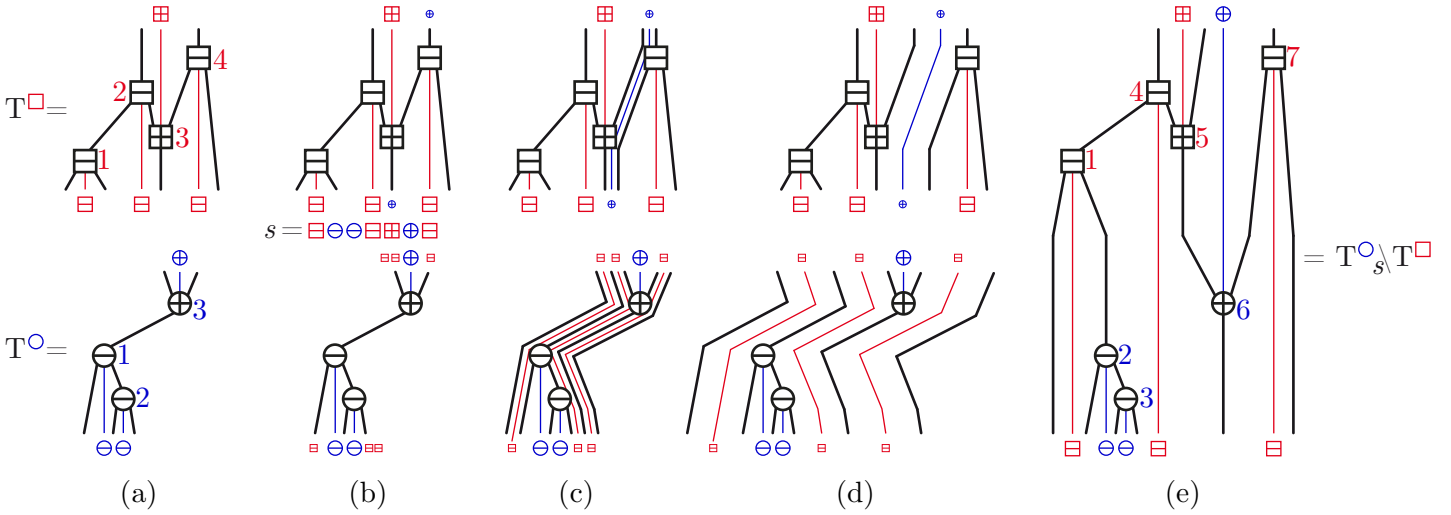


FIGURE 14. (a) The two Cambrian trees T° and T^{\square} . (b) Given the shuffle $s = \square \ominus \ominus \square \square \oplus \square$, the positions of the \square are reported in T° and the positions of the \oplus are reported in T^{\square} . (c) The corresponding laminations. (d) The trees are split according to the laminations. (e) The resulting Cambrian tree $T^{\square} \setminus_s T^{\circ}$.

split T' . This corresponds to the description of $T_s \setminus T'$, where s is the shuffle of the signatures of T and T' given by σ . □

For example, we can compute the product

$$\begin{aligned}
 Q \cdot Q &= G_{12} \cdot G_{213} \\
 &= G_{12435} + G_{13425} + G_{14325} + G_{15324} + G_{23415} + G_{24315} + G_{25314} + G_{34215} + G_{35214} + G_{45213} \\
 &= Q + Q + Q + Q + Q + Q + Q + Q + Q + Q.
 \end{aligned}$$

Note that the 10 resulting Cambrian trees correspond to the 10 possible shuffles of $--$ and $--+$.

COPRODUCT To describe the coproduct of \mathbb{Q} -basis elements of Camb^* , we also use gaps and vertical paths in Cambrian trees. Namely, for a gap γ , we denote by $L(S, \gamma)$ and $R(S, \gamma)$ the left and right Cambrian subtrees of S when split along the path $\lambda(S, \gamma)$. An example is given in Figure 15.

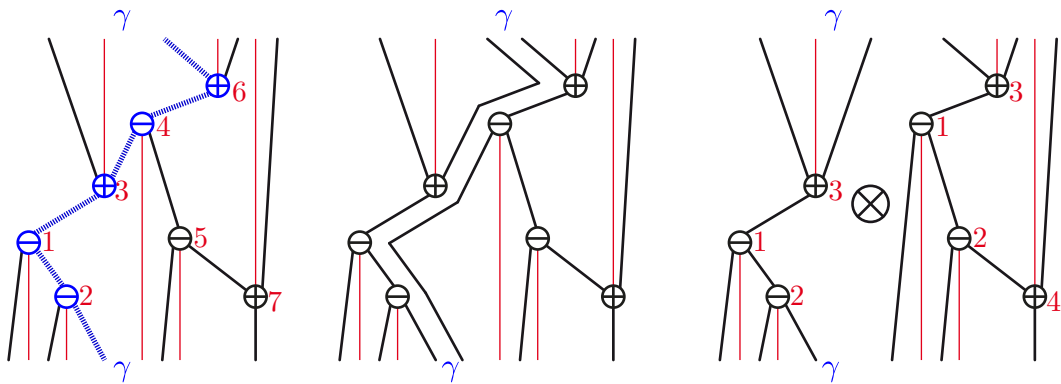


FIGURE 15. A gap γ between 3 and 4 (left) defines a vertical cut (middle) which splits the Cambrian tree (right).

Proposition 30. *For any Cambrian tree S , the coproduct $\Delta \mathbb{Q}_S$ is given by*


$$\Delta \mathbb{Q}_S = \sum_{\gamma} \mathbb{Q}_{L(S,\gamma)} \otimes \mathbb{Q}_{R(S,\gamma)},$$

where γ runs over all gaps between vertices of S .

Proof. Let σ be a linear extension of S and $\tau, \tau' \in \mathfrak{S}_{\pm}$ such that $\sigma \in \tau \sqcup \tau'$. As discussed in Section 1.2.1, τ and τ' respectively appear on the left and right columns of σ . Let γ denote the vertical gap separating τ from τ' . Applying the insertion algorithm to τ and τ' separately then yields the trees $L(S, \gamma)$ and $R(S, \gamma)$. The description follows. \square

For example, we can compute the coproduct

$$\begin{aligned} \Delta \mathbb{Q}_{\begin{array}{c} \text{A} \\ \diagup \quad \diagdown \\ \text{B} \end{array}} &= \Delta \mathbb{G}_{\overline{213}} \\ &= 1 \otimes \mathbb{G}_{\overline{213}} + \mathbb{G}_{\overline{1}} \otimes \mathbb{G}_{\overline{12}} + \mathbb{G}_{\overline{21}} \otimes \mathbb{G}_{\overline{1}} + \mathbb{G}_{\overline{213}} \otimes 1 \\ &= 1 \otimes \mathbb{Q}_{\begin{array}{c} \text{A} \\ \diagup \quad \diagdown \\ \text{B} \end{array}} + \mathbb{Q}_{\begin{array}{c} \text{A} \\ \diagup \\ \text{B} \end{array}} \otimes \mathbb{Q}_{\begin{array}{c} \text{B} \\ \diagdown \\ \text{A} \end{array}} + \mathbb{Q}_{\begin{array}{c} \text{A} \\ \diagdown \\ \text{B} \end{array}} \otimes \mathbb{Q}_{\begin{array}{c} \text{B} \\ \diagup \\ \text{A} \end{array}} + \mathbb{Q}_{\begin{array}{c} \text{A} \\ \diagup \quad \diagdown \\ \text{B} \end{array}} \otimes 1. \end{aligned}$$

Note that the last line can indeed be directly computed using the paths defined by the four possible gaps of the Cambrian tree .

1.2.4. Duality. As proven in [HNT05], the duality $\tau \mapsto \tau^{-1}$ between the Hopf algebras FQSym and FQSym^* induces a duality between the Hopf algebras PBT and PBT^* . That is to say that the composition Ψ of the applications

$$\begin{array}{ccccccc} \text{PBT} & \xleftarrow{\quad} & \text{FQSym} & \xleftarrow{\quad} & \text{FQSym}^* & \xrightarrow{\quad} & \text{PBT}^* \\ & & \mathbb{P}_{\mathbb{T}} \mapsto \sum_{\tau \in \mathcal{L}(\mathbb{T})} \mathbb{F}_{\tau} & & \tau \mapsto \tau^{-1} & & \mathbb{G}_{\tau} \mapsto \mathbb{Q}_{\mathbb{P}(\tau)} \end{array}$$

is an isomorphism between PBT and PBT^* . This property is no longer true for the Cambrian algebra Camb and its dual Camb^* . Namely, the composition Ψ of the applications

$$\begin{array}{ccccccc} \text{Camb} & \xleftarrow{\quad} & \text{FQSym}_{\pm} & \xleftarrow{\quad} & \text{FQSym}_{\pm}^* & \xrightarrow{\quad} & \text{Camb}^* \\ & & \mathbb{P}_{\mathbb{T}} \mapsto \sum_{\tau \in \mathcal{L}(\mathbb{T})} \mathbb{F}_{\tau} & & \mathbb{F}_{\tau} \mapsto \mathbb{G}_{\tau}^{-1} & & \mathbb{G}_{\tau} \mapsto \mathbb{Q}_{\mathbb{P}(\tau)} \end{array}$$

is not an isomorphism. It is indeed not injective as

$$\Psi(\mathbb{P}_{\begin{array}{c} \text{A} \\ \diagup \quad \diagdown \\ \text{B} \end{array}}) = \mathbb{Q}_{\begin{array}{c} \text{A} \\ \diagup \quad \diagdown \\ \text{B} \end{array}} = \Psi(\mathbb{P}_{\begin{array}{c} \text{B} \\ \diagdown \quad \diagup \\ \text{A} \end{array}}).$$

Indeed, their images along the three maps are given by

$$\begin{array}{ccccccc} \mathbb{P}_{\begin{array}{c} \text{A} \\ \diagup \quad \diagdown \\ \text{B} \end{array}} & \mapsto & \mathbb{F}_{\overline{213}} & \mapsto & \mathbb{G}_{\overline{213}} & \mapsto & \mathbb{Q}_{\begin{array}{c} \text{A} \\ \diagup \quad \diagdown \\ \text{B} \end{array}}, \text{ and} \\ \mathbb{P}_{\begin{array}{c} \text{B} \\ \diagdown \quad \diagup \\ \text{A} \end{array}} & \mapsto & \mathbb{F}_{\overline{312}} & \mapsto & \mathbb{G}_{\overline{231}} & \mapsto & \mathbb{Q}_{\begin{array}{c} \text{B} \\ \diagdown \quad \diagup \\ \text{A} \end{array}}. \end{array}$$

1.3. MULTIPLICATIVE BASES

In this section, we define multiplicative bases of Camb and study the indecomposable elements of Camb for these bases. We prove in Sections 1.3.2 and 1.3.3 both structural and enumerative properties of the set of indecomposable elements.

1.3.1. Multiplicative bases and indecomposable elements. For a Cambrian tree \mathbb{T} , we define

$$\mathbb{E}^{\mathbb{T}} := \sum_{\mathbb{T}' \leq \mathbb{T}} \mathbb{P}_{\mathbb{T}'} \quad \text{and} \quad \mathbb{H}^{\mathbb{T}} := \sum_{\mathbb{T}' \leq \mathbb{T}} \mathbb{P}_{\mathbb{T}'}$$

To describe the product of two elements of the \mathbb{E} - or \mathbb{H} -basis, remember that the Cambrian trees

$$\mathbb{T} \nearrow \bar{\mathbb{T}}' \quad \text{and} \quad \mathbb{T} \nwarrow \bar{\mathbb{T}}'$$

are defined to be the trees obtained by shifting all labels of \mathbb{T}' and grafting for the first one the rightmost outgoing leaf of \mathbb{T} on the leftmost incoming leaf of \mathbb{T}' , and for the second one the rightmost incoming leaf of \mathbb{T} on the leftmost outgoing leaf of \mathbb{T}' . Examples are given in Figure 12.

Proposition 31. $(\mathbb{E}^T)_{T \in \text{Camb}}$ and $(\mathbb{H}^T)_{T \in \text{Camb}}$ are multiplicative bases of Camb :

$$\mathbb{E}^T \cdot \mathbb{E}^{T'} = \mathbb{E}^{T \nearrow T'} \quad \text{and} \quad \mathbb{H}^T \cdot \mathbb{H}^{T'} = \mathbb{H}^{T \nwarrow T'}.$$

Proof. Let ω_T denote the maximal linear extension of T in weak order. Since $\{\mathcal{L}(\tilde{T}) \mid \tilde{T} \leq T\}$ partitions the weak order interval $[12 \cdots n, \omega_T]$, we have

$$\mathbb{H}^T = \sum_{\tilde{T} \leq T} \mathbb{P}_{\tilde{T}} = \sum_{\tilde{T} \leq T} \sum_{\tau \in \mathcal{L}(\tilde{T})} \mathbb{F}_\tau = \sum_{\tau \leq \omega_T} \mathbb{F}_\tau.$$

Since the shuffle product of two intervals of the weak order is an interval of the weak order, the product $\mathbb{H}^T \cdot \mathbb{H}^{T'}$ is the sum of \mathbb{F}_τ over the interval

$$[12 \cdots n, \omega_T] \sqcup [12 \cdots n', \omega_{T'}] = [12 \cdots (n+n'), \bar{\omega}_{T'} \omega_T].$$

The result thus follows from the fact that

$$\mathbf{P}(\bar{\omega}_{T'} \omega_T) = T \nwarrow_{\bar{T}'}.$$

The proof is symmetric for \mathbb{E}^T , replacing lower interval and $[12 \cdots n, \omega_T]$ by the upper interval $[\mu_T, n \cdots 21]$. \square

As the multiplicative bases $(\mathbb{E}^T)_{T \in \text{Camb}}$ and $(\mathbb{H}^T)_{T \in \text{Camb}}$ have symmetric properties, we focus our analysis on the \mathbb{E} -basis. The reader is invited to translate the results below to the \mathbb{H} -basis. We consider multiplicative decomposability. Remember that an *edge cut* in a Cambrian tree S is the ordered partition $(X \parallel Y)$ of the vertices of S into the set X of vertices in the source set and the set Y of vertices in the target set of an oriented edge e of S .

Proposition 32. *The following properties are equivalent for a Cambrian tree S :*

- (i) \mathbb{E}^S can be decomposed into a product $\mathbb{E}^S = \mathbb{E}^T \cdot \mathbb{E}^{T'}$ for non-empty Cambrian trees T, T' ;
- (ii) $([k] \parallel [n] \setminus [k])$ is an edge cut of S for some $k \in [n-1]$;
- (iii) at least one linear extension τ of S is decomposable, i.e. $\tau([k]) = [k]$ for some $k \in [n]$.

The tree S is then called **\mathbb{E} -decomposable** and the edge cut $([k] \parallel [n] \setminus [k])$ is called **splitting**.

Proof. The equivalence (i) \iff (ii) is an immediate consequence of the description of the product $\mathbb{E}^T \cdot \mathbb{E}^{T'}$ in Proposition 31. The implication (ii) \implies (iii) follows from the fact that for any cut $(X \parallel Y)$ of a directed acyclic graph G , there exists a linear extension of G which starts with X and finishes with Y . Reciprocally, if τ is a decomposable linear extension of S , then the insertion algorithm creates two blocks and necessarily relates the bottom-left block to the top-right block by a splitting edge. \square

For example, Figure 12 shows that $\mathbf{P}(2\bar{7}51\bar{3}4\bar{6})$ is both \mathbb{E} - and \mathbb{H} -decomposable. In the remaining of this section, we study structural and enumerative properties of \mathbb{E} -indecomposable elements of Camb . We denote by Ind_ε the set of \mathbb{E} -indecomposable elements of $\text{Camb}(\varepsilon)$.

Example 33. For $\varepsilon = (-)^n$, the \mathbb{E} -indecomposable ε -Cambrian trees are *right-tilting* binary trees, i.e. binary trees whose root has no left child. Similarly, for $\varepsilon = (+)^n$, the \mathbb{E} -indecomposable ε -Cambrian trees are *left-tilting* binary trees oriented upwards. See Figure 16 for illustrations.

1.3.2. Structural properties. The objective of this section is to prove the following property of the \mathbb{E} -indecomposable elements of $\text{Camb}(\varepsilon)$.

Proposition 34. *For any signature $\varepsilon \in \pm^n$, the set Ind_ε of \mathbb{E} -indecomposable ε -Cambrian trees forms a principal upper ideal of the ε -Cambrian lattice.*

To prove this statement, we need the following result.

Lemma 35. *Let T be a ε -Cambrian tree, let $i \rightarrow j$ be an edge of T with $i < j$, and let T' be the ε -Cambrian tree obtained by rotating $i \rightarrow j$ in T . Then*

- (i) if T is \mathbb{E} -indecomposable, then so is T' ;
- (ii) if T is \mathbb{E} -decomposable while T' is not, then $\varepsilon_i = +$ or $i = 1$, and $\varepsilon_j = -$ or $j = n$.

Proof. As observed in Proposition 18, the Cambrian trees T and T' have the same edge cuts, except the cut defined by edge $i \rightarrow j$. Using notations of Figure 7, the edge cut $C := (i \cup L \cup B \parallel j \cup R \cup A)$ of T is replaced by the edge cut $C' := (j \cup R \cup B \parallel i \cup L \cup A)$ of T' . Since $i < j$, the edge cut C' cannot be splitting. Therefore, T' is always \mathbb{E} -indecomposable when T is \mathbb{E} -indecomposable.

Assume conversely that T is \mathbb{E} -decomposable while T' is not. This implies that C is splitting while C' is not. Since C is splitting we have $i \cup L \cup B < j \cup R \cup A$ (where we write $X < Y$ if $x < y$ for all $x \in X$ and $y \in Y$). If $\varepsilon_i = -$, then $L < i < B$, and thus $L < \{i, j\} \cup R \cup A \cup B$. If moreover $1 < i$, then $1 < \{i, j\} \cup R \cup A \cup B$ and thus $1 \in L \neq \emptyset$. This would imply that the cut of T' defined by the edge $L \rightarrow i$ would be splitting. Contradiction. We prove similarly that $\varepsilon_j = -$ or $j = n$. \square

Proof or Proposition 34. We already know from Lemma 35 (i) that Ind_ε is an upper set of the ε -Cambrian lattice. To see that this upper set is a principal upper ideal, we characterize the unique \mathbb{E} -indecomposable ε -Cambrian tree T_\bullet whose decreasing rotations all create a splitting edge cut. We proceed in three steps.

CLAIM A All negative vertices $i > 1$ of T_\bullet have no right child, while all positive vertices $j < n$ of T_\bullet have no left child.

Proof. Assume by means of contradiction that a negative vertex $i > 1$ has a right child j . Let T be the Cambrian tree obtained by rotation of the edge $i \leftarrow j$ in T_\bullet . Since this rotation is decreasing (because $i < j$), T is decomposable while T_\bullet is not. This contradicts Lemma 35 (ii).

Claim A ensures that the Cambrian tree T_\bullet is a path with additional leaves incoming at negative vertices and outgoing at positive vertices. Therefore, T_\bullet admits a unique linear extension τ_\bullet . The next two claims determine τ_\bullet and thus $T_\bullet = \mathbf{P}(\tau_\bullet)$.

As vertex 1 has no left child and vertex n has no right child, we consider that 1 behaves as a positive vertex and n behaves as a negative vertex. We thus define $N := \{n_1 < \dots < n_{N-1} < n_N = n\}$ and $P := \{1 = p_1 < p_2 < \dots < p_P\}$, where $n_1 < \dots < n_{N-1}$ are the negative vertices and $p_2 < \dots < p_P$ are the positive vertices among $\{2, \dots, n-1\}$.

CLAIM B The sets N and P both appear in increasing order in τ_\bullet .

Proof. If i appears in τ_\bullet before $j \in N$, then i lies in the left child of j (since j has no right child), so that $i < j$. In particular, N is sorted in τ_\bullet . The proof is symmetric for positive vertices.

CLAIM C In τ_\bullet , vertex p_k appears immediately after the first vertex in N larger than p_{k+1} .

Proof. Let n_ℓ denote the first vertex in N larger than p_{k+1} . If p_k appears before n_ℓ in τ_\bullet , then τ_\bullet is a decomposable permutation (since $\tau([p_{k+1}-1]) = [p_{k+1}-1]$). If p_k appears after $n_{\ell+1}$ in τ_\bullet , then the Cambrian tree obtained by rotation of the incoming edge at p_k in T_\bullet remains indecomposable. Therefore, p_k appears precisely in between n_ℓ and $n_{\ell+1}$. \square

For example, Figure 16 illustrates the generator of the principal upper ideals of \mathbb{E} -indecomposable ε -Cambrian trees for $\varepsilon = -+--++$, $\varepsilon = (-)^7$, and $\varepsilon = (+)^7$. The last two are right- and left-tilting trees respectively.

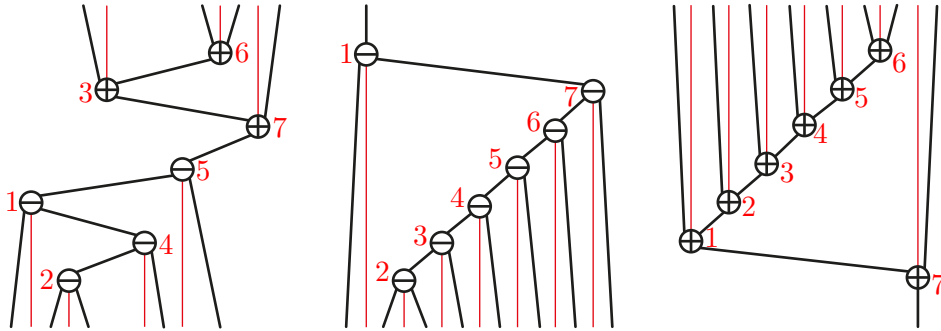


FIGURE 16. The generators of the principal upper ideals of \mathbb{E} -indecomposable ε -Cambrian trees for $\varepsilon = -+--++$ (left), $\varepsilon = (-)^7$ (middle), $\varepsilon = (+)^7$ (right).

1.3.3. Enumerative properties. We now consider enumerative properties of \mathbb{E} -indecomposable elements. We want to show that the number of \mathbb{E} -indecomposable ε -Cambrian trees is independent of the signature ε .

Proposition 36. *For any signature $\varepsilon \in \pm^n$, there are C_{n-1} \mathbb{E} -indecomposable ε -Cambrian trees. Therefore, there are $2^n C_{n-1}$ \mathbb{E} -indecomposable Cambrian trees on n vertices.*

This result is immediate for the signature $\varepsilon = (-)^n$ as \mathbb{E} -indecomposable elements are right-tilting binary trees (see Example 33), which are clearly counted by the Catalan number C_{n-1} . To show Proposition 36, we study the behavior of Cambrian trees and their decompositions under local transformations on signatures of $[n]$. We believe that these transformations are interesting *per se*. For example, they provide an alternative proof that there are C_n ε -Cambrian trees for any signature $\varepsilon \in \pm^n$.

Let $\chi_0 : \pm^n \rightarrow \pm^n$ and $\chi_n : \pm^n \rightarrow \pm^n$ denote the transformations which switch the signs of 1 and n , respectively. Denote by $\Psi_0(T)$ and $\Psi_n(T)$ the trees obtained from a Cambrian tree T by changing the direction of the leftmost and rightmost leaf of T respectively. For $i \in [n-1]$, let $\chi_i : \pm^n \rightarrow \pm^n$ denote the transformation which switches the signs at positions i and $i+1$. The transformation $\varepsilon \rightarrow \chi_i(\varepsilon)$ is only relevant when $\varepsilon_i \neq \varepsilon_{i+1}$. In this situation, we denote by $\Psi_i(T)$ the tree obtained from a ε -Cambrian tree T by

- reversing the arc from the positive to the negative vertex of $\{i, i+1\}$ if it exists,
- exchanging the labels of i and $i+1$ otherwise.

This transformation is illustrated on Figure 17 when $\varepsilon_i = +$ and $\varepsilon_{i+1} = -$.

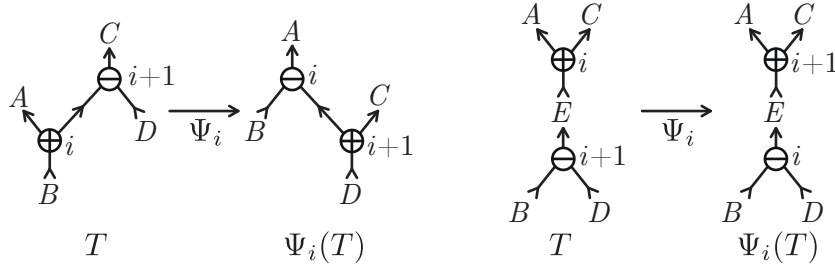


FIGURE 17. The transformation Ψ_i when $\varepsilon_i = +$ and $\varepsilon_{i+1} = -$. The tree $\Psi_i(T)$ is obtained by reversing the arc from i to $i+1$ if it exists (left), and just exchanging the labels of i and $i+1$ otherwise (right).

To show that Ψ_i transforms ε -Cambrian trees to $\chi_i(\varepsilon)$ -Cambrian trees and preserves the number of \mathbb{E} -indecomposable elements, we need the following lemma. Note that this lemma also explains why Figure 17 covers all possibilities when $\varepsilon_i = +$ and $\varepsilon_{i+1} = -$.

Lemma 37. *If $\varepsilon_i = +$ and $\varepsilon_{i+1} = -$, then the following assertions are equivalent for a ε -Cambrian tree T :*

- $([i] \parallel [n] \setminus [i])$ is an edge cut of T ;
- i is smaller than $i+1$ in T ;
- i is in the left subtree of $i+1$ and $i+1$ is in the right subtree of i ;
- i is the left child of $i+1$ and $i+1$ is the right parent of i .

A similar statement holds in the case when $\varepsilon_i = -$ and $\varepsilon_{i+1} = +$.

Proof. Since i and $i+1$ are comparable in T (see Section 1.1.6), the fact that $([i] \parallel [n] \setminus [i])$ is an edge cut of T implies that i is smaller than $i+1$ in T . This shows that (i) \Rightarrow (ii).

If i is smaller than $i+1$ in T , then i is in a subtree of $i+1$, and thus in the left one, and similarly, $i+1$ is in the right subtree of i . This shows that (ii) \Rightarrow (iii).

Assume now that i is in the left subtree of $i+1$ and $i+1$ is in the right subtree of i , and consider the path from i to $i+1$ in T . Since it lies in the right subtree of i and in the left subtree of $i+1$, any label along this path should be greater than i and smaller than $i+1$. This path is thus a single arc. This shows that (iii) \Rightarrow (iv).

Finally, assume that i is the left child of $i + 1$ and $i + 1$ is the right parent of i in T . Then the cut corresponding to the arc e of T from i to $i + 1$ is $([i] \parallel [n] \setminus [i])$. Indeed, all elements in the source of e are in the left subtree and thus smaller than $i + 1$, while all elements in the target of e are in the right subtree and thus greater than i . This shows that (iv) \Rightarrow (i). \square

Lemma 38. *For $0 \leq i \leq n$, the map Ψ_i defines a bijection from ε -Cambrian trees to $\chi_i(\varepsilon)$ -Cambrian trees and preserves the number of \mathbb{E} -indecomposable elements.*

Proof. The result is immediate for $i = 0$ and $i = n$. Assume thus that $i \in [n - 1]$ and that $\varepsilon_i = +$ while $\varepsilon_{i+1} = -$. We first prove that Ψ_i sends ε -Cambrian trees to $\chi_i(\varepsilon)$ -Cambrian trees. It clearly transforms trees to trees. To see that $\Psi_i(T)$ is $\chi_i(\varepsilon)$ -Cambrian, we distinguish two cases:

- Figure 17 (left) illustrates the case when T has an arc in from i to $i + 1$. All labels in B are smaller than i since they are distinct from i and in the left subtree of $i + 1$, and all labels in the right subtree of i in $\Psi_i(T)$ are greater than i since they were in the right subtree of i in T . Therefore, the labels around vertex i of $\Psi_i(T)$ respect the Cambrian rules. We argue similarly around $i + 1$. All other vertices have the same signs and subtrees.
- Figure 17 (right) illustrates the case when T has no arc in from i to $i + 1$. All labels in B (resp. D) are smaller (resp. greater) than i since they are distinct from i and in the left (resp. right) subtree of $i + 1$, so the labels around vertex i of $\Psi_i(T)$ respect the Cambrian rules. We argue similarly around $i + 1$. All other vertices have the same signs and subtrees.

Alternatively, it is also easy to see Ψ_i transforms ε -Cambrian trees to $\chi_i(\varepsilon)$ -Cambrian trees using the interpretation of Cambrian trees as dual trees of triangulations (see Remark 4).

Although Ψ_i does not preserve \mathbb{E} -indecomposable elements, we now check that Ψ_i preserves the number of \mathbb{E} -indecomposable elements. Write $\varepsilon = \underline{\varepsilon}\bar{\varepsilon}$ with $\underline{\varepsilon} : [i] \rightarrow \{\pm\}$ and $\bar{\varepsilon} : [n] \setminus [i] \rightarrow \{\pm\}$, and let $\underline{I} = |\text{Ind}_{\underline{\varepsilon}}|$ and $\bar{I} = |\text{Ind}_{\bar{\varepsilon}}|$. We claim that

- the map Ψ_i transforms precisely $\underline{I} \cdot \bar{I}$ \mathbb{E} -decomposable ε -Cambrian trees to \mathbb{E} -indecomposable $\chi_i(\varepsilon)$ -Cambrian trees. Indeed, T is \mathbb{E} -decomposable while $\Psi_i(T)$ is \mathbb{E} -indecomposable if and only if T has an arc from i to $i + 1$ whose source and target subtrees are \mathbb{E} -indecomposable $\underline{\varepsilon}$ - and $\bar{\varepsilon}$ -Cambrian trees, respectively.
- the map Ψ_i transforms precisely $\underline{I} \cdot \bar{I}$ \mathbb{E} -indecomposable ε -Cambrian trees to \mathbb{E} -decomposable $\chi_i(\varepsilon)$ -Cambrian trees. Indeed, assume that T is \mathbb{E} -indecomposable while $\Psi_i(T)$ is \mathbb{E} -decomposable. We claim that $([i] \parallel [n] \setminus [i])$ is the only splitting edge cut of $\Psi_i(T)$. Indeed, for $j \neq i$, both i and $i + 1$ belong either to $[j]$ or to $[n] \setminus [j]$, and $([j] \parallel [n] \setminus [j])$ is an edge cut of $\Psi_i(T)$ if and only if it is an edge cut of T . Moreover, the $\underline{\varepsilon}$ - and $\bar{\varepsilon}$ -Cambrian trees \underline{S} and \bar{S} induced by $\Psi_i(T)$ on $[i]$ and $[n] \setminus [i]$ are both \mathbb{E} -indecomposable. Otherwise, a splitting edge cut $([j] \parallel [i] \setminus [j])$ of \underline{S} would define a splitting edge cut $([j] \parallel [n] \setminus [j])$ of $\Psi_i(T)$. Conversely, if \underline{S} and \bar{S} are both \mathbb{E} -indecomposable, then so is T .

We conclude that Ψ_i globally preserves the number of \mathbb{E} -indecomposable Cambrian trees. \square

Proof of Proposition 36. Starting from the fully negative signature $(-)^n$, we can reach any signature ε by the transformations $\chi_0, \dots, \chi_{n-1}$: we can make positive signs appear on vertex 1 (using the map χ_0) and make these positive signs travel towards their final position in ε (using the maps χ_i). More precisely, if $p_1 < \dots < p_P$ denote the positions of the positive signs of ε , then $\varepsilon = (\prod_{j \in [P]} \chi_{p_j} \circ \chi_{p_{j-1}} \circ \dots \circ \chi_{p_1} \circ \chi_0)((-)^n)$. The result thus follows from Lemma 38. \square

Proposition 39. *The Cambrian algebra Camb is free.*

Proof. As the generating function $B(u)$ of the Catalan numbers satisfies the functional equation $B(u) = 1 + uB(u)^2$, we obtain by substitution $u = 2t$ that

$$\frac{1}{1 - \sum_{n \geq 1} 2^n C_{n-1} t^n} = \sum_{n \geq 0} 2^n C_n t^n.$$

The result immediately follows from Proposition 36. \square

Part 2. The Baxter-Cambrian Hopf Algebra

2.1. TWIN CAMBRIAN TREES

We now consider twin Cambrian trees and the resulting Baxter-Cambrian algebra. It provides a straightforward generalization to the Cambrian setting of the work of S. Law and N. Reading on quadrangulations [LR12] and S. Giraudo on twin binary trees [Gir12]. The bases of these algebras are counted by the Baxter numbers. In Section 2.1.5 we provide references for the various Baxter families and their bijective correspondences, and we discuss the Cambrian counterpart of these numbers. Definitions and combinatorial properties of twin Cambrian trees are given in this section, while the algebraic aspects are treated in the next section.

2.1.1. Twin Cambrian trees. This section deals with the following pairs of Cambrian trees.

Definition 40. Two ε -Cambrian trees T_\circ, T_\bullet are **twin** if the union $T_\circ \updownarrow T_\bullet$ of T_\circ with the reverse of T_\bullet (reversing the orientations of all edges) is acyclic.

Definition 41. Let T_\circ, T_\bullet be two leveled ε -Cambrian trees with labelings p_\circ, q_\circ and p_\bullet, q_\bullet respectively. We say that they are **twin** if $q_\circ(p_\circ^{-1}(i)) = n - q_\bullet(p_\bullet^{-1}(i))$ for all $i \in [n]$. In other words, when labeled as Cambrian trees, the bottom-up order of the vertices of T_\circ and T_\bullet are opposite.

Examples of twin Cambrian trees and twin leveled Cambrian trees are represented in Figure 18. Note that twin leveled Cambrian trees are twin Cambrian trees T_\circ, T_\bullet endowed with a linear extension of the transitive closure of $T_\circ \updownarrow T_\bullet$.

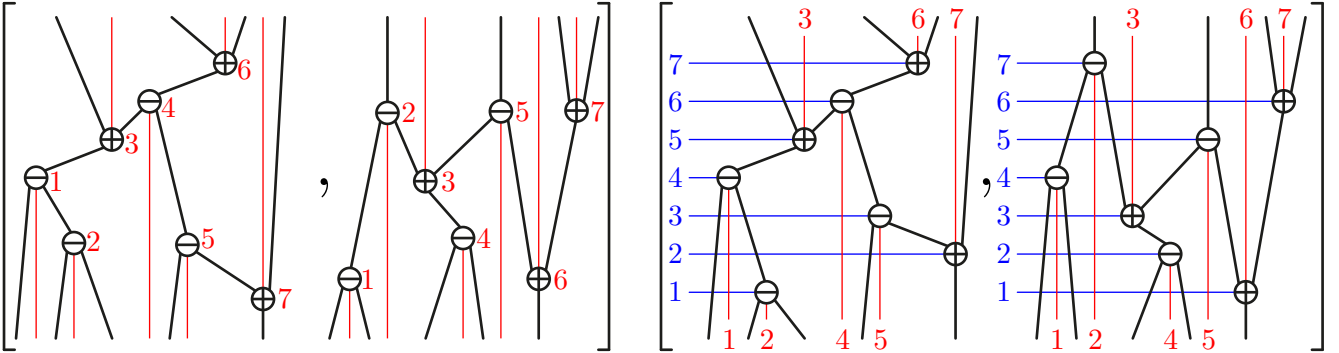


FIGURE 18. A pair of twin Cambrian trees (left), and a pair of twin leveled Cambrian trees (right).

If T_\circ, T_\bullet are two ε -Cambrian trees, they necessarily have opposite canopy (see Section 1.1.6), meaning that $\mathbf{can}(T_\circ)_i = -\mathbf{can}(T_\bullet)_i$ for all $i \in [n-1]$. The reciprocal statement for the constant signature $(-)^n$ is proved by S. Giraudo in [Gir12].

Proposition 42 ([Gir12]). *Two binary trees are twin if and only if they have opposite canopy.*

We conjecture that this statement holds for general signatures. Consider two ε -Cambrian trees T_\circ, T_\bullet with opposite canopies. It is easy to show that $T_\circ \updownarrow T_\bullet$ cannot have trivial cycles, meaning that T_\circ and T_\bullet cannot both have a path from i to j for $i \neq j$. To prove that $T_\circ \updownarrow T_\bullet$ has no cycles at all, a good method is to design an algorithm to extract a linear extension of $T_\circ \updownarrow T_\bullet$. This approach was used in [Gir12] for the signature $(-)^n$. In this situation, it is clear that the root of T_\bullet is minimal in T_\circ (by the canopy assumption), and we therefore pick it as the first value of a linear extension of $T_\circ \updownarrow T_\bullet$. The remaining of the linear extension is constructed inductively. In the general situation, it turns out that not all maximums in T_\bullet are minimums in T_\circ (and reciprocally). It is thus not clear how to choose the first value of a linear extension of $T_\circ \updownarrow T_\bullet$.

Remark 43 (Reversing T_\bullet). It is sometimes useful to reverse the second tree T_\bullet in a pair $[T_\circ, T_\bullet]$ of twin Cambrian trees. The resulting Cambrian trees have opposite signature and their union is acyclic. In this section, we have chosen the orientation of Definition 40 to fit with the notations and results in [Gir12]. We will have to switch to the opposite convention in Section 2.3 when we will extend our results on twin Cambrian trees to arbitrary tuples of Cambrian trees.

2.1.2. Baxter-Cambrian correspondence. We obtain the *Baxter-Cambrian correspondence* between permutations of \mathfrak{S}^ε and pairs of twin leveled ε -Cambrian trees by inserting with the map Θ from Section 1.1.2 a permutation $\tau = \tau_1 \cdots \tau_n \in \mathfrak{S}^\varepsilon$ and its *mirror* $\overleftarrow{\tau} = \tau_n \cdots \tau_1 \in \mathfrak{S}^\varepsilon$.

Proposition 44. *The map Θ^\natural defined by $\Theta^\natural(\tau) = [\Theta(\tau), \Theta(\overleftarrow{\tau})]$ is a bijection from signed permutations to pairs of twin leveled Cambrian trees.*

Proof. If $p, q : V \rightarrow [n]$ denote the Cambrian and increasing labelings of the Cambrian tree $\Theta(\tau)$, then $\tau = q \circ p$. This yields that the leveled ε -Cambrian trees $\Theta(\tau)$ and $\Theta(\overleftarrow{\tau})$ are twin and the map Θ^\natural is bijective. \square

As for Cambrian trees, we focus on the \mathbf{P}^\natural -symbol of this correspondence.

Proposition 45. *The map \mathbf{P}^\natural defined by $\mathbf{P}^\natural(\tau) = [\mathbf{P}(\tau), \mathbf{P}(\overleftarrow{\tau})]$ is a surjection from signed permutations to pairs of twin Cambrian trees.*

Proof. The fiber $(\mathbf{P}^\natural)^{-1}([\mathbf{T}_\circ, \mathbf{T}_\bullet])$ of a pair of twin ε -Cambrian trees $\mathbf{T}_\circ, \mathbf{T}_\bullet$ is the set $\mathcal{L}(\mathbf{T}_\circ \downarrow \mathbf{T}_\bullet)$ of linear extensions of the graph $\mathbf{T}_\circ \downarrow \mathbf{T}_\bullet$. This set is non-empty since $\mathbf{T}_\circ \downarrow \mathbf{T}_\bullet$ is acyclic by definition of twin Cambrian trees. \square

2.1.3. Baxter-Cambrian congruence. We now characterize by a congruence relation the signed permutations $\tau \in \mathfrak{S}^\varepsilon$ which have the same \mathbf{P}^\natural -symbol.

Definition 46. *For a signature $\varepsilon \in \pm^n$, the ε -Baxter-Cambrian congruence is the equivalence relation on \mathfrak{S}^ε defined as the transitive closure of the rewriting rules*

$$\begin{aligned} UbVadWcX &\equiv_\varepsilon^1 UbVdaWcX && \text{if } a < b, c < d \text{ and } \varepsilon_b = \varepsilon_c, \\ UbVcWadX &\equiv_\varepsilon^1 UbVcWdaX && \text{if } a < b, c < d \text{ and } \varepsilon_b \neq \varepsilon_c, \\ UadVbWcX &\equiv_\varepsilon^1 UdaVbWcX && \text{if } a < b, c < d \text{ and } \varepsilon_b \neq \varepsilon_c, \end{aligned}$$

where a, b, c, d are elements of $[n]$ while U, V, W, X are words on $[n]$. The *Baxter-Cambrian congruence* is the equivalence relation on all signed permutations \mathfrak{S}_\pm obtained as the union of all ε -Baxter-Cambrian congruences:

$$\equiv^\natural := \bigsqcup_{\substack{n \in \mathbb{N} \\ \varepsilon \in \pm^n}} \equiv_\varepsilon^1.$$

Proposition 47. *Two signed permutations $\tau, \tau' \in \mathfrak{S}^\varepsilon$ are ε -Baxter-Cambrian congruent if and only if they have the same \mathbf{P}^\natural -symbol:*

$$\tau \equiv_\varepsilon^1 \tau' \iff \mathbf{P}^\natural(\tau) = \mathbf{P}^\natural(\tau').$$

Proof. The proof of this proposition consists essentially in seeing that $\mathbf{P}^\natural(\tau) = \mathbf{P}^\natural(\tau')$ if and only if $\tau \equiv_\varepsilon^1 \tau'$ and $\overleftarrow{\tau} \equiv_\varepsilon^1 \overleftarrow{\tau}'$ (by definition of \mathbf{P}^\natural). The definition of the ε -Baxter-Cambrian equivalence \equiv_ε^1 is exactly the translation of this observation in terms of rewriting rules. \square

Proposition 48. *The ε -Baxter-Cambrian class indexed by a pair $[\mathbf{T}_\circ, \mathbf{T}_\bullet]$ of twin ε -Cambrian trees is the intersection of the ε -Cambrian class indexed by \mathbf{T}_\circ with the $(-\varepsilon)$ -Cambrian class indexed by the reverse of \mathbf{T}_\bullet .*

Proof. The ε -Baxter-Cambrian class indexed by $[\mathbf{T}_\circ, \mathbf{T}_\bullet]$ is the set of linear extensions of $\mathbf{T}_\circ \downarrow \mathbf{T}_\bullet$, i.e. of permutations which are both linear extensions of \mathbf{T}_\circ and linear extensions of the reverse of \mathbf{T}_\bullet . The former form the ε -Cambrian class indexed by \mathbf{T}_\circ while the latter form the $(-\varepsilon)$ -Cambrian class indexed by the reverse of \mathbf{T}_\bullet . This is illustrated in Figure 19. \square

2.1.4. Rotations and Baxter-Cambrian lattices. We now present the rotation operation on pairs of twin ε -Cambrian trees.

Definition 49. *Let $[\mathbf{T}_\circ, \mathbf{T}_\bullet]$ be a pair of ε -Cambrian trees and $i \rightarrow j$ be an edge of $\mathbf{T}_\circ \downarrow \mathbf{T}_\bullet$. We say that the edge $i \rightarrow j$ is *rotatable* if*

- either $i \rightarrow j$ is an edge in \mathbf{T}_\circ and $j \rightarrow i$ is an edge in \mathbf{T}_\bullet ,
- or $i \rightarrow j$ is an edge in \mathbf{T}_\circ while i and j are incomparable in \mathbf{T}_\bullet ,
- or i and j are incomparable in \mathbf{T}_\circ while $j \rightarrow i$ is an edge in \mathbf{T}_\bullet .

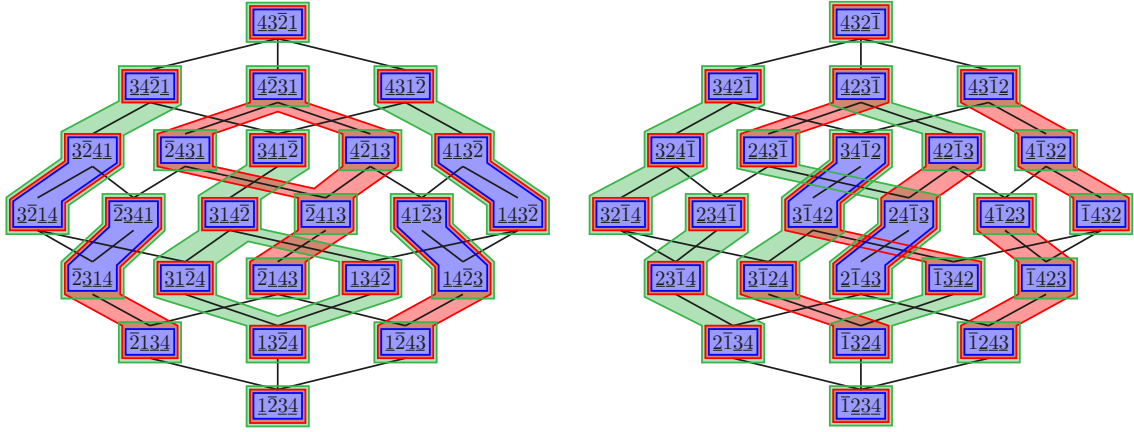


FIGURE 19. The Baxter-Cambrian classes of \equiv_{ε}^1 (blue) are the intersections of the Cambrian classes of \equiv_{ε} (red) and $\equiv_{-\varepsilon}$ (green). Illustrated for the signatures $\varepsilon = -+---$ (left) and $\varepsilon = +----$ (right).

If $i \rightarrow j$ is rotatable in $[T_{\circ}, T_{\bullet}]$, its **rotation** transforms $[T_{\circ}, T_{\bullet}]$ to the pair of trees $[T'_{\circ}, T'_{\bullet}]$, where

- T'_{\circ} is obtained by rotation of $i \rightarrow j$ in T_{\circ} if possible and $T'_{\circ} = T_{\circ}$ otherwise, and
- T'_{\bullet} is obtained by rotation of $j \rightarrow i$ in T_{\bullet} if possible and $T'_{\bullet} = T_{\bullet}$ otherwise.

Proposition 50. *Rotating a rotatable edge $i \rightarrow j$ in a pair $[T_{\circ}, T_{\bullet}]$ of twin ε -Cambrian trees yields a pair $[T'_{\circ}, T'_{\bullet}]$ of twin ε -Cambrian trees.*

Proof. By Proposition 18, the trees T_{\circ}, T_{\bullet} are ε -Cambrian trees. To see that they are twins, observe that switching i and j in a linear extension of $T_{\circ} \Downarrow T_{\bullet}$ yields a linear extension of $T'_{\circ} \Downarrow T'_{\bullet}$. \square

Remark 51 (Number of rotatable edges). Note that a pair $[T_{\circ}, T_{\bullet}]$ of ε -Cambrian trees has always at least $n - 1$ rotatable edges. This will be immediate from the considerations of Section 2.1.6.

Consider the **increasing rotation graph** whose vertices are pairs of twin ε -Cambrian trees and whose arcs are increasing rotations $[T_{\circ}, T_{\bullet}] \rightarrow [T'_{\circ}, T'_{\bullet}]$, i.e. for which $i < j$ in Definition 49. This graph is illustrated on Figure 20 for the signatures $\varepsilon = -+---$ and $\varepsilon = +----$.

Proposition 52. *For any cover relation $\tau < \tau'$ in the weak order on $\mathfrak{S}^{\varepsilon}$, either $\mathbf{P}^1(\tau) = \mathbf{P}^1(\tau')$ or $\mathbf{P}^1(\tau) \rightarrow \mathbf{P}^1(\tau')$ in the increasing rotation graph.*

Proof. Let $i, j \in [n]$ be such that τ' is obtained from τ by switching two consecutive values ij to ji . If i and j are incomparable in $\mathbf{P}(\tau)$, then $\mathbf{P}(\tau) = \mathbf{P}(\tau')$. Otherwise, there is an edge $i \rightarrow j$ in $\mathbf{P}(\tau)$, and $\mathbf{P}(\tau')$ is obtained by rotating $i \rightarrow j$ in $\mathbf{P}(\tau)$. The same discussion is valid for the trees $\mathbf{P}(\overleftarrow{\tau})$ and $\mathbf{P}(\overleftarrow{\tau}')$ and edge $j \rightarrow i$. The result immediately follows. \square

It follows that the increasing rotation graph on pairs of twin ε -Cambrian trees is acyclic and we call **ε -Baxter-Cambrian poset** its transitive closure. In other words, the previous statement says that the map \mathbf{P}^1 defines a poset homomorphism from the weak order on $\mathfrak{S}^{\varepsilon}$ to the ε -Baxter-Cambrian poset. The following statement extends the results of N. Reading [Rea06] on Cambrian lattices and S. Law and N. Reading [LR12] on the lattice of diagonal rectangulations.

Proposition 53. *The ε -Baxter-Cambrian poset is a lattice quotient of the weak order on $\mathfrak{S}^{\varepsilon}$.*

Proof. By Proposition 48, the ε -Baxter-Cambrian congruence is the intersection of two Cambrian congruences. The statement follows since the Cambrian congruences are lattice congruences of the weak order [Rea06] and an intersection of lattice congruences is a lattice congruence. \square

Remark 54 (Cambrian vs. Baxter-Cambrian lattices). Using the definition of Θ^1 , we also notice that the ε -Cambrian classes are unions of ε -Baxter-Cambrian classes, therefore the Cambrian lattice is a lattice quotient of the Baxter-Cambrian lattice. Figure 21 illustrates the Baxter-Cambrian, Cambrian, and boolean congruence classes on the weak orders of $\mathfrak{S}_{\varepsilon}$ for the signatures $\varepsilon = -+---$ and $\varepsilon = +----$.

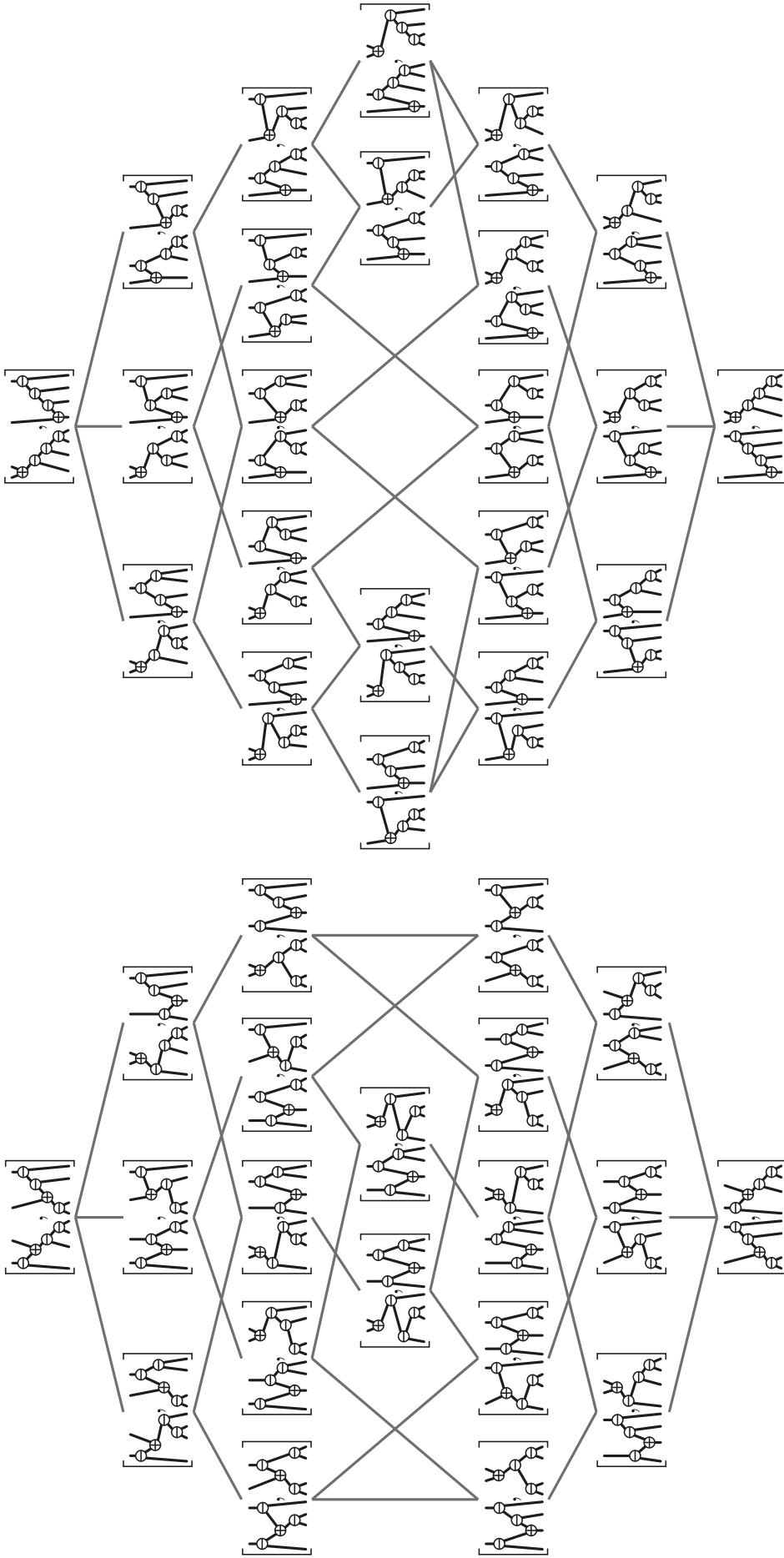


FIGURE 20. The ε -Baxter-Cambrian lattices on pairs of twin ε -Cambrian trees, for the signatures $\varepsilon = -+---$ (left) and $\varepsilon = +----$ (right).

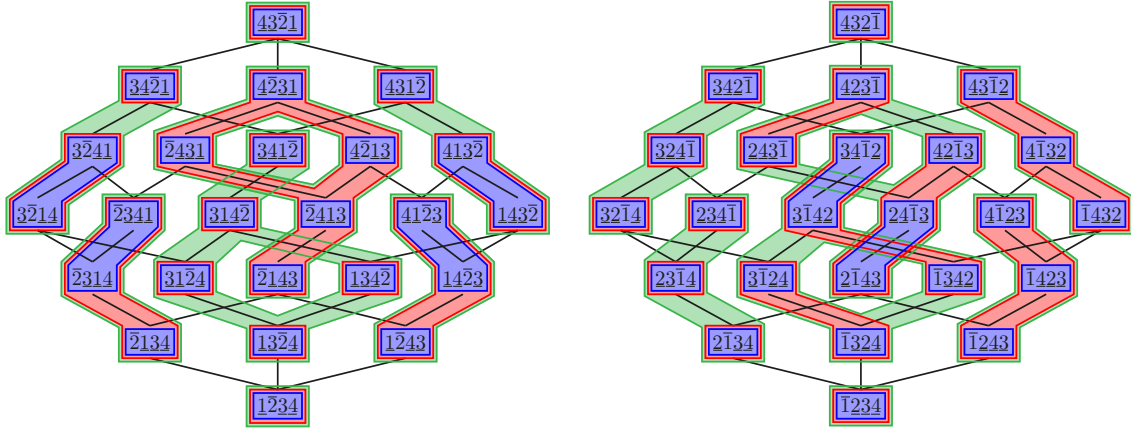


FIGURE 21. Baxter-Cambrian (blue), Cambrian (red), and boolean (green) congruence classes on the weak orders of \mathfrak{S}_ε for the signatures $\varepsilon = -+--$ (left) and $\varepsilon = +---$ (right). The number of Baxter-Cambrian classes is not constant.

Remark 55 (Extremal elements and pattern avoidance). Since the Baxter-Cambrian classes are generated by rewriting rules, we immediately obtain that the minimal elements of the Baxter-Cambrian classes are precisely the signed permutations avoiding the patterns:

$$\underline{b}\text{-}da\text{-}\underline{c}, \bar{b}\text{-}da\text{-}\bar{c}, \underline{c}\text{-}da\text{-}\underline{b}, \bar{c}\text{-}da\text{-}\bar{b}, \underline{b}\text{-}\bar{c}\text{-}da, \bar{b}\text{-}\bar{c}\text{-}da, \underline{c}\text{-}\bar{b}\text{-}da, \bar{c}\text{-}\bar{b}\text{-}da, da\text{-}\underline{b}\text{-}\bar{c}, da\text{-}\bar{b}\text{-}\underline{c}, da\text{-}\underline{c}\text{-}\bar{b}, da\text{-}\bar{c}\text{-}\underline{b}.$$

Similarly, the maximal elements of the Baxter-Cambrian classes are precisely the signed permutations avoiding the patterns:

$$(\star) \underline{b}\text{-}ad\text{-}\underline{c}, \bar{b}\text{-}ad\text{-}\bar{c}, \underline{c}\text{-}ad\text{-}\underline{b}, \bar{c}\text{-}ad\text{-}\bar{b}, \underline{b}\text{-}\bar{c}\text{-}ad, \bar{b}\text{-}\bar{c}\text{-}ad, \underline{c}\text{-}\bar{b}\text{-}ad, \bar{c}\text{-}\bar{b}\text{-}ad, ad\text{-}\underline{b}\text{-}\bar{c}, ad\text{-}\bar{b}\text{-}\underline{c}, ad\text{-}\underline{c}\text{-}\bar{b}, ad\text{-}\bar{c}\text{-}\underline{b}.$$

2.1.5. Baxter-Cambrian numbers. In contrast to the number of ε -Cambrian trees, the number of pairs of twin ε -Cambrian trees does depend on the signature ε . For example, there are 22 pairs of twin $(----)$ -Cambrian trees and only 20 pairs of twin $(-+--)$ -Cambrian trees. See Figures 20, 21 and 22.

For a signature ε , we define the ε -Baxter-Cambrian number B_ε to be the number of pairs of twin ε -Cambrian trees. We immediately observe that B_ε is preserved when we change the first and last sign of ε , inverse simultaneously all signs of ε , or reverse the signature ε :

$$B_\varepsilon = B_{\chi_0(\varepsilon)} = B_{\chi_n(\varepsilon)} = B_{-\varepsilon} = B_{\bar{\varepsilon}},$$

where χ_0 and χ_n change the first and last sign, $(-\varepsilon)_i = -\varepsilon_i$ and $(\bar{\varepsilon})_i = \varepsilon_{n+1-i}$. Table 2 shows the ε -Baxter-Cambrian number B_ε for all small signatures ε up to these transformations. Table 3 records all possible ε -Baxter-Cambrian numbers B_ε for signatures ε of sizes $n \leq 10$.

$n = 4$	$B_{++++} = 22$	$B_{+--+} = 20$	
$n = 5$	$B_{+++++} = 92$	$B_{++++-} = 78$	$B_{+---+} = 70$
$n = 6$	$B_{++++++} = 422$	$B_{+++++-} = 342$	$B_{+---++} = 316$
	$B_{+---+++} = 284$	$B_{+---++-} = 282$	$B_{+---+-+} = 252$
$n = 7$	$B_{+++++++} = 2074$	$B_{++++++-} = 1628$	$B_{+---+---} = 1428$
	$B_{+---+---} = 1298$	$B_{+---+---} = 1270$	$B_{+---+---} = 1172$
	$B_{+---+---} = 1162$	$B_{+---+---} = 1044$	$B_{+---+---} = 1036$
		$B_{+---+---} = 924$	

TABLE 2. The number B_ε of twin ε -Cambrian trees for all small signatures ε (up to first/last sign change, simultaneous inversion of all signs, and reverse).

$n = 4$	22 (1), 20 (1)
$n = 5$	92 (1), 78 (2), 70 (1)
$n = 6$	422 (1), 342 (2), 316 (1), 284 (1), 282 (2), 252 (1)
$n = 7$	2074 (1), 1628 (2), 1428 (2), 1298 (1), 1270 (2), 1172 (2), 1162 (1), 1044 (2), 1036 (2), 924 (1)
$n = 8$	10754 (1), 8244 (2), 6966 (2), 6612 (1), 6388 (1), 6182 (2), 5498 (2), 5380 (2), 5334 (2), 4902 (1), 4884 (2), 4748 (2), 4392 (1), 4362 (2), 4356 (2), 4324 (1), 3882 (1), 3880 (2), 3852 (2), 3432 (1)
$n = 9$	58202 (1), 43812 (2), 35998 (2), 33240 (1), 32908 (2), 31902 (2), 27660 (2), 26602 (2), 26392 (2), 25768 (2), 24888 (1), 24528 (2), 23530 (1), 23466 (2), 22768 (2), 20888 (2), 20886 (2), 20718 (2), 20244 (2), 20218 (2), 20082 (2), 18544 (1), 18518 (2), 18430 (2), 18376 (2), 17874 (2), 16470 (2), 16454 (1), 16358 (2), 16344 (2), 16342 (2), 16234 (1), 14550 (4), 14454 (2), 12870 (1)
$n = 10$	326240 (1), 242058 (2), 194608 (2), 180678 (1), 172950 (2), 172304 (2), 166568 (1), 146622 (2), 139100 (2), 138130 (2), 131994 (2), 129870 (2), 129600 (2), 124896 (2), 122716 (2), 120800 (1), 113754 (2), 111274 (2), 107072 (2), 106854 (1), 106382 (2), 105606 (2), 101084 (3), 101028 (2), 100426 (2), 98730 (2), 97524 (2), 94908 (1), 94372 (1), 93854 (2), 89952 (2), 89324 (2), 89276 (2), 88966 (2), 86638 (2), 86034 (2), 86026 (2), 79826 (2), 79384 (2), 79226 (2), 79076 (2), 79018 (2), 78580 (1), 78528 (2), 76542 (2), 76526 (2), 76484 (2), 76072 (2), 70450 (2), 70316 (1), 69866 (4), 69838 (2), 69810 (2), 69400 (2), 69314 (1), 67694 (2), 62124 (3), 62120 (1), 62096 (2), 61766 (2), 61746 (2), 61706 (2), 61682 (2), 61376 (1), 54956 (2), 54920 (2), 54892 (1), 54626 (2), 48620 (1)

TABLE 3. All possible ε -Baxter-Cambrian numbers B_ε for signatures ε of sizes $n \leq 10$. Numbers in parenthesis indicate the multiplicity of each Baxter number: for example, the second line indicates that there are 8 (resp. 16, resp. 8) signatures ε of \pm^5 such that $B_\varepsilon = 92$ (resp. 78, resp. 70).

In the following statements, we provide an inductive formula to compute all ε -Baxter-Cambrian numbers, using a two-parameters refinement. The proof is based on ideas similar to Proposition 15. The pairs of twin ε -Cambrian trees are in bijection with the weak order maximal permutations of ε -Baxter-Cambrian classes. These permutations are precisely the permutations avoiding the patterns (\star) in Remark 55. We consider the generating tree $\mathcal{T}_\varepsilon^1$ for these permutations. This tree has n levels, and the nodes at level m are labeled by permutations of $[m]$ whose values are signed by the restriction of ε to $[m]$ and avoiding the patterns (\star) . The parent of a permutation in $\mathcal{T}_\varepsilon^1$ is obtained by deleting its maximal value. See Figure 22.

As in the proof of Proposition 15, we consider the possible positions of $m + 1$ in the children of a permutation τ at level m in this generating tree $\mathcal{T}_\varepsilon^1$. Index by $\{0, \dots, m\}$ from left to right the gaps before the first letter, between two consecutive letters, and after the last letter of τ . *Free gaps* are those where placing $m + 1$ does not create a pattern of (\star) . Free gaps are marked with a blue dot in Figure 22. It is important to observe that gap 0 as well as the gaps immediately after $m - 1$ and m are always free, no matter τ or the signature ε .

Define the *free-gap-type* of τ to be the pair (ℓ, r) where ℓ (resp. r) denote the number of free gaps on the left (resp. right) of m in τ . For a signature ε , let $B_\varepsilon(\ell, r)$ denote the number of free-gap-type (ℓ, r) weak order maximal permutations of ε -Baxter-Cambrian classes. These refined Baxter-Cambrian numbers enables us to write inductive equations.

Proposition 56. *Consider two signatures $\varepsilon \in \pm^n$ and $\varepsilon' \in \pm^{n-1}$, where ε' is obtained by deleting the last sign of ε . Then*

$$B_\varepsilon(\ell, r) = \begin{cases} \sum_{\ell' \geq \ell} B_{\varepsilon'}(\ell', r - 1) + \sum_{r' \geq r} B_{\varepsilon'}(\ell - 1, r') & \text{if } \varepsilon_{n-1} = \varepsilon_n, \quad (=) \\ \delta_{\ell=1} \cdot \delta_{r \geq 2} \cdot \sum_{\substack{\ell' \geq r-1 \\ r' \geq 1}} B_{\varepsilon'}(\ell', r') + \delta_{\ell \geq 2} \cdot \delta_{r=1} \cdot \sum_{\substack{\ell' \geq 1 \\ r' \geq \ell-1}} B_{\varepsilon'}(\ell', r') & \text{if } \varepsilon_{n-1} \neq \varepsilon_n, \quad (\neq) \end{cases}$$

where δ denote the Kronecker δ (defined by $\delta_X = 1$ if X is satisfied and 0 otherwise).

Proof. Assume first that $\varepsilon_{n-1} = \varepsilon_n$. Consider two permutations τ and τ' at level n and $n-1$ in $\mathcal{T}_\varepsilon^{\mathbb{1}}$ such that τ' is obtained by deleting n in τ . Denote by α and β the gaps immediately after $n-1$ and n in τ , by α' the gap immediately after $n-1$ in τ' , and by β' the gap in τ' where we insert n to get τ . Then, besides gaps 0 , α and β , the free gaps of τ are precisely the free gaps of τ' not located between gaps α' and β' . Indeed,

- inserting $d := n+1$ just after a value a located between $b := n-1$ and $c := n$ in τ would create a pattern $b-ad-c$ or $c-ad-b$ with $\varepsilon_b = \varepsilon_c$;
- conversely, consider a gap γ of τ not located between α and β . If inserting $n+1$ at γ in τ creates a forbidden pattern of (\star) with $c = n$, then inserting n at γ in τ' would also create the same forbidden pattern of (\star) with $c = n-1$. Therefore, all free gaps not located between gaps α' and β' remain free.

Let (ℓ, r) denote the free-gap-type of τ and (ℓ', r') denote the free-gap-type of τ' . We obtain that

- $\ell' \geq \ell$ and $r' = r-1$ if n is inserted on the left of $n-1$;
- $\ell' = \ell-1$ and $r' \geq r$ if n is inserted on the right of $n-1$.

The formula follows immediately when $\varepsilon_{n-1} = \varepsilon_n$.

Assume now that $\varepsilon_{n-1} = -\varepsilon_n$, and keep the same notations as before. Using similar arguments, we observe that besides gaps 0 , α and β , the free gaps of τ are precisely the free gaps of τ' located between gaps α' and β' . Therefore, we obtain that

- $\ell = 1$, $r \geq 2$, and $\ell' \geq r-1$ if n is inserted on the left of $n-1$;
- $\ell \geq 2$, $r = 1$, and $r' \geq \ell-1$ if n is inserted on the right of $n-1$.

The formula follows for $\varepsilon_{n-1} = -\varepsilon_n$. □

Before applying these formulas to obtain bounds on B_ε for arbitrary signatures ε , let us consider two special signatures: the constant and the alternating signature.

ALTERNATING SIGNATURE Since it is the easiest, we start with the *alternating signature* $(+-)^{\frac{n}{2}}$ (where we define $(+-)^{\frac{n}{2}}$ to be $(+-)^m+$ when $n = 2m+1$ is odd).

Proposition 57. *The Baxter-Cambrian numbers for alternating signatures are central binomial coefficients (see [OEIS, A000984]):*

$$B_{(+ -)^{\frac{n}{2}}} = \binom{2n-2}{n-1}.$$

Proof. We prove by induction on n that the refined Baxter-Cambrian numbers are

$$B_{(+ -)^{\frac{n}{2}}}(\ell, r) = \delta_{\ell=1} \cdot \delta_{r \geq 2} \cdot \binom{2n-2-r}{n-r} + \delta_{\ell \geq 2} \cdot \delta_{r=1} \cdot \binom{2n-2-\ell}{n-\ell}.$$

This is true for $n = 2$ since $B_{+-}(1, 2) = 1$ (counting the permutation 21) and $B_{+-}(2, 1) = 1$ (counting the permutation 12). Assume now that it is true for some $n \in \mathbb{N}$. Then Equation (\neq) of Proposition 56 shows that

$$\begin{aligned} B_{(+ -)^{\frac{n+1}{2}}}(\ell, r) &= \delta_{\ell=1} \cdot \delta_{r \geq 2} \cdot \sum_{\ell' \geq r-1} \binom{2n-2-\ell'}{n-\ell'} + \delta_{\ell \geq 2} \cdot \delta_{r=1} \cdot \sum_{r' \geq \ell-1} \binom{2n-2-r'}{n-r'} \\ &= \delta_{\ell=1} \cdot \delta_{r \geq 2} \cdot \binom{2n-r}{n+1-r} + \delta_{\ell \geq 2} \cdot \delta_{r=1} \cdot \binom{2n-\ell}{n+1-\ell}, \end{aligned}$$

since a sum of binomial coefficients along a diagonal $\sum_{i=0}^p \binom{q+i}{i}$ simplifies to the binomial coefficient $\binom{q+p+1}{p}$ by multiple applications of Pascal's rule. Finally, we conclude observing that

$$B_{(+ -)^{\frac{n}{2}}} = \sum_{\ell, r \in [n]} B_{(+ -)^{\frac{n}{2}}}(\ell, r) = 2 \sum_{u \geq 2} \binom{2n-2-u}{n-u} = 2 \binom{2n-3}{n-2} = \binom{2n-2}{n-1}.$$

Remark 59 provides an alternative analytic proof for this result. □

Remark 58 (Properties of the generating tree $\mathcal{T}_{(+ -)^{\frac{n}{2}}}^{\mathbb{1}}$). Observe that:

- A permutation at level m with k free gaps has k children, whose numbers of free gaps are $3, 3, 4, 5, \dots, k+1$ respectively (compare to Lemma 16). This can already be observed on the generating tree $\mathcal{T}_{+-}^{\mathbb{1}}$ of Figure 22.

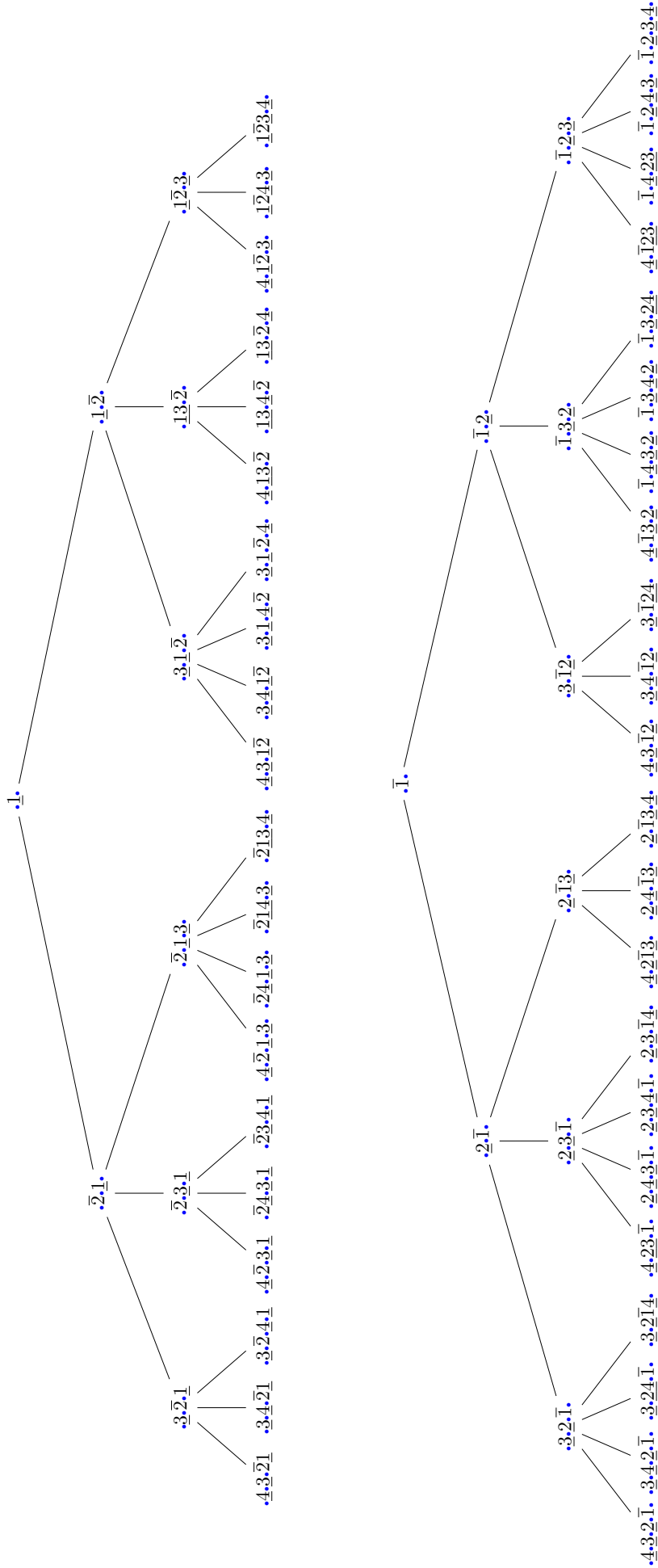


FIGURE 22. The generating trees \mathcal{T}_ε for the signatures $\varepsilon = -+---$ (top) and $\varepsilon = ++---$ (bottom). Free gaps are marked with a blue dot.

- (ii) For a permutation τ at level m with k free gaps, there are precisely $\binom{k+2p-2}{p}$ permutations at level $m+p$ that have τ as a subword, for any $p \in \mathbb{N}$.
- (iii) The number of permutations at level m with k free gaps is $2\binom{2m-1-k}{m+1-k}$. Counting permutations at level m and $m+1$ according to their number of free gaps gives

$$\binom{2m-2}{m-1} = \sum_{k \geq 3} 2\binom{2m-1-k}{m+1-k} \quad \text{and} \quad \binom{2m}{m} = \sum_{k \geq 3} 2k\binom{2m-1-k}{m+1-k}.$$

- (iv) Slight perturbations of the alternating signature yields interesting signatures for which we can give closed formulas for the Baxter-Cambrian number. For example, consider the signature $++(+ -)^{\frac{n}{2}-1}$ obtained from the alternating one by switching the second sign. Its Baxter-Cambrian number is given by a sum of three almost-central binomial coefficients:

$$B_{++(+ -)^{\frac{n}{2}-1}} = 2\binom{2n-6}{n-4} + \binom{2n-2}{n-1}.$$

CONSTANT SIGNATURE We now consider the *constant signature* $(+)^n$. The number $B_{(+)^n}$ is the classical *Baxter number* (see [OEIS, A001181]) defined by

$$B_{(+)^n} = B_n = \binom{n+1}{1}^{-1} \binom{n+1}{2}^{-1} \sum_{k=1}^n \binom{n+1}{k-1} \binom{n+1}{k} \binom{n+1}{k+1}.$$

These numbers have been extensively studied, see in particular [CGHK78, Mal79, DG96, DG98, YCCG03, FFNO11, BBMF11, LR12, Gir12]. The Baxter number B_n counts several families:

- Baxter permutations of $[n]$, *i.e.* permutations avoiding the patterns $b\text{-}da\text{-}c$ and $c\text{-}ad\text{-}b$,
- weak order maximal (resp. minimal) permutations of Baxter congruence classes on \mathfrak{S}_n , *i.e.* permutations avoiding the patterns $b\text{-}ad\text{-}c$ and $c\text{-}ad\text{-}b$ (resp. $b\text{-}da\text{-}c$ and $c\text{-}da\text{-}b$),
- pairs of twin binary trees on n nodes,
- diagonal rectangulations of an $n \times n$ grid,
- plane bipolar orientations with n edges,
- non-crossing triples of path with $k-1$ north steps and $n-k$ east steps, for all $k \in [n]$,
- etc.

Bijections between all these *Baxter families* are discussed in [DG96, DG98, FFNO11, BBMF11].

Remark 59 (Two proofs of the summation formula). There are essentially two ways to obtain the above summation formula for Baxter numbers: it was first proved analytically in [CGHK78], and then bijectively in [Vie81, DG98, FFNO11]. Let us shortly comment on these two techniques and discuss the limits of their extension to the Baxter-Cambrian setting.

- (i) The *bijective proofs* in [DG98, FFNO11] transform pairs of binary trees to triples of non-crossing paths, and then use the Gessel-Viennot determinant lemma [GV85] to get the summation formula. The middle path of these triples is given by the canopy of the twin binary trees, while the other two paths are given by the structure of the trees. We are not yet able to adapt this technique to provide summation formulas for all Baxter-Cambrian numbers.
- (ii) The *analytic proof* in [CGHK78] is based on Equation (=) of Proposition 56 and can be partially adapted to arbitrary signatures as follows. Define the *extension* of a signature $\varepsilon \in \pm^n$ by a signature $\delta \in \pm^m$ to be the signature $\varepsilon \triangleleft \delta \in \pm^{n+m}$ such that $(\varepsilon \triangleleft \delta)_i = \varepsilon_i$ for $i \in [n]$ and $(\varepsilon \triangleleft \delta)_{n+j} = \delta_j \cdot (\varepsilon \triangleleft \delta)_{n+j-1}$ for $j \in [m]$. For example, $++- \triangleleft +--+ = ++-+--+$. Then for any $\varepsilon \in \pm^n$ and $\delta \in \pm^m$, we have

$$B_{\varepsilon \triangleleft \delta} = \sum_{\ell, r \geq 1} X_\delta(\ell, r) B_\varepsilon(\ell, r),$$

where the coefficients $X_\delta(\ell, r)$ are obtained inductively from the formulas of Proposition 56. Namely, for any $\ell, r \geq 1$, we have $X_\emptyset(\ell, r) = 1$ and

$$\begin{aligned} X_{(+\delta)}(\ell, r) &= \sum_{1 \leq \ell' \leq \ell} X_\delta(\ell', r+1) + \sum_{1 \leq r' \leq r} X_\delta(\ell+1, r'), \\ X_{(-\delta)}(\ell, r) &= \sum_{2 \leq \ell' \leq r+1} X_\delta(\ell', 1) + \sum_{2 \leq r' \leq \ell+1} X_\delta(1, r'). \end{aligned}$$

These equations translate on the generating function $\mathfrak{X}_\delta(u, v) := \sum_{\ell, r \geq 1} X_\delta(\ell, r) u^{\ell-1} v^{r-1}$ to the formulas $\mathfrak{X}_\emptyset(u, v) = \frac{1}{(1-u)(1-v)}$ and

$$\begin{aligned}\mathfrak{X}_{(+\delta)}(u, v) &= \frac{\mathfrak{X}_\delta(u, v) - \mathfrak{X}_\delta(u, 0)}{(1-u)v} + \frac{\mathfrak{X}_\delta(u, v) - \mathfrak{X}_\delta(0, v)}{u(1-v)}, \\ \mathfrak{X}_{(-\delta)}(u, v) &= \frac{\mathfrak{X}_\delta(v, 0) - \mathfrak{X}_\delta(0, 0)}{(1-u)(1-v)v} + \frac{\mathfrak{X}_\delta(0, u) - \mathfrak{X}_\delta(0, 0)}{u(1-u)(1-v)}.\end{aligned}$$

Note that the u/v -symmetry of $\mathfrak{X}_\delta(u, v)$ is reflected in a symmetry on these inductive equations. We can thus write this generating function $\mathfrak{X}_\delta(u, v)$ as

$$\mathfrak{X}_\delta(u, v) = \sum_{\substack{i, j \geq 0 \\ k \in [|\delta|+1]}} Y_\delta^{i, j, k} \frac{(-u)^i (-v)^j}{(1-u)^{|\delta|+2-k} (1-v)^k},$$

where the non-vanishing coefficients $Y_\delta^{i, j, k}$ are computed inductively by $Y_\emptyset^{0, 0, 1} = 1$ and

$$\begin{aligned}Y_{(+\delta)}^{i, j, k} &= \binom{k}{j+1} Y_\delta^{i, 0, k} - Y_\delta^{i, j+1, k} + \binom{|\delta|+3-k}{i+1} Y_\delta^{0, j, k-1} - Y_\delta^{i+1, j, k-1}, \\ Y_{(-\delta)}^{i, j, k} &= \binom{k-1}{j} \left[\binom{|\delta|+2-k}{i+1} Y_\delta^{0, 0, k} - Y_\delta^{i+1, 0, k} \right] + \binom{|\delta|+2-k}{i} \left[\binom{k-1}{j+1} Y_\delta^{0, 0, k-1} - Y_\delta^{0, j+1, k-1} \right].\end{aligned}$$

We used that $Y_\delta^{i, j, k} = Y_\delta^{j, i, |\delta|+2-k}$ to simplify the second equation. Note that this decomposition of \mathfrak{X}_δ is not unique and the inductive equations on $Y_\delta^{i, j, k}$ follow from a particular choice of such a decomposition.

At that stage, F. Chung, R. Graham, V. Hoggatt, and M. Kleiman [CGHK78], guess and check that the first equation is always satisfied by

$$Y_{(+\delta)}^{i, j, k} = \frac{\binom{n+1}{k} \binom{n+1}{k+i+1} \binom{n+1}{k-j-1} \left[\binom{k+i-2}{i} \binom{n+j-k-1}{j} - \binom{k+i-2}{i-1} \binom{n+j-k-1}{j-1} \right]}{\binom{n+1}{1} \binom{n+1}{2}}$$

from which they derive immediately that

$$\begin{aligned}B_{(+\delta)^n} &= B_{+\triangleleft(+)^{n-1}} = \sum_{\ell, r \geq 1} X_{(+)^{n-1}}(\ell, r) B_+(\ell, r) = X_{(+)^{n-1}}(1, 1) = \mathfrak{X}_{(+)^{n-1}}(0, 0) \\ &= \sum_{k \in [n]} Y_{(+)^{n-1}}^{0, 0, k} = \binom{n+1}{1}^{-1} \binom{n+1}{2}^{-1} \sum_{k=1}^n \binom{n+1}{k-1} \binom{n+1}{k} \binom{n+1}{k+1}.\end{aligned}$$

Unfortunately, we have not been able to guess a closed formula for the coefficients $Y_{(-)^n}^{i, j, k}$. Note that it would be sufficient to understand the coefficients $Y_{(-)^n}^{i, 0, k}$ for which we observed empirically that

$$Y_{(-)^n}^{0, 0, k} = C_n, \quad Y_{(-)^n}^{i, 0, 0} = Y_{(-)^n}^{i, 0, 1} = \binom{2n}{n-1-i} \binom{n-1+i}{i} / n \quad \text{and} \quad Y_{(-)^n}^{i, 0, n+1-i} = \sum_{p=i}^{n-1} C_{n-1-p} C_p.$$

See [OEIS, A000108], [OEIS, A234950], and [OEIS, A028364]. This would provide an alternative proof of Proposition 57 as we would obtain that

$$B_{(+\delta)^{\frac{n}{2}}} = B_{+\triangleleft(-)^{n-1}} = \mathfrak{X}_{(-)^{n-1}}(0, 0) = \sum_{k \in [n]} Y_{(-)^{n-1}}^{0, 0, k} = n C_{n-1} = \binom{2n-2}{n-1}.$$

However, even if we were not able to work out the coefficients $Y_{(-)^n}^{i, 0, k}$, we still obtain another proof Proposition 57 by checking directly on the inductive equations on $\mathfrak{X}_\delta(u, v)$ that

$$\mathfrak{X}_{(-)^n}(u, v) = \sum_{k \in [n]} \binom{2n-1-k}{n-1} \left[\frac{1}{(1-u)(1-v)^{k+1}} + \frac{1}{(1-u)^{k+1}(1-v)} \right],$$

from which we obtain

$$\begin{aligned} B_{(+ -)^{\frac{n}{2}}} &= B_{+\triangleleft(-)^{n-1}} = \mathfrak{X}_{(-)^{n-1}}(0,0) = \sum_{k \in [n-1]} 2 \binom{2n-3-k}{n-2} \\ &= 2 \sum_{k=2}^n \binom{2n-2-k}{n-2} = 2 \binom{2n-2}{n-1} - 2 \binom{2n-3}{n-2} = \binom{2n-2}{n-1}. \end{aligned}$$

For the prior to last equality, choose $n-1$ positions among $2n-2$ and group according to the first position k .

ARBITRARY SIGNATURES We now come back to an arbitrary signature ε . We were not able to derive summation formulas for arbitrary signatures using the techniques presented in Remark 59 above. However, we use here the inductive formulas of Proposition 56 to bound the Baxter-Cambrian number B_ε for an arbitrary signature ε .

For this, we consider the matrix $\mathbf{B}_\varepsilon := (B_\varepsilon(\ell, r))_{\ell, r \in [n]}$. The inductive formulas of Proposition 56 provide an efficient inductive algorithm to compute this matrix \mathbf{B}_ε and thus the ε -Baxter-Cambrian number $B_\varepsilon = \sum_{\ell, r \in [n]} B_\varepsilon(\ell, r)$. Namely, if ε is obtained by adding a sign at the end of ε' , then each entry of \mathbf{B}_ε is the sum of entries of $\mathbf{B}_{\varepsilon'}$ in a region depending on whether $\varepsilon_n = \varepsilon_{n-1}$. These regions are sketched in Figure 23 and examples of such computations appear in Figure 24.

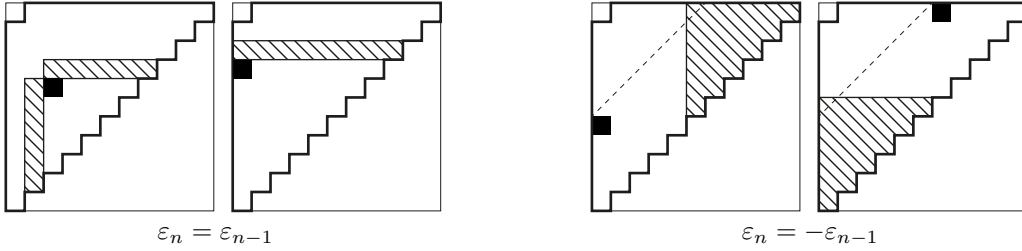


FIGURE 23. Inductive computation of \mathbf{B}_ε : the black entry of \mathbf{B}_ε is the sum of the entries of $\mathbf{B}_{\varepsilon'}$ over the shaded region. Entries outside the upper triangular region always vanish. When $\varepsilon_n = -\varepsilon_{n-1}$, the only non-vanishing entries of \mathbf{B}_ε are in the first row or in the first column.

We observe that the transformations of Figure 23 are symmetric with respect to the diagonal of the matrix. Since $\mathbf{B}_{\varepsilon_1\varepsilon_2} = \begin{bmatrix} 0 & 1 \\ 1 & 0 \end{bmatrix}$ is symmetric, and \mathbf{B}_ε is obtained from $\mathbf{B}_{\varepsilon_1\varepsilon_2}$ by successive applications of these symmetric transformations, we obtain that \mathbf{B}_ε is always symmetric. Although this fact may seem natural to the reader, it is not at all immediate as there is an asymmetry on the three forced free gaps: for example gap 0 is always free.

For a matrix $M := (m_{i,j})$, we consider the matrix $M^{\text{SE}} := (m_{i,j}^{\text{SE}})$ where

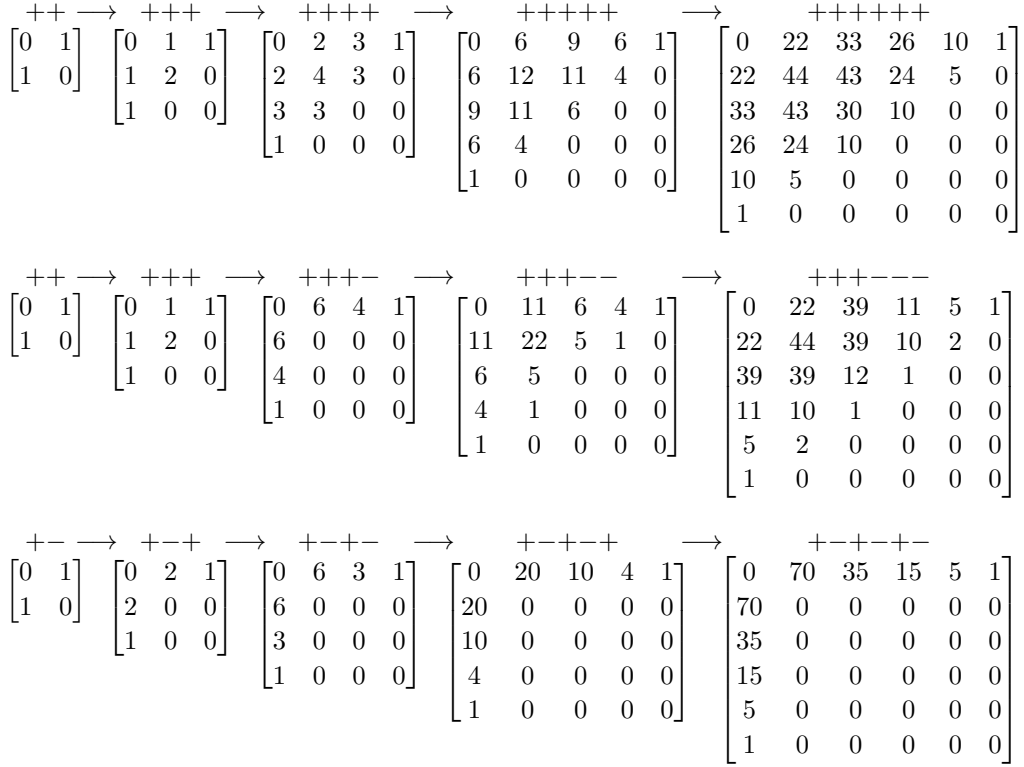
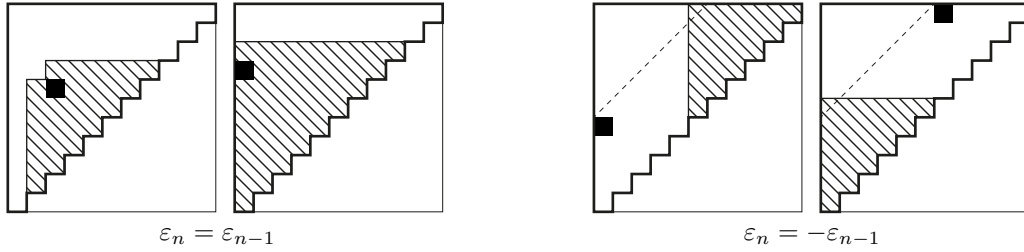
$$m_{i,j}^{\text{SE}} := \sum_{p \geq i, q \geq j} m_{p,q}$$

is the sum of all entries located south-east of (i, j) (in matrix notation). Observe that $(\mathbf{B}_\varepsilon)_{1,1}^{\text{SE}}$ is the sum of all entries of \mathbf{B}_ε , and thus equals the ε -Baxter-Cambrian number B_ε . Using Figure 23, we obtain a similar rule to compute the entries of $B_\varepsilon^{\text{SE}}$ as sums of entries of $B_{\varepsilon'}^{\text{SE}}$ when ε is obtained by adding a sign at the end of ε' . This rule is presented in Figure 25.

This matrix interpretation of the formulas of Proposition 56 provides us with tools to bound the Baxter-Cambrian numbers. For a signature ε , we denote by $\text{switch}(\varepsilon)$ the set of gaps where ε switches sign.

Proposition 60. *For any two signatures $\varepsilon, \tilde{\varepsilon} \in \pm^n$, if $\text{switch}(\varepsilon) \subset \text{switch}(\tilde{\varepsilon})$ then $B_\varepsilon > B_{\tilde{\varepsilon}}$.*

Proof. For two matrices $M := (m_{i,j})$ and $\tilde{M} := (\tilde{m}_{i,j})$, we write $M \succcurlyeq \tilde{M}$ when $m_{i,j} \geq \tilde{m}_{i,j}$ for all indices i, j (entrywise comparison), and we write $M \succ \tilde{M}$ when $M \succcurlyeq \tilde{M}$ and $M \neq \tilde{M}$. Consider


 FIGURE 24. Inductive computation of \mathbf{B}_ε , for $\varepsilon = (+)^6$, $(+)^3(-)^3$ and $(+-)^3$.

 FIGURE 25. Inductive computation of $\mathbf{B}_\varepsilon^{\text{SE}}$: the black entry of $\mathbf{B}_\varepsilon^{\text{SE}}$ is the sum of the entries of $\mathbf{B}_{\varepsilon'}^{\text{SE}}$ over the shaded region. Entries outside the triangular shape always vanish. When $\varepsilon_n = -\varepsilon_{n-1}$, the only non-vanishing entries of $\mathbf{B}_\varepsilon^{\text{SE}}$ are in the first row or in the first column.

four signatures $\varepsilon, \tilde{\varepsilon} \in \pm^n$ and $\varepsilon', \tilde{\varepsilon}' \in \pm^{n-1}$ such that ε' (resp. $\tilde{\varepsilon}'$) is obtained by deleting the last sign of ε (resp. $\tilde{\varepsilon}$). From Figure 25, and using the fact that \mathbf{B}_ε is symmetric, we obtain that:

- if $\varepsilon_n = \varepsilon_{n-1}$ while $\tilde{\varepsilon}_n = -\tilde{\varepsilon}_{n-1}$, then $\mathbf{B}_{\varepsilon'}^{\text{SE}} \succ \mathbf{B}_{\tilde{\varepsilon}'}^{\text{SE}}$ implies $\mathbf{B}_\varepsilon^{\text{SE}} \succ \mathbf{B}_{\tilde{\varepsilon}}^{\text{SE}}$.
- if either both $\varepsilon_n = \varepsilon_{n-1}$ and $\tilde{\varepsilon}_n = \tilde{\varepsilon}_{n-1}$, or both $\varepsilon_n = -\varepsilon_{n-1}$ and $\tilde{\varepsilon}_n = -\tilde{\varepsilon}_{n-1}$, then $\mathbf{B}_{\varepsilon'}^{\text{SE}} \succ \mathbf{B}_{\tilde{\varepsilon}'}^{\text{SE}}$ implies $\mathbf{B}_\varepsilon^{\text{SE}} \succ \mathbf{B}_{\tilde{\varepsilon}}^{\text{SE}}$.

By repeated applications of these observations, we therefore obtain that $\text{switch}(\varepsilon) \subset \text{switch}(\tilde{\varepsilon})$ implies $\mathbf{B}_\varepsilon^{\text{SE}} \succ \mathbf{B}_{\tilde{\varepsilon}}^{\text{SE}}$, and thus $B_\varepsilon > B_{\tilde{\varepsilon}}$. \square

Corollary 61. *Among all signatures of \pm^n , the constant signature maximizes the Baxter-Cambrian number, while the alternating signature minimizes it: for all $\varepsilon \in \pm^n$,*

$$\binom{2n-2}{n-1} = B_{(+ -)^{\frac{n}{2}}} \leq B_\varepsilon \leq B_{(+)^n} = \binom{n+1}{1}^{-1} \binom{n+1}{2}^{-1} \sum_{k=1}^n \binom{n+1}{k-1} \binom{n+1}{k} \binom{n+1}{k-1}.$$

Remark 62. The proof of Proposition 60 may seem unnecessarily intricate. Observe however that the situation is rather subtle:

- If $\text{switch}(\varepsilon) \not\subseteq \text{switch}(\tilde{\varepsilon})$, we may have $B_\varepsilon < B_{\tilde{\varepsilon}}$ even if $|\text{switch}(\varepsilon)| < |\text{switch}(\tilde{\varepsilon})|$. The smallest example is given by $B_{+++++----} = 18376 < 18544 = B_{+++++----}$.
- We may have $\mathbf{B}_\varepsilon^{\text{SE}} \succ \mathbf{B}_{\tilde{\varepsilon}}^{\text{SE}}$ but $\mathbf{B}_\varepsilon \not\succeq \mathbf{B}_{\tilde{\varepsilon}}$. See the third column of Figure 24.

2.1.6. Geometric realizations. Using similar tools as in Section 1.1.7 and following [LR12], we present geometric realizations for pairs of twin Cambrian trees, for the Baxter-Cambrian lattice, and for the Baxter-Cambrian \mathbf{P}^{\perp} -symbol. For a partial order \prec on $[n]$, we still define its *incidence cone* $C(\prec)$ and its *braid cone* $C^\circ(\prec)$ as

$$C(\prec) := \text{cone}\{e_i - e_j \mid \text{for all } i \prec j\} \quad \text{and} \quad C^\circ(\prec) := \{\mathbf{x} \in \mathbb{H} \mid x_i \leq x_j \text{ for all } i \prec j\}.$$

The cones $C(\mathsf{T}_\circ \updownarrow \mathsf{T}_\bullet)$ for all pairs $[\mathsf{T}_\circ, \mathsf{T}_\bullet]$ of twin ε -Cambrian trees form (together with all their faces) a complete polyhedral fan that we call the *ε -Baxter-Cambrian fan*. It is the common refinement of the ε - and $(-\varepsilon)$ -Cambrian fans. It is therefore the normal fan of the Minkowski sum of the associahedra $\text{Asso}(\varepsilon)$ and $\text{Asso}(-\varepsilon)$. We call this polytope *Baxter-Cambrian associahedron* and denote it by $\text{BaxAsso}(\varepsilon)$. Note that $\text{BaxAsso}(\varepsilon)$ is clearly centrally symmetric (since $\text{Asso}(\varepsilon) = -\text{Asso}(-\varepsilon)$) but not necessarily simple. Examples are illustrated on Figure 26. The graph of $\text{BaxAsso}(\varepsilon)$, oriented in the direction $(n, \dots, 1) - (1, \dots, n) = \sum_{i \in [n]} (n+1-2i)e_i$, is the Hasse diagram of the ε -Baxter-Cambrian lattice. Finally, the Baxter-Cambrian \mathbf{P}^{\perp} -symbol can be read geometrically as

$$[\mathsf{T}_\circ, \mathsf{T}_\bullet] = \mathbf{P}^{\perp}(\tau) \iff C(\mathsf{T}_\circ \updownarrow \mathsf{T}_\bullet) \subseteq C(\tau) \iff C^\circ(\mathsf{T}_\circ \updownarrow \mathsf{T}_\bullet) \supseteq C^\circ(\tau).$$

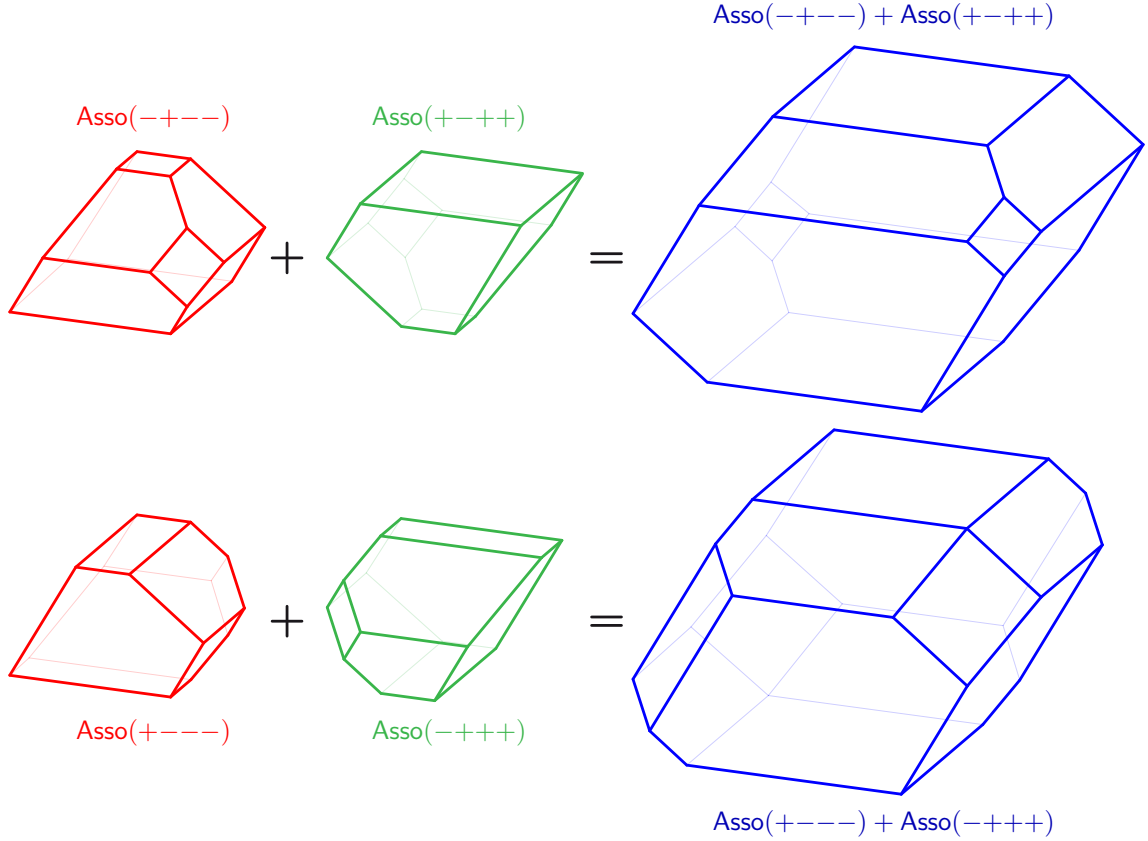


FIGURE 26. The Minkowski sum (blue, right) of the associahedra $\text{Asso}(\varepsilon)$ (red, left) and $\text{Asso}(-\varepsilon)$ (green, middle) gives a realization of the ε -Baxter-Cambrian lattice. Illustrated with the signatures $\varepsilon = -+---$ (top) and $\varepsilon = +----$ (bottom) whose ε -Baxter-Cambrian lattice are represented in Figures 19, 20, and 21.

2.2. BAXTER-CAMBRIAN HOPF ALGEBRA

In this section, we define the Baxter-Cambrian Hopf algebra BaxCamb , extending simultaneously the Cambrian Hopf algebra and the Baxter Hopf algebra studied by S. Law and N. Reading [LR12] and S. Giraud [Gir12]. We present again the construction of BaxCamb as a subalgebra of FQSym_\pm and that of its dual BaxCamb^* as a quotient of FQSym_\pm^* .

2.2.1. Subalgebra of FQSym_\pm . We denote by BaxCamb the vector subspace of FQSym_\pm generated by the elements

$$\mathbb{P}_{[T_\circ, T_\bullet]} := \sum_{\substack{\tau \in \mathfrak{S}_\pm \\ \mathbf{P}^\natural(\tau) = [T_\circ, T_\bullet]}} \mathbb{F}_\tau = \sum_{\tau \in \mathcal{L}(T_\circ \uparrow T_\bullet)} \mathbb{F}_\tau,$$

for all pairs of twin Cambrian trees $[T_\circ, T_\bullet]$. For example, for the pair of twin Cambrian trees of Figure 18 (left), we have

$$\mathbb{P} \left[\begin{array}{c} \text{Diagram 1} \\ \text{Diagram 2} \end{array} \right] = \mathbb{F}_{\underline{21\bar{7}5\bar{3}4\bar{6}}} + \mathbb{F}_{\underline{2\bar{7}15\bar{3}4\bar{6}}} + \mathbb{F}_{\underline{2\bar{7}51\bar{3}4\bar{6}}} + \mathbb{F}_{\underline{7\bar{2}15\bar{3}4\bar{6}}} + \mathbb{F}_{\underline{7\bar{2}51\bar{3}4\bar{6}}} + \mathbb{F}_{\underline{7\bar{5}21\bar{3}4\bar{6}}}.$$

Theorem 63. BaxCamb is a Hopf subalgebra of FQSym_\pm .

Proof. The proof of this theorem is left to the reader as it is very similar to that of Theorem 24. Exchanges in a permutation τ of the product $\mathbb{P}_{[T_\circ, T_\bullet]} \cdot \mathbb{P}_{[T'_\circ, T'_\bullet]}$ are due to exchanges either in the linear extensions of $T_\circ \uparrow T_\bullet$ and $T'_\circ \uparrow T'_\bullet$, or in the shuffle product of these linear extensions. The coproduct is treated similarly. \square

As for the Cambrian algebra, we can describe combinatorially the product and coproduct of \mathbb{P} -basis elements of BaxCamb in terms of operations on pairs of twin Cambrian trees.

PRODUCT The product in the Baxter-Cambrian algebra BaxCamb can be described in terms of intervals in Baxter-Cambrian lattices.

Proposition 64. For any two pairs $[T_\circ, T_\bullet]$ and $[T'_\circ, T'_\bullet]$ of twin Cambrian trees, the product $\mathbb{P}_{[T_\circ, T_\bullet]} \cdot \mathbb{P}_{[T'_\circ, T'_\bullet]}$ is given by

$$\mathbb{P}_{[T_\circ, T_\bullet]} \cdot \mathbb{P}_{[T'_\circ, T'_\bullet]} = \sum_{[S_\circ, S_\bullet]} \mathbb{P}_{[S_\circ, S_\bullet]},$$

where $[S_\circ, S_\bullet]$ runs over the interval between $\left[T_\circ \nearrow \bar{T}'_\circ, T_\bullet \nwarrow \bar{T}'_\bullet \right]$ and $\left[T_\circ \nwarrow \bar{T}'_\circ, T_\bullet \nearrow \bar{T}'_\bullet \right]$ in the $\varepsilon(T_\circ)\varepsilon(T'_\circ)$ -Baxter-Cambrian lattice.

Proof. The result relies on the fact that the ε -Baxter-Cambrian classes are intervals of the weak order on \mathfrak{S}^ε , and that the shuffle product of two intervals of the weak order is again an interval of the weak order. See the similar proof of Proposition 25. \square

For example, we can compute the product

$$\begin{aligned} & \mathbb{P} \left[\begin{array}{c} \text{Diagram 1} \\ \text{Diagram 2} \end{array} \right] \cdot \mathbb{P} \left[\begin{array}{c} \text{Diagram 3} \\ \text{Diagram 4} \end{array} \right] = \mathbb{F}_{\underline{21}} \cdot (\mathbb{F}_{\underline{2341}} + \mathbb{F}_{\underline{2314}}) \\ &= \begin{pmatrix} \mathbb{F}_{\underline{214536}} + \mathbb{F}_{\underline{241536}} \\ +\mathbb{F}_{\underline{245136}} + \mathbb{F}_{\underline{214563}} \\ +\mathbb{F}_{\underline{241563}} + \mathbb{F}_{\underline{245163}} \\ +\mathbb{F}_{\underline{245613}} \end{pmatrix} + \begin{pmatrix} \mathbb{F}_{\underline{245316}} + \mathbb{F}_{\underline{245361}} \\ +\mathbb{F}_{\underline{245631}} \end{pmatrix} + \begin{pmatrix} \mathbb{F}_{\underline{421536}} + \mathbb{F}_{\underline{425136}} \\ +\mathbb{F}_{\underline{421563}} + \mathbb{F}_{\underline{425163}} \\ +\mathbb{F}_{\underline{425613}} + \mathbb{F}_{\underline{452136}} \\ +\mathbb{F}_{\underline{452163}} + \mathbb{F}_{\underline{452613}} \\ +\mathbb{F}_{\underline{456213}} \end{pmatrix} + \begin{pmatrix} \mathbb{F}_{\underline{425316}} + \mathbb{F}_{\underline{425361}} \\ +\mathbb{F}_{\underline{425631}} + \mathbb{F}_{\underline{452316}} \\ +\mathbb{F}_{\underline{452361}} + \mathbb{F}_{\underline{452631}} \\ +\mathbb{F}_{\underline{456231}} \end{pmatrix} + \begin{pmatrix} \mathbb{F}_{\underline{453216}} + \mathbb{F}_{\underline{453261}} \\ +\mathbb{F}_{\underline{453621}} + \mathbb{F}_{\underline{456321}} \end{pmatrix} \\ &= \mathbb{P} \left[\begin{array}{c} \text{Diagram 5} \\ \text{Diagram 6} \end{array} \right] + \mathbb{P} \left[\begin{array}{c} \text{Diagram 7} \\ \text{Diagram 8} \end{array} \right] + \mathbb{P} \left[\begin{array}{c} \text{Diagram 9} \\ \text{Diagram 10} \end{array} \right] + \mathbb{P} \left[\begin{array}{c} \text{Diagram 11} \\ \text{Diagram 12} \end{array} \right] + \mathbb{P} \left[\begin{array}{c} \text{Diagram 13} \\ \text{Diagram 14} \end{array} \right]. \end{aligned}$$

Remark 65 (Multiplicative bases). Similar to the multiplicative bases defined in Section 1.3, the bases $\mathbb{E}^{[T_\circ, T_\bullet]}$ and $\mathbb{H}^{[T_\circ, T_\bullet]}$ defined by

$$\mathbb{E}^{[T_\circ, T_\bullet]} := \sum_{[T_\circ, T_\bullet] \leq [T'_\circ, T'_\bullet]} \mathbb{P}_{[T'_\circ, T'_\bullet]} \quad \text{and} \quad \mathbb{H}^{[T_\circ, T_\bullet]} := \sum_{[T'_\circ, T'_\bullet] \leq [T_\circ, T_\bullet]} \mathbb{P}_{[T'_\circ, T'_\bullet]}$$

are multiplicative since

$$\mathbb{E}^{[T_\circ, T_\bullet]} \cdot \mathbb{E}^{[T'_\circ, T'_\bullet]} = \mathbb{E}^{[T_\circ \nearrow T'_\circ, T_\bullet \nwarrow T'_\bullet]} \quad \text{and} \quad \mathbb{H}^{[T_\circ, T_\bullet]} \cdot \mathbb{H}^{[T'_\circ, T'_\bullet]} = \mathbb{H}^{[T_\circ \nwarrow T'_\circ, T_\bullet \nearrow T'_\bullet]}.$$

The \mathbb{E} -indecomposable elements are precisely the pairs $[T_\circ, T_\bullet]$ for which all linear extensions of $T_\circ \updownarrow T_\bullet$ are indecomposable. In particular, $[T_\circ, T_\bullet]$ is \mathbb{E} -indecomposable as soon as T_\circ is \mathbb{E} -indecomposable or T_\bullet is \mathbb{H} -indecomposable. This condition is however not necessary. For example $\mathbf{P}^1(3142)$ is \mathbb{E} -indecomposable while $\mathbf{P}(3142) = \mathbf{P}(1342)$ is \mathbb{E} -decomposable and $\mathbf{P}(2413) = \mathbf{P}(4213)$ is \mathbb{H} -decomposable. The enumerative and structural properties studied in Section 1.3 do not hold anymore for the set of \mathbb{E} -indecomposable pairs of twin Cambrian trees: they form an ideal of the Baxter-Cambrian lattice, but this ideal is not principal as in Proposition 34, and they are not counted by simple formulas as in Proposition 36. Let us however mention that

- the numbers of \mathbb{E} -indecomposable elements with constant signature $(-)^n$ are given by 1, 1, 3, 11, 47, 221, ... See [OEIS, A217216].
- the numbers of \mathbb{E} -indecomposable elements with constant signature $(+-)^{n/2}$ are given by 1, 1, 3, 9, 29, 97, 333, 1165, 4135, ... These numbers are the coefficients of the Taylor series of $\frac{1}{x + \sqrt{1-4x}}$. See [OEIS, A081696] for references and details.

COPRODUCT A *cut* of a pair of twin Cambrian trees $[S_\circ, S_\bullet]$ is a pair $\gamma = [\gamma_\circ, \gamma_\bullet]$ where γ_\circ is a cut of S_\circ and γ_\bullet is a cut of S_\bullet such that the labels of S_\circ below γ_\circ coincide with the labels of S_\bullet above γ_\bullet . Equivalently, it can be seen as a lower set of $T_\circ \updownarrow T_\bullet$. An example is illustrated in Figure 27.

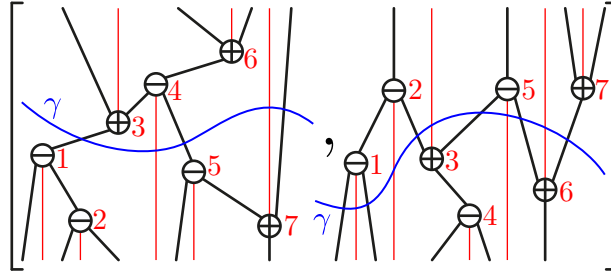


FIGURE 27. A cut γ of a pair of twin Cambrian trees.

We denote by $AB([S_\circ, S_\bullet], [\gamma_\circ, \gamma_\bullet])$ the set of pairs $[A_\circ, B_\bullet]$, where A_\circ appears in the product $\prod_{T \in A(S_\circ)} \mathbb{P}_T$ while B_\bullet appears in the product $\prod_{T \in B(S_\bullet)} \mathbb{P}_T$, and A_\circ and B_\bullet are twin Cambrian trees. We define $BA([S_\circ, S_\bullet], [\gamma_\circ, \gamma_\bullet])$ similarly exchanging the role of A and B . We obtain the following description of the coproduct in the Baxter-Cambrian algebra BaxCamb .

Proposition 66. *For any pair of twin Cambrian trees $[S_\circ, S_\bullet]$, the coproduct $\Delta \mathbb{P}_{[S_\circ, S_\bullet]}$ is given by*

$$\Delta \mathbb{P}_{[S_\circ, S_\bullet]} = \sum_{\gamma} \left(\sum_{[B_\circ, A_\bullet]} \mathbb{P}_{[B_\circ, A_\bullet]} \right) \otimes \left(\sum_{[A_\circ, B_\bullet]} \mathbb{P}_{[A_\circ, B_\bullet]} \right),$$

where γ runs over all cuts of $[S_\circ, S_\bullet]$, $[B_\circ, A_\bullet]$ runs over $BA([S_\circ, S_\bullet], [\gamma_\circ, \gamma_\bullet])$ and $[A_\circ, B_\bullet]$ runs over $AB([S_\circ, S_\bullet], [\gamma_\circ, \gamma_\bullet])$.

Proof. The proof is similar to that of Proposition 26. The difficulty here is to describe the linear extensions of the union of the forest $A(S_\circ, \gamma_\circ)$ with the opposite of the forest $B(S_\bullet, \gamma_\bullet)$. This difficulty is hidden in the definition of $AB([S_\circ, S_\bullet], [\gamma_\circ, \gamma_\bullet])$. \square

For example, we can compute the coproduct

$$\begin{aligned}
\Delta \mathbb{P} \left[\begin{array}{c} \text{Diagram 1} \\ \text{Diagram 2} \end{array} \right] &= \Delta (\mathbb{F}_{\bar{2}\bar{3}\bar{1}\bar{4}} + \mathbb{F}_{\bar{2}\bar{3}\bar{4}\bar{1}}) \\
&= 1 \otimes (\mathbb{F}_{\bar{2}\bar{3}\bar{1}\bar{4}} + \mathbb{F}_{\bar{2}\bar{3}\bar{4}\bar{1}}) + \mathbb{F}_{\bar{1}} \otimes (\mathbb{F}_{\bar{2}\bar{1}\bar{3}} + \mathbb{F}_{\bar{2}\bar{3}\bar{1}}) + \mathbb{F}_{\bar{1}\bar{2}} \otimes (\mathbb{F}_{\bar{1}\bar{2}} + \mathbb{F}_{\bar{2}\bar{1}}) + \mathbb{F}_{\bar{2}\bar{3}\bar{1}} \otimes \mathbb{F}_{\bar{1}} + \mathbb{F}_{\bar{1}\bar{2}\bar{3}} \otimes \mathbb{F}_{\bar{1}} + (\mathbb{F}_{\bar{2}\bar{3}\bar{1}\bar{4}} + \mathbb{F}_{\bar{2}\bar{3}\bar{4}\bar{1}}) \otimes 1 \\
&= 1 \otimes \mathbb{P} \left[\begin{array}{c} \text{Diagram 1} \\ \text{Diagram 2} \end{array} \right] + \mathbb{P} \left[\begin{array}{c} \text{Diagram 3} \\ \text{Diagram 4} \end{array} \right] \otimes (\mathbb{P} \left[\begin{array}{c} \text{Diagram 5} \\ \text{Diagram 6} \end{array} \right] + \mathbb{P} \left[\begin{array}{c} \text{Diagram 7} \\ \text{Diagram 8} \end{array} \right]) + \mathbb{P} \left[\begin{array}{c} \text{Diagram 9} \\ \text{Diagram 10} \end{array} \right] \otimes (\mathbb{P} \left[\begin{array}{c} \text{Diagram 11} \\ \text{Diagram 12} \end{array} \right] + \mathbb{P} \left[\begin{array}{c} \text{Diagram 13} \\ \text{Diagram 14} \end{array} \right]) \\
&\quad + \mathbb{P} \left[\begin{array}{c} \text{Diagram 15} \\ \text{Diagram 16} \end{array} \right] \otimes \mathbb{P} \left[\begin{array}{c} \text{Diagram 17} \\ \text{Diagram 18} \end{array} \right] + \mathbb{P} \left[\begin{array}{c} \text{Diagram 19} \\ \text{Diagram 20} \end{array} \right] \otimes \mathbb{P} \left[\begin{array}{c} \text{Diagram 21} \\ \text{Diagram 22} \end{array} \right] + \mathbb{P} \left[\begin{array}{c} \text{Diagram 23} \\ \text{Diagram 24} \end{array} \right] \otimes 1.
\end{aligned}$$

In the result line, we have grouped the summands according to the six possible cuts of the pair of twin Cambrian trees $\left[\begin{array}{c} \text{Diagram 1} \\ \text{Diagram 2} \end{array} \right]$.

MATRIOCHKA ALGEBRAS As the Baxter-Cambrian classes refine the Cambrian classes, the Baxter-Cambrian Hopf algebra is sandwiched between the Hopf algebra on signed permutations and the Cambrian Hopf algebra. It completes our sequence of subalgebras:

$$\text{Rec} \subset \text{Camb} \subset \text{BaxCamb} \subset \text{FQSym}_{\pm}.$$

2.2.2. Quotient algebra of FQSym_{\pm}^* . As for the Cambrian algebra, the following result is automatic from Theorem 63.

Theorem 67. *The graded dual BaxCamb^* of the Baxter-Cambrian algebra is isomorphic to the image of FQSym_{\pm}^* under the canonical projection*

$$\pi : \mathbb{C}\langle A \rangle \longrightarrow \mathbb{C}\langle A \rangle / \equiv^{\mathbb{1}},$$

where $\equiv^{\mathbb{1}}$ denotes the Baxter-Cambrian congruence. The dual basis $\mathbb{Q}_{[\text{T}_o, \text{T}_\bullet]}$ of $\mathbb{P}_{[\text{T}_o, \text{T}_\bullet]}$ is expressed as $\mathbb{Q}_{[\text{T}_o, \text{T}_\bullet]} = \pi(\mathbb{G}_\tau)$, where τ is any linear extension of $\text{T}_o \uparrow \text{T}_\bullet$.

We now describe the product and coproduct in BaxCamb^* by combinatorial operations on pairs of twin Cambrian trees. We use the definitions and notations introduced in Section 1.2.3.

PRODUCT The product in BaxCamb^* can be described using gaps and laminations similarly to Proposition 29. An example is illustrated on Figure 28. For two Cambrian trees T and T' and a shuffle s of the signatures $\varepsilon(T)$ and $\varepsilon(T')$, we still denote by $T \mathbin{\vphantom{T}}_s \mathbin{\vphantom{T}} T'$ the tree described in Section 1.2.3.

Proposition 68. *For any two pairs of twin Cambrian trees $[\text{T}_o, \text{T}_\bullet]$ and $[\text{T}'_o, \text{T}'_\bullet]$, the product $\mathbb{Q}_{[\text{T}_o, \text{T}_\bullet]} \cdot \mathbb{Q}_{[\text{T}'_o, \text{T}'_\bullet]}$ is given by*

$$\mathbb{Q}_{[\text{T}_o, \text{T}_\bullet]} \cdot \mathbb{Q}_{[\text{T}'_o, \text{T}'_\bullet]} = \sum_s \mathbb{Q}_{[\text{T}_o \mathbin{\vphantom{T}_o} \mathbin{\vphantom{T}_o} \text{T}'_o, \text{T}'_\bullet \mathbin{\vphantom{T}'_\bullet} \mathbin{\vphantom{T}'_\bullet} \text{T}_\bullet]},$$

where s runs over all shuffles of the signatures $\varepsilon(\text{T}_o) = \varepsilon(\text{T}_\bullet)$ and $\varepsilon(\text{T}'_o) = \varepsilon(\text{T}'_\bullet)$.

Proof. The proof follows the same lines as that of Proposition 29. The only difference is that if $\tau \in \mathcal{L}(\text{T}_o \uparrow \text{T}_\bullet)$, $\tau' \in \mathcal{L}(\text{T}'_o \uparrow \text{T}'_\bullet)$, and $\sigma \in \tau \star \tau'$, then $\text{T}_o = \mathbf{P}(\tau)$ appears below $\text{T}'_o = \mathbf{P}(\tau')$ in $\mathbf{P}(\sigma)$ since σ is inserted from left to right in $\mathbf{P}(\sigma)$, while $\text{T}_\bullet = \mathbf{P}(\overleftarrow{\tau})$ appears above $\text{T}'_\bullet = \mathbf{P}(\overleftarrow{\tau}')$ in $\mathbf{P}(\overleftarrow{\sigma})$ since σ is inserted from right to left in $\mathbf{P}(\overleftarrow{\sigma})$. \square

For example, we can compute the product

$$\begin{aligned}
\mathbb{Q} \left[\begin{array}{c} \text{Diagram 1} \\ \text{Diagram 2} \end{array} \right] \cdot \mathbb{Q} \left[\begin{array}{c} \text{Diagram 3} \\ \text{Diagram 4} \end{array} \right] &= \mathbb{G}_{\bar{2}\bar{1}} \cdot \mathbb{G}_{\bar{1}\bar{2}} \\
&= \mathbb{G}_{\bar{2}\bar{1}\bar{3}\bar{4}} + \mathbb{G}_{\bar{3}\bar{1}\bar{2}\bar{4}} + \mathbb{G}_{\bar{4}\bar{1}\bar{2}\bar{3}} + \mathbb{G}_{\bar{3}\bar{2}\bar{1}\bar{4}} + \mathbb{G}_{\bar{4}\bar{2}\bar{1}\bar{3}} + \mathbb{G}_{\bar{4}\bar{3}\bar{1}\bar{2}} \\
&= \mathbb{Q} \left[\begin{array}{c} \text{Diagram 5} \\ \text{Diagram 6} \end{array} \right] + \mathbb{Q} \left[\begin{array}{c} \text{Diagram 7} \\ \text{Diagram 8} \end{array} \right] + \mathbb{Q} \left[\begin{array}{c} \text{Diagram 9} \\ \text{Diagram 10} \end{array} \right] + \mathbb{Q} \left[\begin{array}{c} \text{Diagram 11} \\ \text{Diagram 12} \end{array} \right] + \mathbb{Q} \left[\begin{array}{c} \text{Diagram 13} \\ \text{Diagram 14} \end{array} \right] + \mathbb{Q} \left[\begin{array}{c} \text{Diagram 15} \\ \text{Diagram 16} \end{array} \right].
\end{aligned}$$

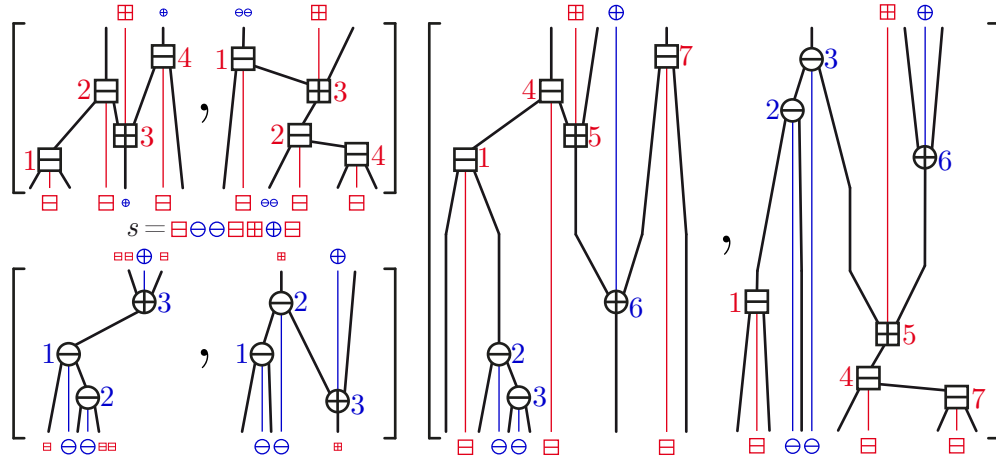


FIGURE 28. Two pairs of twin Cambrian trees $[T_\circ, T_\bullet]$ and $[T'_\circ, T'_\bullet]$ (left), and a pair of twin Cambrian trees which appear in the product $\mathbb{Q}_{[T_\circ, T_\bullet]} \cdot \mathbb{Q}_{[T'_\circ, T'_\bullet]}$ (right).

COPRODUCT The coproduct in $\mathbf{BaxCamb}^*$ can be described combinatorially as in Proposition 30. For a Cambrian tree S and a gap γ between two consecutive vertices of S , we still denote by $L(S, \gamma)$ and $R(S, \gamma)$ the left and right Cambrian subtrees of S when split along the path $\lambda(S, \gamma)$.

Proposition 69. For any pair of twin Cambrian trees $[S_\circ, S_\bullet]$, the coproduct $\Delta \mathbb{Q}_{[S_\circ, S_\bullet]}$ is given by

$$\Delta \mathbb{Q}_{[S_\circ, S_\bullet]} = \sum_{\gamma} \mathbb{Q}_{[L(S_\circ, \gamma), L(S_\bullet, \gamma)]} \otimes \mathbb{Q}_{[R(S_\circ, \gamma), R(S_\bullet, \gamma)]},$$

where γ runs over all gaps between consecutive positions in $[n]$.

Proof. The proof is identical to that of Proposition 30. \square

For example, we can compute the coproduct

$$\begin{aligned} \Delta \mathbb{Q} \left[\begin{array}{c} \text{Tree with 4 vertices} \\ \text{Tree with 4 vertices} \end{array} \right] &= \Delta G_{\bar{2}34\bar{1}} \\ &= 1 \otimes G_{\bar{2}34\bar{1}} + G_{\bar{1}} \otimes G_{\bar{1}23} + G_{\bar{2}\bar{1}} \otimes G_{\bar{1}2} + G_{\bar{2}3\bar{1}} \otimes G_{\bar{1}} + G_{\bar{2}34\bar{1}} \otimes 1 \\ &= 1 \otimes \mathbb{Q} \left[\begin{array}{c} \text{Tree with 4 vertices} \\ \text{Tree with 4 vertices} \end{array} \right] + \mathbb{Q} \left[\begin{array}{c} \text{Tree with 2 vertices} \\ \text{Tree with 2 vertices} \end{array} \right] \otimes \mathbb{Q} \left[\begin{array}{c} \text{Tree with 2 vertices} \\ \text{Tree with 2 vertices} \end{array} \right] + \mathbb{Q} \left[\begin{array}{c} \text{Tree with 2 vertices} \\ \text{Tree with 2 vertices} \end{array} \right] \otimes \mathbb{Q} \left[\begin{array}{c} \text{Tree with 2 vertices} \\ \text{Tree with 2 vertices} \end{array} \right] \\ &\quad + \mathbb{Q} \left[\begin{array}{c} \text{Tree with 2 vertices} \\ \text{Tree with 2 vertices} \end{array} \right] \otimes \mathbb{Q} \left[\begin{array}{c} \text{Tree with 2 vertices} \\ \text{Tree with 2 vertices} \end{array} \right] + \mathbb{Q} \left[\begin{array}{c} \text{Tree with 2 vertices} \\ \text{Tree with 2 vertices} \end{array} \right] \otimes 1. \end{aligned}$$

2.3. CAMBRIAN TUPLES

This section is devoted to a natural extension of our results on twin Cambrian trees and the Baxter-Cambrian algebra to arbitrary intersections of Cambrian congruences. Since the results presented here are straightforward generalizations of that of Sections 2.1 and 2.2, all proofs of this section are left to the reader.

2.3.1. Combinatorics of Cambrian tuples. As observed in Remark 43, pairs of twin Cambrian trees can as well be thought of as pairs of Cambrian trees on opposite signature whose union is acyclic. We extend this idea to arbitrary signatures. For an ℓ -tuple \mathcal{T} and $k \in [\ell]$, we denote by $\mathcal{T}_{[k]}$ the k th element of \mathcal{T} .

Definition 70. A **Cambrian ℓ -tuple** is a ℓ -tuple \mathcal{T} of Cambrian trees $\mathcal{T}_{[k]}$ on the same vertex set, and whose union forms an acyclic graph. The **signature** of \mathcal{T} is the ℓ -tuple of signatures $\mathcal{E}(\mathcal{T}) := [\varepsilon(\mathcal{T}_{[1]}), \dots, \varepsilon(\mathcal{T}_{[\ell]})]$. Let $\mathbf{Camb}(\mathcal{E})$ denote the set of Cambrian ℓ -tuples of signature \mathcal{E} .

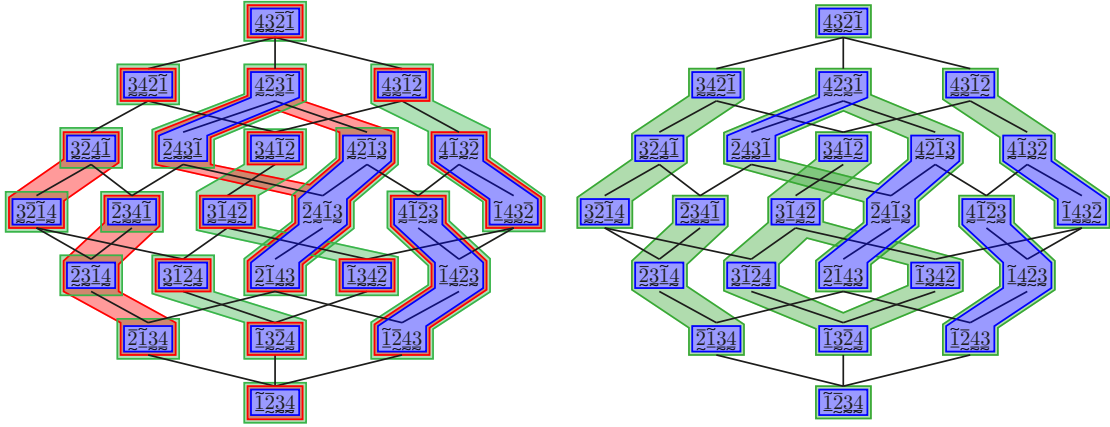


FIGURE 30. (Left) The $[-+---, +----]$ -Cambrian classes (blue) are the intersections of the $(-+---)$ -Cambrian classes (red) and the $(+----)$ -Cambrian classes (green). (Right) $[-+---, +----]$ -Cambrian (blue) and boolean (green) congruence classes on the weak order.

Proposition 74. *Two ℓ -signed permutations $\tau, \tau' \in \mathfrak{S}_{\pm\ell}$ are Cambrian congruent if and only if they have the same \mathbf{P}_ℓ -symbol:*

$$\tau \equiv_\ell \tau' \iff \mathbf{P}_\ell(\tau) = \mathbf{P}_\ell(\tau').$$

Proposition 75. *The ε -Cambrian class indexed by the Cambrian ℓ -tuple \mathcal{T} is the intersection of the $\mathcal{E}_{[k]}$ -Cambrian classes indexed by $\mathcal{T}_{[k]}$ over $k \in [\ell]$.*

We now present the rotation operation on Cambrian ℓ -tuples.

Definition 76. *Let \mathcal{T} be a Cambrian ℓ -tuple and consider an edge $i \rightarrow j$ of the union $\bigcup_{k \in [\ell]} \mathcal{T}_{[k]}$. We say that the edge $i \rightarrow j$ is **rotatable** if either $i \rightarrow j$ is an edge or i and j are incomparable in each tree $\mathcal{T}_{[k]}$ (note that $i \rightarrow j$ is an edge in at least one of these trees since it belongs to their union). If $i \rightarrow j$ is rotatable in \mathcal{T} , its **rotation** transforms \mathcal{T} to the ℓ -tuple of trees $\mathcal{T}' := [\mathcal{T}'_1, \dots, \mathcal{T}'_\ell]$, where \mathcal{T}'_k is obtained by rotation of $i \rightarrow j$ in $\mathcal{T}_{[k]}$ if possible and $\mathcal{T}'_k = \mathcal{T}_{[k]}$ otherwise.*

Proposition 77. *Rotating a rotatable edge $i \rightarrow j$ in a Cambrian ℓ -tuple \mathcal{T} yields a Cambrian ℓ -tuple \mathcal{T}' with the same signature.*

Consider the **increasing rotation graph** whose vertices are \mathcal{E} -Cambrian tuples and whose arcs are increasing rotations $\mathcal{T} \rightarrow \mathcal{T}'$, i.e. for which $i < j$ in Definition 76. This graph is illustrated on Figure 31 for the signature 2-tuple $\mathcal{E} = [-+---, +----]$.

Proposition 78. *For any cover relation $\tau < \tau'$ in the weak order on $\mathfrak{S}^\mathcal{E}$, either $\mathbf{P}_\ell(\tau) = \mathbf{P}_\ell(\tau')$ or $\mathbf{P}_\ell(\tau) \rightarrow \mathbf{P}_\ell(\tau')$ in the increasing rotation graph.*

It follows that the increasing rotation graph on \mathcal{E} -Cambrian tuples is acyclic. We call **\mathcal{E} -Cambrian poset** its transitive closure. In other words, the previous statement says that the map \mathbf{P}_ℓ defines a poset homomorphism from the weak order on $\mathfrak{S}^\mathcal{E}$ to the \mathcal{E} -Cambrian poset. This homomorphism is in fact a lattice homomorphism.

Proposition 79. *The \mathcal{E} -Cambrian poset is a lattice quotient of the weak order on $\mathfrak{S}^\mathcal{E}$.*

The \mathcal{E} -Cambrian lattice has natural geometric realizations, similar to the geometric realizations of the Baxter-Cambrian lattice. Namely, for a signature ℓ -tuple \mathcal{E} , the cones $C(\mathcal{T}) := C(\bigcup_{k \in [\ell]} \mathcal{T}_{[k]})$ for all \mathcal{E} -Cambrian tuples \mathcal{T} form (together with all their faces) a complete polyhedral fan that we call the **\mathcal{E} -Cambrian fan**. It is the common refinement of the $\mathcal{E}_{[k]}$ -Cambrian fans for $k \in [\ell]$. It is therefore the normal fan of the Minkowski sum of the associahedra $\text{Asso}(\mathcal{E}_{[k]})$ for $k \in [\ell]$. An example is illustrated on Figure 32. The 1-skeleton of this polytope, oriented in the direction

of $(n, \dots, 1) - (1, \dots, n) = \sum_{i \in [n]} (n+1-2i)e_i$, is the Hasse diagram of the \mathcal{E} -Cambrian lattice. Finally, the \mathcal{E} -Cambrian \mathbf{P}_ℓ -symbol can be read geometrically as

$$\mathcal{T} = \mathbf{P}_\ell(\tau) \iff C(\mathcal{T}) \subseteq C(\tau) \iff C^\circ(\mathcal{T}) \supseteq C^\circ(\tau).$$

2.3.2. Cambrian tuple Hopf Algebra. In this section, we construct a Hopf algebra indexed by Cambrian ℓ -tuples, similar to the Baxter-Cambrian algebra. Exactly as we needed to consider the Hopf algebra \mathbf{FQSym}_\pm on signed permutations when constructing the Cambrian algebra to keep track of the signature, we now need to consider a natural extension of \mathbf{FQSym} on ℓ -signed permutation to keep track of the ℓ signatures of \mathcal{E} .

The *shifted shuffle product* $\tau \sqcup \tau'$ (resp. *convolution product* $\tau \star \tau'$) of two ℓ -signed permutations τ, τ' is still defined as the shifted product (resp. convolution product) where signs travel with their values (resp. stay at their positions). When $\ell = 2$ and the two signatures are marked with $\bar{}/_-$ and $\tilde{}/_-$ respectively, we have for example

$$\begin{aligned} \bar{1}\bar{2} \sqcup \bar{2}\bar{3}\bar{1} &= \{\bar{1}\bar{2}\bar{4}\bar{5}\bar{3}, \bar{1}\bar{4}\bar{2}\bar{5}\bar{3}, \bar{1}\bar{4}\bar{5}\bar{2}\bar{3}, \bar{1}\bar{4}\bar{5}\bar{3}\bar{2}, \bar{4}\bar{1}\bar{2}\bar{5}\bar{3}, \bar{4}\bar{1}\bar{5}\bar{2}\bar{3}, \bar{4}\bar{1}\bar{5}\bar{3}\bar{2}, \bar{4}\bar{5}\bar{1}\bar{2}\bar{3}, \bar{4}\bar{5}\bar{1}\bar{3}\bar{2}, \bar{4}\bar{5}\bar{3}\bar{1}\bar{2}\}, \\ \bar{1}\bar{2} \star \bar{2}\bar{3}\bar{1} &= \{\bar{1}\bar{2}\bar{4}\bar{5}\bar{3}, \bar{1}\bar{3}\bar{4}\bar{5}\bar{2}, \bar{1}\bar{4}\bar{3}\bar{5}\bar{2}, \bar{1}\bar{5}\bar{3}\bar{4}\bar{2}, \bar{2}\bar{3}\bar{4}\bar{5}\bar{1}, \bar{2}\bar{4}\bar{3}\bar{5}\bar{1}, \bar{2}\bar{5}\bar{3}\bar{4}\bar{1}, \bar{3}\bar{4}\bar{2}\bar{5}\bar{1}, \bar{3}\bar{5}\bar{2}\bar{4}\bar{1}, \bar{4}\bar{5}\bar{2}\bar{3}\bar{1}\}. \end{aligned}$$

We denote by $\mathbf{FQSym}_{\pm\ell}$ the Hopf algebra with basis $(F_\tau)_{\tau \in \mathfrak{S}_{\pm\ell}}$ indexed by ℓ -signed permutations and whose product and coproduct are defined by

$$F_\tau \cdot F_{\tau'} = \sum_{\sigma \in \tau \sqcup \tau'} F_\sigma \quad \text{and} \quad \Delta F_\sigma = \sum_{\tau \in \tau \star \tau'} F_\tau \otimes F_{\tau'}.$$

Remark 80 (Cambrian algebra vs. G -colored binary tree algebra). Checking that these product and coproduct produce a Hopf algebra is standard. It even extends to a Hopf algebra \mathbf{FQSym}_G on G -colored permutations for an arbitrary semigroup G , see *e.g.* [NT10, BH08, BH06]. In these papers, the authors use this algebra \mathbf{FQSym}_G to defined G -colored subalgebras from congruence relations on permutations, see in particular [BH06]. Note that our construction of the Cambrian algebra and of the tuple Cambrian algebra really differs from the construction of [BH06] as our congruence relations depend on the signs, while their congruences do not.

We denote by \mathbf{Camb}_ℓ the vector subspace of $\mathbf{FQSym}_{\pm\ell}$ generated by the elements

$$\mathbb{P}_\mathcal{T} := \sum_{\substack{\tau \in \mathfrak{S}_{\pm\ell} \\ \mathbf{P}_\ell(\tau) = \mathcal{T}}} F_\tau = \sum_{\tau \in \mathcal{L}\left(\bigcup_{k \in [\ell]} \mathcal{T}_{[k]}\right)} F_\tau,$$

for all Cambrian ℓ -tuples \mathcal{T} . For example, for the Cambrian tuple of Figure 29 (left), we have

$$\mathbb{P} \left[\begin{array}{c} \text{Diagram of Cambrian tuple} \end{array} \right] = \mathbb{F}_{\bar{2}\bar{1}\bar{7}\bar{5}\bar{3}\bar{4}\bar{6}} + \mathbb{F}_{\bar{2}\bar{7}\bar{1}\bar{5}\bar{3}\bar{4}\bar{6}} + \mathbb{F}_{\bar{2}\bar{7}\bar{5}\bar{1}\bar{3}\bar{4}\bar{6}} + \mathbb{F}_{\bar{7}\bar{2}\bar{1}\bar{5}\bar{3}\bar{4}\bar{6}} + \mathbb{F}_{\bar{7}\bar{2}\bar{5}\bar{1}\bar{3}\bar{4}\bar{6}} + \mathbb{F}_{\bar{7}\bar{5}\bar{2}\bar{1}\bar{3}\bar{4}\bar{6}}.$$

Theorem 81. \mathbf{Camb}_ℓ is a Hopf subalgebra of $\mathbf{FQSym}_{\pm\ell}$.

As for the Cambrian algebra, the product and coproduct of \mathbb{P} -basis elements of the ℓ -Cambrian algebra \mathbf{Camb}_ℓ can be described directly in terms of combinatorial operations on Cambrian ℓ -tuples.

PRODUCT The product in the ℓ -Cambrian algebra \mathbf{Camb}_ℓ can be described in terms of intervals in ℓ -Cambrian lattices. We denote by $\mathcal{E}\mathcal{E}' := [\mathcal{E}_{[1]}\mathcal{E}'_{[1]}, \dots, \mathcal{E}_{[\ell]}\mathcal{E}'_{[\ell]}]$ the componentwise concatenation of two signature ℓ -tuples $\mathcal{E}, \mathcal{E}'$. Similarly, for two Cambrian ℓ -tuples $\mathcal{T}, \mathcal{T}'$, we define

$$\mathcal{T} \nearrow \bar{\mathcal{T}}' := \left[\mathcal{T}_{[1]} \nearrow \bar{\mathcal{T}}'_{[1]}, \dots, \mathcal{T}_{[\ell]} \nearrow \bar{\mathcal{T}}'_{[\ell]} \right] \quad \text{and} \quad \mathcal{T} \searrow \bar{\mathcal{T}}' := \left[\mathcal{T}_{[1]} \searrow \bar{\mathcal{T}}'_{[1]}, \dots, \mathcal{T}_{[\ell]} \searrow \bar{\mathcal{T}}'_{[\ell]} \right].$$

Proposition 82. For any two Cambrian ℓ -tuples \mathcal{T} and \mathcal{T}' , the product $\mathbb{P}_\mathcal{T} \cdot \mathbb{P}_{\mathcal{T}'}$ is given by

$$\mathbb{P}_\mathcal{T} \cdot \mathbb{P}_{\mathcal{T}'} = \sum_S \mathbb{P}_S,$$

where S runs over the interval between $\mathcal{T} \nearrow \bar{\mathcal{T}}'$ and $\mathcal{T} \searrow \bar{\mathcal{T}}'$ in the $\mathcal{E}(\mathcal{T})\mathcal{E}(\mathcal{T}')$ -Cambrian lattice.

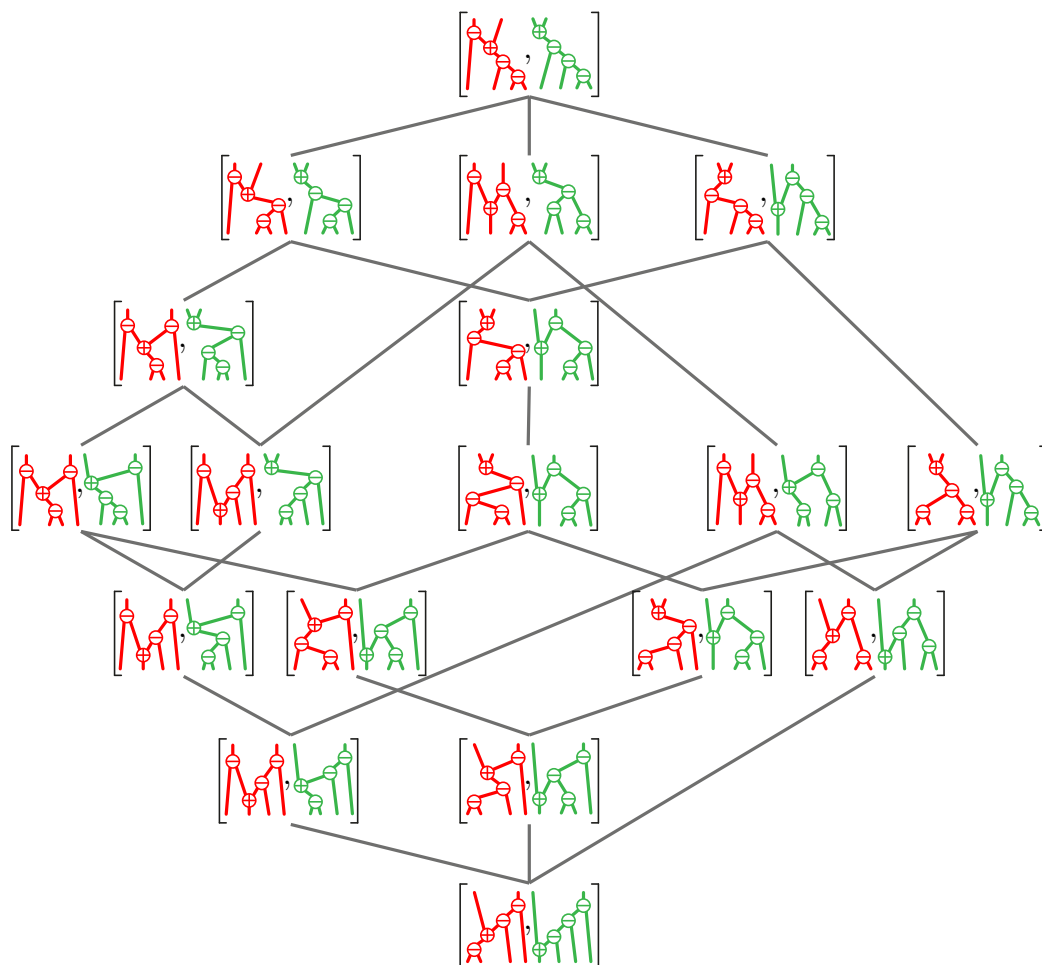


FIGURE 31. The $[-+---, +----]$ -Cambrian lattice on Cambrian tuples. See also Figure 30.

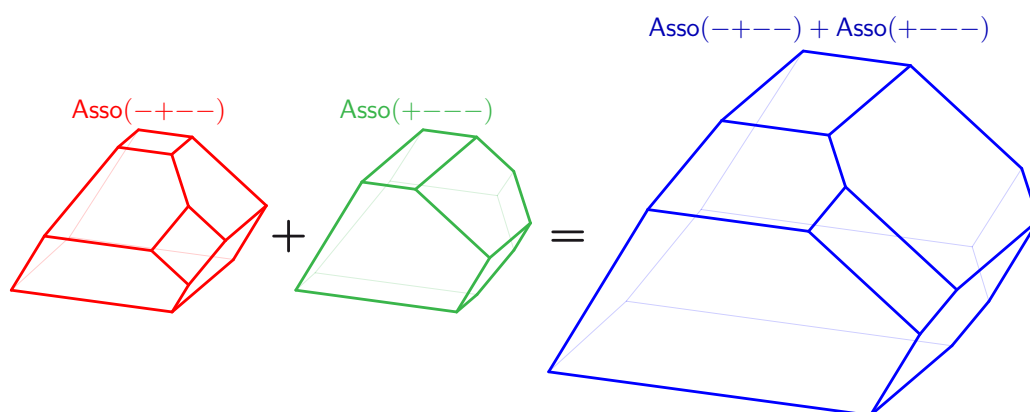


FIGURE 32. The Minkowski sum (blue, right) of the associahedra $\text{Asso}(-+---)$ (red, left) and $\text{Asso}(+----)$ (green, middle) gives a realization of the $[-+---, +----]$ -Cambrian lattice, represented in Figures 30 and 31.

Remark 83 (Multiplicative bases). Similar to the multiplicative bases defined in Section 1.3 and Remark 65, the bases $\mathbb{E}^{\mathcal{T}}$ and $\mathbb{H}^{\mathcal{T}}$ defined by

$$\mathbb{E}^{\mathcal{T}} := \sum_{\mathcal{T} \leq \mathcal{T}'} \mathbb{P}_{\mathcal{T}'} \quad \text{and} \quad \mathbb{H}^{\mathcal{T}} := \sum_{\mathcal{T}' \leq \mathcal{T}} \mathbb{P}_{\mathcal{T}'}$$

are multiplicative since

$$\mathbb{E}^{\mathcal{T}} \cdot \mathbb{E}^{\mathcal{T}'} = \mathbb{E}^{\mathcal{T} \nearrow \mathcal{T}'} \quad \text{and} \quad \mathbb{H}^{\mathcal{T}} \cdot \mathbb{H}^{\mathcal{T}'} = \mathbb{H}^{\mathcal{T} \nwarrow \mathcal{T}'}$$

The \mathbb{E} -indecomposable elements are precisely the Cambrian ℓ -tuples \mathcal{T} such that all linear extensions of the union $\bigcup_{k \in [\ell]} \mathcal{T}_{[k]}$ are indecomposable. In particular, \mathcal{T} is \mathbb{E} -indecomposable as soon as one of the $\mathcal{T}_{[k]}$ is \mathbb{E} -indecomposable, but this condition is not necessary. The \mathbb{E} -indecomposable \mathcal{E} -Cambrian tuples form an ideal of the \mathcal{E} -Cambrian lattice, but this ideal is not principal.

COPRODUCT A *cut* γ of a Cambrian ℓ -tuple \mathcal{S} is a cut of the union $\bigcup_{k \in [\ell]} \mathcal{S}_{[k]}$. It defines a cut $\gamma_{[k]}$ on each Cambrian tree $\mathcal{S}_{[k]}$. We denote by

$$A(\mathcal{S}, \gamma) := A(\mathcal{S}_{[1]}, \gamma_{[1]}) \times \cdots \times A(\mathcal{S}_{[\ell]}, \gamma_{[\ell]}) \quad \text{and} \quad B(\mathcal{S}, \gamma) := B(\mathcal{S}_{[1]}, \gamma_{[1]}) \times \cdots \times B(\mathcal{S}_{[\ell]}, \gamma_{[\ell]}).$$

Proposition 84. *For any Cambrian ℓ -tuple \mathcal{S} , the coproduct $\Delta \mathbb{P}_{\mathcal{S}}$ is given by*

$$\Delta \mathbb{P}_{\mathcal{S}} = \sum_{\gamma} \left(\sum_{\mathcal{B} \in B(\mathcal{S}, \gamma)} \mathbb{P}_{\mathcal{B}} \right) \otimes \left(\sum_{\mathcal{A} \in A(\mathcal{S}, \gamma)} \mathbb{P}_{\mathcal{A}} \right),$$

where γ runs over all cuts of \mathcal{S} .

2.3.3. Dual Cambrian tuple Hopf Algebra. We now consider the dual Hopf algebra of Camb_{ℓ} . Again, the following statement is automatic from Theorem 81.

Theorem 85. *The graded dual Camb_{ℓ}^* of the ℓ -Cambrian algebra is isomorphic to the image of $\text{FQSym}_{\pm \ell}^*$ under the canonical projection*

$$\pi : \mathbb{C}\langle A \rangle \longrightarrow \mathbb{C}\langle A \rangle / \equiv_{\ell},$$

where \equiv_{ℓ} denotes the ℓ -Cambrian congruence. The dual basis $\mathbb{Q}_{\mathcal{T}}$ of $\mathbb{P}_{\mathcal{T}}$ is expressed as $\mathbb{Q}_{\mathcal{T}} = \pi(\mathbb{G}_{\mathcal{T}})$, where τ is any linear extension of $\bigcup_{k \in [\ell]} \mathcal{T}_{[k]}$.

We now describe the product and coproduct in Camb_{ℓ}^* in terms of combinatorial operations on Cambrian ℓ -tuples. We use the definitions and notations introduced in Section 1.2.3.

PRODUCT The product in Camb_{ℓ}^* can be described using gaps and laminations similarly to Proposition 29. For two Cambrian trees T and T' and a shuffle s of the signatures $\varepsilon(T)$ and $\varepsilon(T')$, we still denote by $T_s \setminus T'$ the tree described in Section 1.2.3. For two Cambrian ℓ -tuples \mathcal{T} and \mathcal{T}' , with trees of size n and n' respectively, and for a shuffle s of $[n]$ and $[n']$, we write

$$\mathcal{T}_s \setminus \mathcal{T}' := [\mathcal{T}_{[1]} \setminus_s \mathcal{T}'_{[1]}, \dots, \mathcal{T}_{[\ell]} \setminus_s \mathcal{T}'_{[\ell]}],$$

where we see s as a shuffle of the signatures $\varepsilon(\mathcal{T}_{[k]})$ and $\varepsilon(\mathcal{T}'_{[k]})$.

Proposition 86. *For any two Cambrian ℓ -tuples $\mathcal{T}, \mathcal{T}'$, the product $\mathbb{Q}_{\mathcal{T}} \cdot \mathbb{Q}_{\mathcal{T}'}$ is given by*

$$\mathbb{Q}_{\mathcal{T}} \cdot \mathbb{Q}_{\mathcal{T}'} = \sum_s \mathbb{Q}_{\mathcal{T}_s \setminus \mathcal{T}'},$$

where s runs over all shuffles of $[n]$ and $[n']$ (where n and n' denote the respective sizes of the trees of \mathcal{T} and \mathcal{T}').

COPRODUCT The coproduct in Camb_{ℓ}^* can be described combinatorially as in Proposition 30. For a Cambrian ℓ -tuple \mathcal{S} , with trees of size n , and a gap $\gamma \in \{0, \dots, n\}$, we define

$$L(\mathcal{S}, \gamma) = [L(\mathcal{T}_{[1]}, \gamma), \dots, L(\mathcal{T}_{[\ell]}, \gamma)] \quad \text{and} \quad R(\mathcal{S}, \gamma) = [R(\mathcal{T}_{[1]}, \gamma), \dots, R(\mathcal{T}_{[\ell]}, \gamma)].$$

Proposition 87. *For any Cambrian ℓ -tuple \mathcal{S} , the coproduct $\Delta \mathbb{Q}_{\mathcal{S}}$ is given by*

$$\Delta \mathbb{Q}_{\mathcal{S}} = \sum_{\gamma} \mathbb{Q}_{L(\mathcal{S}, \gamma)} \otimes \mathbb{Q}_{R(\mathcal{S}, \gamma)},$$

where γ runs over all gaps between consecutive positions in $[n]$ (where n denotes the size of the trees of \mathcal{T}).

Part 3. The Schröder-Cambrian Hopf Algebra

3.1. SCHRÖDER-CAMBRIAN TREES

We already insisted on the fact that the bases of M. Malvenuto and C. Reutenauer’s algebra on permutations, of J.-L. Loday and M. Ronco’s algebra on binary trees, and of L. Solomon’s descent algebra correspond to the vertices of the permutahedra, of the associahedra, and of the cubes respectively. In [Cha00], F. Chapoton generalized these algebras to three Hopf algebras with bases indexed by all faces of the permutahedra, of the associahedra, and of the cubes. To conclude the paper, we show that F. Chapoton’s construction extends as well to the Cambrian setting. We obtain the Schröder-Cambrian Hopf algebra with basis indexed by all faces of all associahedra of C. Hohlweg and C. Lange. It is also a good occasion to observe relevant combinatorial properties of Schröder-Cambrian trees, which correspond to the faces of these associahedra.

3.1.1. Schröder-Cambrian trees. The faces of J.-L. Loday’s n -dimensional associahedron correspond to *Schröder trees* with $n + 1$ leaves, *i.e.* trees where each internal node has at least 2 children. We first recall the Cambrian counterpart of these trees, which correspond to all faces of C. Hohlweg and C. Lange’s associahedra (see Section 3.1.6). These trees were defined in [LP13] as “spines” of dissections of polygons, see Remark 90.

Definition 88. Consider a signature $\varepsilon \in \pm^n$. For $X \subseteq [n]$, we denote by $X^+ := \{x \in X \mid \varepsilon_x = +\}$ and $X^- := \{x \in X \mid \varepsilon_x = -\}$. A *Schröder ε -Cambrian tree* is a directed tree T with vertex set V endowed with a vertex labeling $p : V \rightarrow 2^{[n]} \setminus \emptyset$ such that

- (i) the labels of T partition $[n]$, *i.e.* $v \neq w \in V \Rightarrow p(v) \cap p(w) = \emptyset$ and $\bigcup_{v \in V} p(v) = [n]$;
- (ii) each vertex $v \in V$ has one incoming (resp. outgoing) subtree $T_{v,I}$ for each interval I of $[n] \setminus p(v)^-$ (resp. of $[n] \setminus p(v)^+$) and all labels of $T_{v,I}$ are subsets of I .

For $p \geq 0$ and $\varepsilon \in \pm^n$, we denote by $\text{SchrCamb}^{\geq p}(\varepsilon)$ the set of Schröder ε -Cambrian trees with at most $n - p$ internal nodes, and we define $\text{SchrCamb}^{\geq p}(n) := \bigsqcup_{\varepsilon \in \pm^n} \text{SchrCamb}^{\geq p}(\varepsilon)$ and $\text{SchrCamb}^{\geq p} := \bigsqcup_{n \in \mathbb{N}} \text{SchrCamb}^{\geq p}(n)$. They correspond to associahedron faces of dimension at least p . Finally, we simply omit the superscript $\geq p$ in the previous notations to denote Schröder-Cambrian trees with arbitrary many internal nodes. Note that this defines a filtration

$$\text{SchrCamb} = \bigcup_{p \geq 1} \text{SchrCamb}^{\geq p} \quad \text{with} \quad \text{SchrCamb}^{\geq 0} \supset \text{SchrCamb}^{\geq 1} \supset \dots$$

Definition 89. A *k -leveled Schröder ε -Cambrian tree* is a directed tree with vertex set V endowed with two labelings $p : V \rightarrow 2^{[n]} \setminus \emptyset$ and $q : V \rightarrow [k]$ which respectively define a Schröder ε -Cambrian tree and an increasing tree (meaning that q is surjective and $v \rightarrow w$ in T implies that $q(v) < q(w)$).

A Schröder-Cambrian tree and a 3-leveled Schröder-Cambrian tree are represented in Figure 33. Note that each level of a k -leveled Schröder ε -Cambrian tree may contain more than one node.

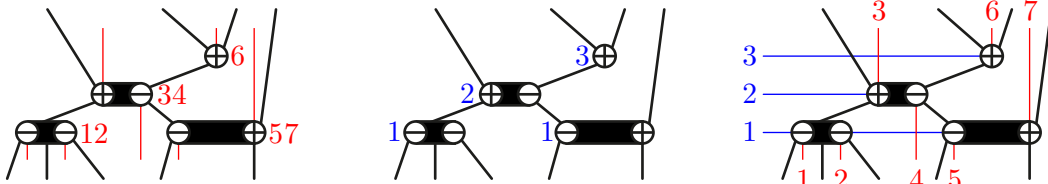


FIGURE 33. A Schröder-Cambrian tree (left), an increasing tree (middle), and a 3-leveled Schröder-Cambrian tree (right).

Remark 90 (Spines of dissections). Exactly as ε -Cambrian trees correspond to triangulations of the $(n + 2)$ -gon P^ε (see Remark 4), Schröder ε -Cambrian trees correspond to all dissections of P^ε . See Figure 34 and refer to [LP13] for details.

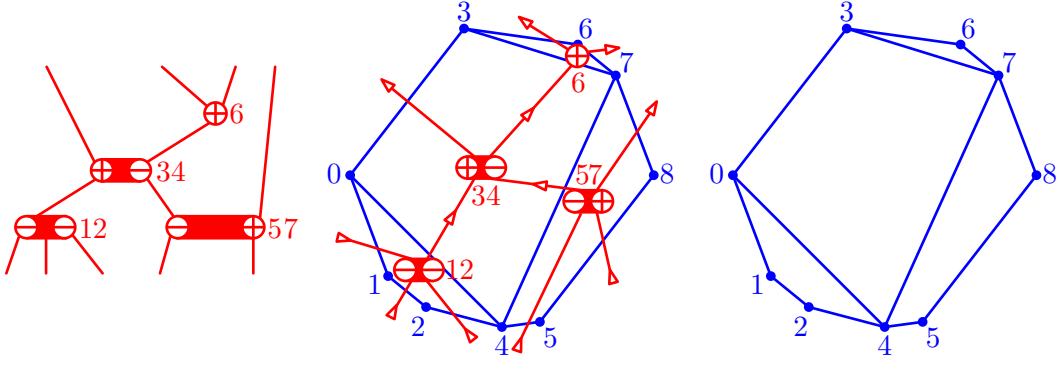


FIGURE 34. Schröder-Cambrian trees (left) and dissections (right) are dual to each other (middle).

Remark 90 immediately implies that the number of Schröder ε -Cambrian trees with k nodes is the number of $(n - k)$ -dimensional faces of the associahedron, and is therefore independent of the signature ε . An alternative proof based on generating trees is mentioned in Remark 108.

Proposition 91. *For any signature $\varepsilon \in \pm^n$, the number of Schröder ε -Cambrian trees with k internal nodes is*

$$\frac{1}{k+1} \binom{n+2+k}{k+1} \binom{n-1}{k+1},$$

see [OEIS, A033282].

3.1.2. Schröder-Cambrian correspondence. We now define an analogue of the Cambrian correspondence and Cambrian \mathbf{P} -symbol, which will map the faces of the permutahedron to the faces of C. Hohlweg and C. Lange’s associahedra. Recall first that the $(n - k)$ -dimensional faces of the n -dimensional permutahedron correspond to *surjections* from $[n]$ to $[k]$, or equivalently to *ordered partitions* of $[n]$ into k parts. See Figure 35. We denote (abusively) by π^{-1} the ordered partition corresponding to a surjection $\pi : [n] \rightarrow [k]$, i.e. given by $\pi^{-1} := \pi^{-1}(\{1\}) \mid \pi^{-1}(\{2\}) \mid \cdots \mid \pi^{-1}(\{k\})$. Conversely, we denote (abusively) by λ^{-1} the surjection corresponding to an ordered partition $\lambda = \lambda_1 \mid \lambda_2 \mid \cdots \mid \lambda_k$, i.e. such that each i belongs to the part $\lambda_{\lambda^{-1}(i)}$. We represent graphically a surjection $\pi : [n] \rightarrow [k]$ by the $(k \times n)$ -table with a dot in row $\pi(j)$ in each column j . Therefore, we represent an ordered partition $\lambda := \lambda_1 \mid \cdots \mid \lambda_k$ of $[n]$ by the $(k \times n)$ -table with a dot in row i and column j for each $j \in \lambda_i$. See Figure 36 (left). In this paper, we work with ordered partitions rather than surjections to match better the presentation of the previous sections: the permutations of $[n]$ used in the previous sections have to be thought of as ordered partitions of $[n]$ into n parts. We denote by $\mathfrak{P}_n^{\geq p}$ the set of ordered partitions of $[n]$ into at most $n - p$ parts, and we set $\mathfrak{P}^{\geq p} := \bigsqcup_{n \in \mathbb{N}} \mathfrak{P}_n^{\geq p}$. It correspond to permutahedron faces of dimension at least p . As previously, we omit the superscript $\geq p$ in these notations to forget this dimension restriction.

A *signed ordered partition* is an ordered partition table where each dot receives a $+$ or $-$ sign. For a signature $\varepsilon \in \pm^n$, we denote by $\mathfrak{P}_\varepsilon^{\geq p}$ the set of ordered partitions of $[n]$ into at most $n - p$ parts signed by ε , and we set

$$\mathfrak{P}_\pm^{\geq p} := \bigsqcup_{n \in \mathbb{N}, \varepsilon \in \pm^n} \mathfrak{P}_\varepsilon^{\geq p}.$$

We omit again the superscript $\geq p$ in the previous notations to denote signed ordered partitions with arbitrarily many parts. This gives again a filtration

$$\mathfrak{P}_\pm = \bigcup_{p \geq 1} \mathfrak{P}_\pm^{\geq p} \quad \text{with} \quad \mathfrak{P}_\pm^{\geq 0} \supset \mathfrak{P}_\pm^{\geq 1} \supset \dots$$

Given such a signed ordered partition λ , we construct a leveled Schröder-Cambrian tree $\Theta^*(\lambda)$ as follows. As a preprocessing, we represent the table of λ , we draw a vertical wall below the negative dots and above the positive dots, and we connect into nodes the dots at the same level which are not separated by a wall. Note that we might obtain several nodes per level. We then

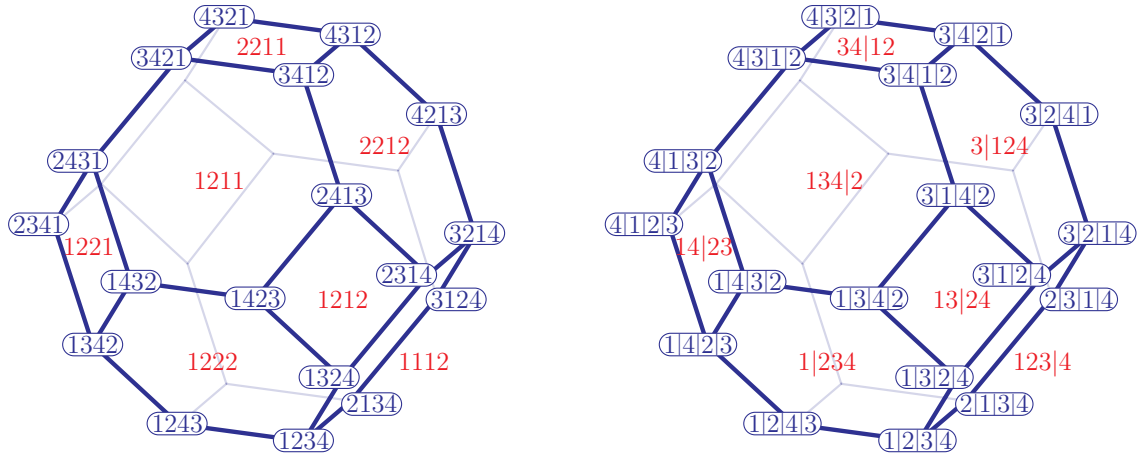


FIGURE 35. The 3-dimensional permutahedron $\text{Perm}([4])$. Its $(4-k)$ -dimensional faces correspond equivalently to the surjections from $[4]$ to $[k]$ (left), or to the ordered partitions of $[4]$ into k parts (right). Vertices are in blue and facets in red. The reader is invited to label the edges accordingly.

sweep the table from bottom to top as follows. The procedure starts with an incoming strand in between any two consecutive negative values. At each level, each node v (connected set of dots) gathers all strands in the region below and visible from v (*i.e.* not hidden by a vertical wall) and produces one strand in each region above and visible from v . The procedure finished with an outgoing strand in between any two consecutive positive values. See Figure 36.

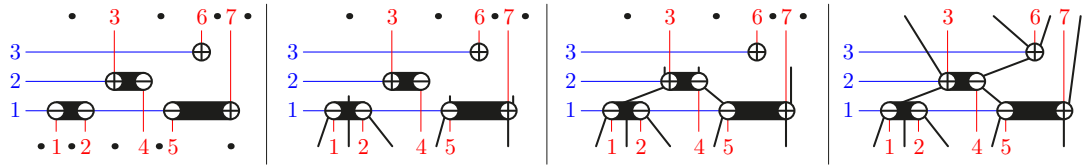


FIGURE 36. The insertion algorithm on the signed ordered partition $\underline{1257}|\overline{34}|\overline{6}$.

Proposition 92 ([LP13]). *The map Θ^* is a bijection from signed ordered partitions to leveled Schröder-Cambrian trees.*

We define the \mathbf{P}^* -symbol of a signed ordered partition λ as the Schröder-Cambrian tree $\mathbf{P}^*(\lambda)$ defined by $\Theta^*(\lambda)$. Note that an ordered partition of $[n]$ into k parts is sent to a Schröder-Cambrian tree with at least k internal nodes, since some levels can be split into several nodes. In other words, the fibers of the Schröder-Cambrian \mathbf{P}^* -symbol respect the filtrations $(\mathfrak{P}_{\pm}^{\geq p})_{p \in \mathbb{N}}$ and $(\text{SchrCamb}^{\geq p})_{p \in \mathbb{N}}$, in the sense that

$$(\mathbf{P}^*)^{-1}(\text{SchrCamb}^{\geq p}) \subseteq \mathfrak{P}_{\pm}^{\geq p}.$$

The following characterization of the fibers of the map \mathbf{P}^* is immediate from the description of the Schröder-Cambrian correspondence. For a Schröder-Cambrian tree T , we write $i \rightarrow j$ in T if the node of T containing i is below the node of T containing j , and $i \sim j$ in T if i and j belong to the same node of T . We say that i and j are *incomparable* in T when $i \not\rightarrow j$, $j \not\rightarrow i$, and $i \not\sim j$.

Proposition 93. *For any Schröder ε -Cambrian tree T and signed ordered partition $\lambda \in \mathfrak{P}_{\varepsilon}$, we have $\mathbf{P}^*(\lambda) = T$ if and only if $i \sim j$ in T implies $\lambda^{-1}(i) = \lambda^{-1}(j)$ and $i \rightarrow j$ in T implies $\lambda^{-1}(i) < \lambda^{-1}(j)$. In other words, λ is obtained from a linear extension of T by merging parts which label incomparable vertices of T .*

Example 94. When $\varepsilon = (+)^n$, the Schröder-Cambrian tree $\mathbf{P}^*(\lambda)$ is the increasing tree of λ^{-1} . Here, the *increasing tree* $\text{IT}(\pi)$ of a surjection $\pi = \pi^{(1)}1\pi^{(2)}1\dots1\pi^{(p)}$ is defined inductively by grafting the increasing trees $\text{IT}(\pi^{(1)}), \dots, \text{IT}(\pi^{(p)})$ from left to right on a bottom root labeled by 1. Similarly, when $\varepsilon = (-)^n$, the Schröder-Cambrian tree $\mathbf{P}^*(\lambda)$ is the decreasing tree of λ^{-1} . Here, the *decreasing tree* $\text{DT}(\pi)$ of a surjection $\pi = \pi^{(1)}k\pi^{(2)}k\dots k\pi^{(p)}$ from $[n]$ to $[k]$ is defined inductively by grafting the decreasing trees $\text{DT}(\pi^{(1)}), \dots, \text{DT}(\pi^{(p)})$ from left to right on a top root labeled by k . See Figure 37.

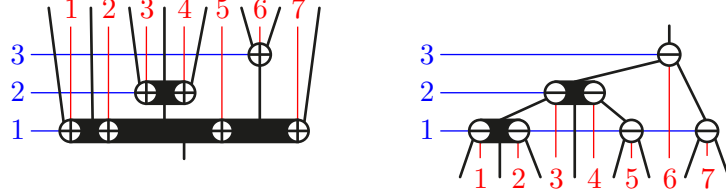


FIGURE 37. The insertion procedure produces increasing Schröder trees when the signature is constant positive (left) and decreasing Schröder trees when the signature is constant negative (right).

Remark 95 (Schröder-Cambrian correspondence on dissections). Similar to Remark 11, we can describe the map \mathbf{P}^* on the dissections of the polygon P^ε . Namely the dissection dual to the Schröder-Cambrian tree $\mathbf{P}^*(\lambda)$ is the union of the paths π_0, \dots, π_n where π_i is the path between vertices 0 and $n+1$ of P^ε passing through the vertices in the symmetric difference $\varepsilon^{-1}(-) \triangle (\bigcup_{j \in [i]} \lambda_j)$.

3.1.3. Schröder-Cambrian congruence. As for the Cambrian congruence, the fibers of the Schröder-Cambrian \mathbf{P}^* -symbol define a congruence relation on signed ordered partitions, which can be expressed by rewriting rules.

Definition 96. For a signature $\varepsilon \in \pm^n$, the Schröder ε -Cambrian congruence is the equivalence relation on \mathfrak{P}_ε defined as the transitive closure of the rewriting rules

$$U|\mathbf{a}|c|V \equiv_\varepsilon^* U|\mathbf{a}c|V \equiv_\varepsilon^* U|c|\mathbf{a}|V,$$

where \mathbf{a}, \mathbf{c} are parts while U, V are sequences of parts of $[n]$, and there exists $\mathbf{a} < b < \mathbf{c}$ such that $\varepsilon_b = +$ and $b \in \bigcup U$, or $\varepsilon_b = -$ and $b \in \bigcup V$. The Schröder-Cambrian congruence is the equivalence relation \equiv^* on \mathfrak{P}_\pm obtained as the union of all Schröder ε -Cambrian congruences.

For example, $\underline{1257}|\underline{34}|\underline{6} \equiv^* \underline{12}|\underline{57}|\underline{34}|\underline{6} \equiv^* \underline{57}|\underline{12}|\underline{34}|\underline{6} \not\equiv^* \underline{57}|\underline{34}|\underline{12}|\underline{6}$.

Proposition 97. Two signed ordered partitions $\lambda, \lambda' \in \mathfrak{P}_\pm$ are Schröder-Cambrian congruent if and only if they have the same \mathbf{P}^* -symbol:

$$\lambda \equiv^* \lambda' \iff \mathbf{P}^*(\lambda) = \mathbf{P}^*(\lambda').$$

Proof. It boils down to observe that two consecutive parts \mathbf{a} and \mathbf{c} of an ordered partition $U|\mathbf{a}|c|V$ in a fiber $(\mathbf{P}^*)^{-1}(T)$ can be merged to $U|\mathbf{a}c|V$ and even exchanged to $U|c|\mathbf{a}|V$ while staying in $(\mathbf{P}^*)^{-1}(T)$ precisely when they belong to distinct subtrees of a node of T . They are therefore separated by the vertical wall below (resp. above) a value b with $\mathbf{a} < b < \mathbf{c}$ and such that $\varepsilon_b = -$ and $b \in V$ (resp. $\varepsilon_b = +$ and $b \in U$). \square

3.1.4. Weak order on ordered partitions and Schröder-Cambrian lattices. In order to define the Schröder counterpart of the Cambrian lattice, we first need to extend the weak order on permutations to all ordered partitions. This was done by D. Krob, M. Latapy, J.-C. Novelli, H. D. Phan and S. Schwer in [KLN⁺01]. See also [BHK^N01] for representation theoretic properties of this order and [PR06] for an extension to all finite Coxeter systems.

Definition 98. The **coinversion map** $\text{coinv}(\lambda) : \binom{[n]}{2} \rightarrow \{-1, 0, 1\}$ of an ordered partition $\lambda \in \mathfrak{P}_n$ is the map defined for $i < j$ by

$$\text{coinv}(\lambda)(i, j) = \begin{cases} -1 & \text{if } \lambda^{-1}(i) < \lambda^{-1}(j), \\ 0 & \text{if } \lambda^{-1}(i) = \lambda^{-1}(j), \\ 1 & \text{if } \lambda^{-1}(i) > \lambda^{-1}(j). \end{cases}$$

It is also called the **inversion map** of the surjection λ^{-1} .

Definition 99. There are two natural poset structures on \mathfrak{P}_n :

- The **refinement poset** \subseteq defined by $\lambda \subseteq \lambda'$ if $|\text{coinv}(\lambda)(i, j)| \geq |\text{coinv}(\lambda')(i, j)|$ for all $i < j$. It is isomorphic to the face lattice of the permutahedron $\text{Perm}(n)$, and respects the filtration $(\mathfrak{P}_n^{\geq p})_{p \in [n]}$.
- The **weak order** \leq defined by $\lambda \leq \lambda'$ if $\text{coinv}(\lambda)(i, j) \leq \text{coinv}(\lambda')(i, j)$ for all $i < j$.

These two posets are represented in Figure 38 for $n = 3$.

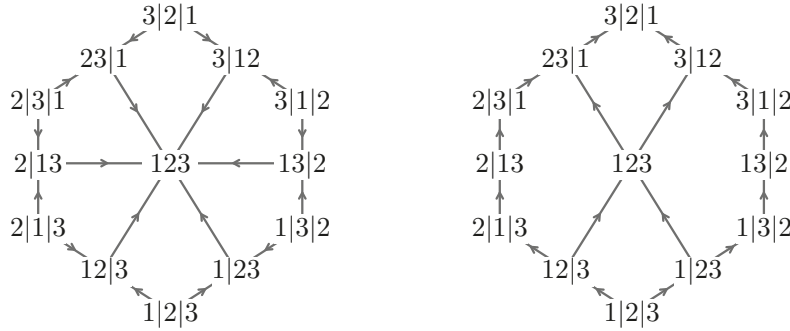


FIGURE 38. The refinement poset (left) and the weak order (right) on \mathfrak{P}_3 .

Note that the restriction of the weak order to \mathfrak{S}_n is the classical weak order on permutations, which is a lattice. This property was extended to the weak order on \mathfrak{P}_n in [KLN⁺01].

Proposition 100 ([KLN⁺01]). *The weak order $<$ on the set of ordered partitions \mathfrak{P}_n is a lattice.*

In the following statement and throughout the remaining of the paper, we define for $X, Y \subset \mathbb{N}$

$$X \ll Y \iff \max(X) < \min(Y) \iff x < y \text{ for all } x \in X \text{ and } y \in Y.$$

Proposition 101 ([KLN⁺01]). *The cover relations of the weak order $<$ on \mathfrak{P}_n are given by*

$$\begin{aligned} \lambda_1 | \cdots | \lambda_i | \lambda_{i+1} | \cdots | \lambda_k &< \lambda_1 | \cdots | \lambda_i \lambda_{i+1} | \cdots | \lambda_k && \text{if } \lambda_i \ll \lambda_{i+1}, \\ \lambda_1 | \cdots | \lambda_i \lambda_{i+1} | \cdots | \lambda_k &< \lambda_1 | \cdots | \lambda_i | \lambda_{i+1} | \cdots | \lambda_k && \text{if } \lambda_{i+1} \ll \lambda_i. \end{aligned}$$

We now extend the Cambrian lattice on Cambrian trees to a lattice on all Schröder-Cambrian trees. For the constant signature $\varepsilon = (-)^n$, the order considered below was already defined by P. Palacios and M. Ronco in [PR06], although its lattice structure (Proposition 105) was not discussed in there.

Definition 102. Consider a Schröder ε -Cambrian tree T , and an edge $e = \{v, w\}$ of T . We denote by T/e the tree obtained by contracting e in T . It is again a Schröder ε -Cambrian tree. We say that the contraction is **increasing** if $p(u) \ll p(v)$ and **decreasing** if $p(v) \ll p(u)$. Otherwise, we say that the contraction is **non-monotone**.

Definition 103. There are two natural poset structures on $\text{SchrCamb}_\varepsilon$:

- The **contraction poset** \subseteq defined as the transitive closure of the relation $T \subseteq T/e$ for any Schröder ε -Cambrian tree T and edge $e \in T$. It is isomorphic to the face lattice of the associahedron $\text{Asso}(\varepsilon)$, and respects the filtration $(\text{SchrCamb}_\varepsilon^{\geq p})_{p \in [n]}$.
- The **Schröder ε -Cambrian poset** $<$ defined as the transitive closure of the relation $T < T/e$ (resp. $T/e < T$) for any Schröder ε -Cambrian tree T and any edge $e \in T$ defining an increasing (resp. decreasing) contraction.

These two posets are represented in Figure 39 for the signature $+--$. Observe that there are two non-monotone contractions. Note also that the restriction of the Schröder ε -Cambrian poset $<$ to the ε -Cambrian trees is the ε -Cambrian lattice.

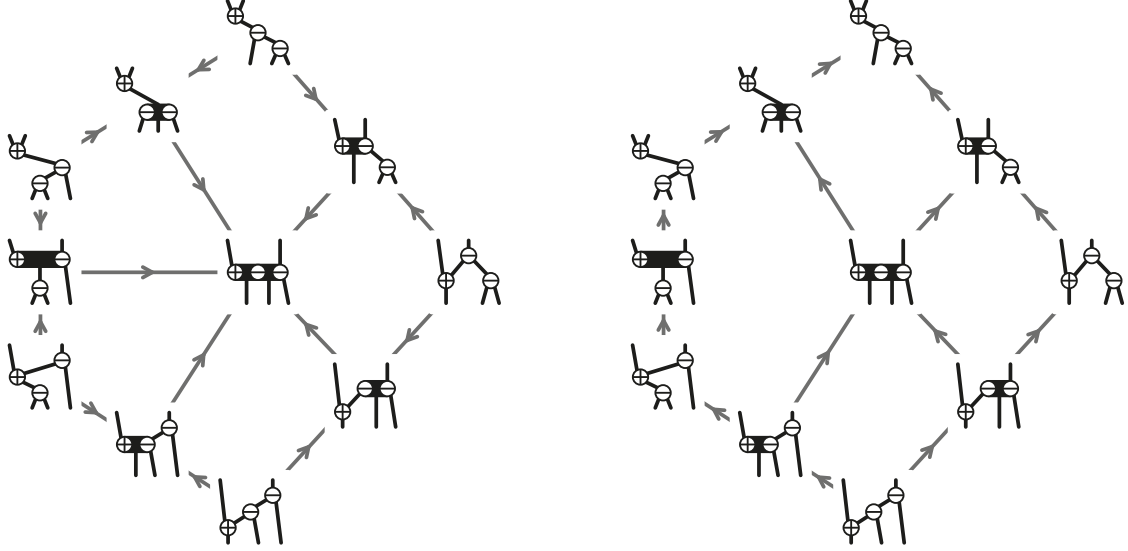


FIGURE 39. The contraction poset (left) and the Schröder $(+--)$ -Cambrian poset (right) on Schröder $(+--)$ -Cambrian trees.

Proposition 104. *The map \mathbf{P}^* defines a poset homomorphism from the weak order on \mathfrak{P}_ε to the Schröder ε -Cambrian poset on $\text{SchrCamb}(\varepsilon)$.*

Proof. Let $\lambda < \lambda'$ be a cover relation in the weak order on \mathfrak{P}_ε . Assume that λ' is obtained by merging the parts $\lambda_i \ll \lambda_{i+1}$ of λ (the other case being symmetric). Let u denote the rightmost node of $\mathbf{P}^*(\lambda)$ at level i , and v the leftmost node of $\mathbf{P}^*(\lambda)$ at level $i + 1$. If u and v are not comparable, then $\mathbf{P}^*(\lambda) = \mathbf{P}^*(\lambda')$. Otherwise, there is an edge $u \rightarrow v$ in $\mathbf{P}^*(\lambda)$ and $\mathbf{P}^*(\lambda')$ is obtained by the increasing contraction of $u \rightarrow v$ in $\mathbf{P}^*(\lambda)$. \square

Proposition 105. *For any signature $\varepsilon \in \pm^n$, the Schröder ε -Cambrian poset on Schröder ε -Cambrian trees is a lattice quotient of the weak order on ordered partitions of $[n]$.*

This proposition is proved by the following two lemmas, similar to N. Reading’s approach [Rea06].

Lemma 106. *The Schröder ε -Cambrian classes are intervals of the weak order.*

Proof. Let T be a Schröder ε -Cambrian tree, with vertex labeling $p : V \rightarrow 2^{[n]} \setminus \emptyset$. Consider a linear extension of T , *i.e.* an ordered partition λ whose parts are the labels of T and such that $p(v)$ appears before $p(w)$ for $v \rightarrow w$ in T . If v and w are two incomparable nodes of T , then either $p(v) \ll p(w)$ or $p(w) \ll p(v)$ since they are separated by a wall. By successive exchanges, there exists a linear extension λ_{\min} (resp. λ_{\max}) of T such that $p(v)$ appears before (resp. after) $p(w)$ for any two incomparable nodes v and w such that $p(v) \ll p(w)$. By construction, the (i, j) -entries of the coinversion tables of λ_{\min} and λ_{\max} are given for $i < j$ by

$$\text{coinv}(\lambda_{\min})(i, j) = \begin{cases} 1 & \text{if } j \rightarrow i \text{ in } T, \\ 0 & \text{if } i \sim j \text{ in } T, \\ -1 & \text{otherwise,} \end{cases} \quad \text{and} \quad \text{coinv}(\lambda_{\max})(i, j) = \begin{cases} -1 & \text{if } i \rightarrow j \text{ in } T, \\ 0 & \text{if } i \sim j \text{ in } T, \\ 1 & \text{otherwise.} \end{cases}$$

It follows that the fiber of T under \mathbf{P}^* is the weak order interval $[\lambda_{\min}, \lambda_{\max}]$. \square

Lemma 107. *Let λ and λ' be two signed ordered partitions from distinct Schröder ε -Cambrian classes C and C' . If $\lambda < \lambda'$ then $\min(C) < \min(C')$ and $\max(C) < \max(C')$ (all in weak order).*

Proof. We prove the result for maximums, the proof for the minimums being similar. We first observe that we can assume that λ' covers λ in weak order, so that there exists a position i such that either $\lambda'_i = \lambda_i \cup \lambda_{i+1}$ and $\lambda_i \ll \lambda_{i+1}$, or $\lambda_i = \lambda'_i \cup \lambda'_{i+1}$ and $\lambda'_{i+1} \ll \lambda'_i$. The proof then works by induction on the weak order distance between λ and $\max(C)$. If $\lambda = \max(C)$, the result is immediate as $\max(C) = \lambda < \lambda' \leq \max(C')$. Otherwise, consider an ordered partition μ in C covering λ in weak order. There exists a position $j \neq i$ such that $\mu_j = \lambda_j \cup \lambda_{j+1}$ and $\lambda_j \ll \lambda_{j+1}$, or $\lambda_j = \mu_j \cup \mu_{j+1}$ and $\mu_{j+1} \ll \mu_j$. We now distinguish four cases, according to the relative positions of i and j :

- (1) If $|i - j| > 1$, then the local changes from λ to λ' at position i and from λ to μ at position j are independent. Define μ' to be the ordered partition obtained from λ by performing both local changes at i and at j . We then check that $\lambda' \equiv^* \mu'$ since any witness for the equivalence $\lambda \equiv^* \mu$ is also a witness for the equivalence $\lambda' \equiv^* \mu'$. Moreover, $\mu < \mu'$.
- (2) Otherwise, the local changes at i and j are not independent anymore. We therefore need to treat various cases separately, depending on whether the local changes from λ to λ' and from λ to μ are merging or splitting, and on the respective positions of these local changes. In all cases below, $\mathbf{a}, \mathbf{b}, \mathbf{c}$ are parts of $[n]$ such that $\mathbf{a} \ll \mathbf{b} \ll \mathbf{c}$, while U, V are sequences of parts of $[n]$.
 - If $\lambda = U|\mathbf{a}|\mathbf{b}|\mathbf{c}|V$, $\lambda' = U|\mathbf{ab}|\mathbf{c}|V$, and $\mu = U|\mathbf{a}|\mathbf{bc}|V$, then define $\mu' := U|\mathbf{abc}|V$. Any witness for the Schröder-Cambrian congruence $\lambda \equiv^* \mu$ is also a witness for the Schröder-Cambrian congruence $\lambda' \equiv^* \mu'$. Moreover, we have $\mu < \mu'$ since $\mathbf{a} \ll \mathbf{bc}$. The same arguments yield the same conclusions in the following cases:
 - if $\lambda = U|\mathbf{a}|\mathbf{b}|\mathbf{c}|V$, $\lambda' = U|\mathbf{a}|\mathbf{bc}|V$, and $\mu = U|\mathbf{ab}|\mathbf{c}|V$, then define $\mu' := U|\mathbf{abc}|V$.
 - if $\lambda = U|\mathbf{abc}|V$, $\lambda' = U|\mathbf{c}|\mathbf{ab}|V$, and $\mu = U|\mathbf{bc}|\mathbf{a}|V$, then define $\mu' := U|\mathbf{c}|\mathbf{b}|\mathbf{a}|V$.
 - if $\lambda = U|\mathbf{abc}|V$, $\lambda' = U|\mathbf{bc}|\mathbf{a}|V$, and $\mu = U|\mathbf{c}|\mathbf{ab}|V$, then define $\mu' := U|\mathbf{c}|\mathbf{b}|\mathbf{a}|V$.
 - If $\lambda = U|\mathbf{a}|\mathbf{bc}|V$, $\lambda' = U|\mathbf{abc}|V$, and $\mu = U|\mathbf{a}|\mathbf{c}|\mathbf{b}|V$, then define $\mu' := U|\mathbf{c}|\mathbf{ab}|V$. Any witness for the Schröder-Cambrian congruence $\lambda \equiv^* \mu$ is also a witness for the Schröder-Cambrian congruence $\lambda' \equiv^* \mu'$. Moreover $\mu < \mu'$ by comparison of the coinversion tables. The same arguments yield the same conclusions in the case:
 - if $\lambda = U|\mathbf{ab}|\mathbf{c}|V$, $\lambda' = U|\mathbf{abc}|V$, and $\mu = U|\mathbf{b}|\mathbf{a}|\mathbf{c}|V$, then define $\mu' := U|\mathbf{bc}|\mathbf{a}|V$.
 - If $\lambda = U|\mathbf{a}|\mathbf{bc}|V$, $\lambda' = U|\mathbf{a}|\mathbf{c}|\mathbf{b}|V$, and $\mu = U|\mathbf{abc}|V$, then define $\mu' := U|\mathbf{c}|\mathbf{ab}|V$. Let d be a witness for the Schröder-Cambrian congruence $\lambda \equiv^* \mu$, that is, $\mathbf{a} < d < \mathbf{bc}$ and either $\varepsilon_d = -$ and $d \in V$, or $\varepsilon_d = +$ and $d \in U$. Then d is also a witness for the Schröder-Cambrian congruences $\lambda' = U|\mathbf{a}|\mathbf{c}|\mathbf{b}|V \equiv^* U|\mathbf{ac}|\mathbf{b}|V \equiv^* U|\mathbf{c}|\mathbf{a}|\mathbf{b}|V \equiv^* U|\mathbf{c}|\mathbf{ab}|V = \mu'$. Moreover, we have $\mu < \mu'$ since $\mathbf{ab} \ll \mathbf{c}$. The same arguments yield the same conclusions in the case:
 - if $\lambda = U|\mathbf{ab}|\mathbf{c}|V$, $\lambda' = U|\mathbf{b}|\mathbf{a}|\mathbf{c}|V$, and $\mu = U|\mathbf{abc}|V$, then define $\mu' := U|\mathbf{bc}|\mathbf{a}|V$.

In all cases, we have $\lambda \equiv^* \mu < \mu' \equiv^* \lambda'$. Since μ is closer to $\max(C)$ than λ , we obtain that $\max(C) < \max(C')$ by induction hypothesis. The proof for minimums is identical. \square

Remark 108 (Extremal elements and pattern avoidance). Since the Schröder-Cambrian classes are generated by rewriting rules, their minimal elements are precisely the ordered partitions avoiding the patterns $\mathbf{c}|\mathbf{a} - \mathbf{b}$ and $\bar{\mathbf{b}} - \mathbf{c}|\mathbf{a}$, while their maximal elements are precisely the ordered partitions avoiding the patterns $\mathbf{a}|\mathbf{c} - \mathbf{b}$ and $\bar{\mathbf{b}} - \mathbf{a}|\mathbf{c}$. This enables us to construct a generating tree for these permutations. Similar arguments as in Section 1.1.4 could thus provide an alternative proof of Proposition 91.

3.1.5. Canopy. We define the canopy of a Schröder-Cambrian tree using the same observation as for Cambrian trees: in any Schröder-Cambrian tree, the numbers i and $i + 1$ appear either in the same label, or in two comparable labels.

Definition 109. The *canopy* of a Schröder-Cambrian tree T is the sequence $\mathbf{can}^*(T) \in \{-, 0, +\}$ defined by

$$\mathbf{can}^*(T)_i = \begin{cases} - & \text{if } i \text{ appears above } i + 1 \text{ in } T, \\ 0 & \text{if } i \text{ and } i + 1 \text{ appear in the same label in } T, \\ + & \text{if } i \text{ is below } i + 1 \text{ in } T. \end{cases}$$

For example, the canopy of the Schröder-Cambrian tree of Figure 33 (left) is $0+0-+-$. The following statement provides an immediate analogue of Proposition 23 in the Schröder-Cambrian setting. We define the *recoil* sequence of an ordered partition $\lambda \in \mathfrak{P}_n$ as $\mathbf{rec}^*(\lambda) \in \{-, 0, +\}^{n-1}$, where $\mathbf{rec}^*(\lambda)_i = \text{coinv}(\lambda)(i, i+1)$.

Proposition 110. *The maps \mathbf{P}^* , \mathbf{can}^* , and \mathbf{rec}^* define the following commutative diagram of lattice homomorphism*

$$\begin{array}{ccc} \mathfrak{P}_\varepsilon & \xrightarrow{\mathbf{rec}^*} & \{-, 0, +\}^{n-1} \\ & \searrow \mathbf{P}^* & \nearrow \mathbf{can}^* \\ & \text{SchrCamb}(\varepsilon) & \end{array}$$

Figure 40 (left) illustrates this proposition for the signature $+--$.

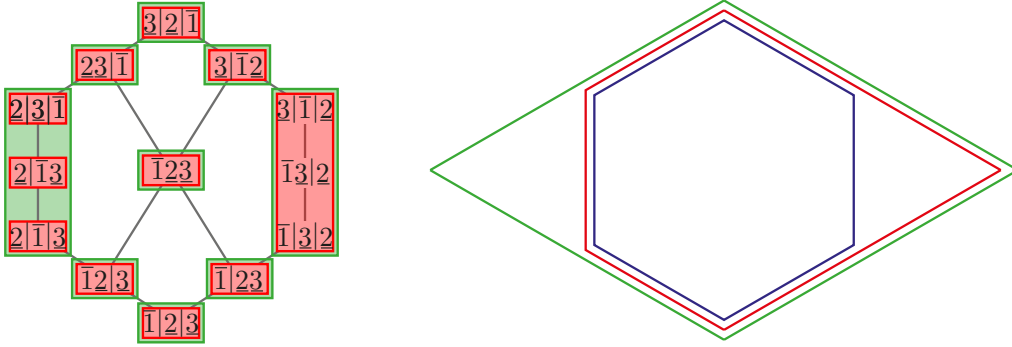


FIGURE 40. The fibers of the maps \mathbf{P}^* (red) and \mathbf{rec}^* (green) on the weak orders of \mathfrak{S}_{+--} (left), and the geometric realization of these maps (right).

3.1.6. Geometric realizations. We close this section with the geometric motivation of Schröder-Cambrian trees. More details can be found in [LP13]. We still denote by e_1, \dots, e_n the canonical basis of \mathbb{R}^n and by \mathbb{H} the hyperplane of \mathbb{R}^n orthogonal to $\sum e_i$. We define the *incidence cone* $C(\mathbb{T})$ and the *braid cone* $C^\circ(\mathbb{T})$ of a directed tree \mathbb{T} with vertices labeled by subsets of $[n]$ as

$$\begin{aligned} C(\mathbb{T}) &:= \text{cone}\{e_i - e_j \mid \text{for all } i \rightarrow j \text{ or } i \sim j \text{ in } \mathbb{T}\} \quad \text{and} \\ C^\circ(\mathbb{T}) &:= \{x \in \mathbb{H} \mid x_i \leq x_j \text{ for all } i \rightarrow j \text{ or } i \sim j \text{ in } \mathbb{T}\}. \end{aligned}$$

These two cones lie in the space \mathbb{H} and are polar to each other. Note that if \mathbb{T} has k nodes, then $\dim(C^\circ(\mathbb{T})) = k - 1$. For an ordered partition $\lambda \in \mathfrak{P}_n$, we denote by $C(\lambda)$ and $C^\circ(\lambda)$ the incidence and braid cone of the chain $\lambda_1 \rightarrow \dots \rightarrow \lambda_n$. Finally, for a vector $\chi \in \{-, 0, +\}^{n-1}$, we denote by $C(\chi)$ and $C^\circ(\chi)$ the incidence and braid cone of the oriented path $1 - \dots - n$, where $i \rightarrow i+1$ if $\chi_i = +$, $i \leftarrow i+1$ if $\chi_i = -$, and i and $i+1$ are merged to the same node if $\chi_i = 0$.

As explained in Section 1.1.7, the collections of cones

$$\{C^\circ(\lambda) \mid \lambda \in \mathfrak{P}_n\}, \quad \{C^\circ(\mathbb{T}) \mid \mathbb{T} \in \text{SchrCamb}_\varepsilon\}, \quad \text{and} \quad \{C^\circ(\chi) \mid \chi \in \{-, 0, +\}^{n-1}\}$$

form complete simplicial fans, which are the normal fans of the classical permutahedron $\text{Perm}(n)$, of C. Hohlweg and C. Lange's associahedron $\text{Asso}(\varepsilon)$, and of the parallelepiped $\text{Para}(n)$ respectively. See Figures 40 (right) and 10 for 2- and 3-dimensional examples of these polytopes.

The incidence and braid cones also characterize the maps \mathbf{P}^* , \mathbf{can}^* , and \mathbf{rec}^* as follows

$$\begin{aligned} \mathbb{T} = \mathbf{P}^*(\lambda) &\iff C(\mathbb{T}) \subseteq C(\lambda) \iff C^\circ(\mathbb{T}) \supseteq C^\circ(\lambda), \\ \chi = \mathbf{can}^*(\mathbb{T}) &\iff C(\chi) \subseteq C(\mathbb{T}) \iff C^\circ(\chi) \supseteq C^\circ(\mathbb{T}), \\ \chi = \mathbf{rec}^*(\lambda) &\iff C(\chi) \subseteq C(\lambda) \iff C^\circ(\chi) \supseteq C^\circ(\lambda). \end{aligned}$$

Finally, the weak order, the Schröder-Cambrian lattice and the boolean lattice correspond to the lattice of faces of the permutahedron $\text{Perm}(n)$, associahedron $\text{Asso}(\varepsilon)$ and parallelepiped $\text{Para}(n)$, oriented in the direction $(n, \dots, 1) - (1, \dots, n) = \sum_{i \in [n]} (n+1-2i)e_i$.

3.2. SCHRÖDER-CAMBRIAN HOPF ALGEBRA

In this section, we define the Schröder-Cambrian Hopf algebra SchrCamb , extending simultaneously the Cambrian Hopf algebra and F. Chapoton's Hopf algebra on Schröder trees [Cha00]. We construct the algebra SchrCamb as a subalgebra of a signed version of F. Chapoton's Hopf algebra on ordered partitions [Cha00]. We then also consider the dual algebra SchrCamb^* as a quotient of the dual Hopf algebra on signed ordered partitions.

3.2.1. Shuffle and convolution products on signed ordered partitions. We define here a natural analogue of the shifted shuffle and convolution products of Section 1.2.1 on ordered partitions. Equivalent definitions in the world of surjections can be found in [Cha00]. Here, we stick to ordered partitions to match our presentation of the Cambrian algebra in Section 1.2.

We first define two restrictions on ordered partitions. Consider an ordered partition μ of $[n]$ into k parts. As already mentioned earlier, we represent graphically μ by the $(k \times n)$ -table with a dot in row i and column j for each $j \in \mu_i$. For $I \subseteq [k]$, we let $n_I := |\{j \in [n] \mid \exists i \in I, j \in \mu_i\}|$ and we denote by $\mu|_I$ the ordered partition of $[n_I]$ into $|I|$ parts whose table is obtained from the table of μ by deleting all rows not in I and standardizing to get a $(|I| \times n_I)$ -table. Similarly, for $J \subseteq [n]$, we let $k_J := |\{i \in [k] \mid \exists j \in J, j \in \mu_i\}|$ and we denote by $\mu^{[J]}$ the ordered partition of $[|J|]$ into k_J parts whose table is obtained from the table of μ by deleting all columns not in J and standardizing to get a $(k_J \times |J|)$ -table. These restrictions are illustrated in Figure 41.

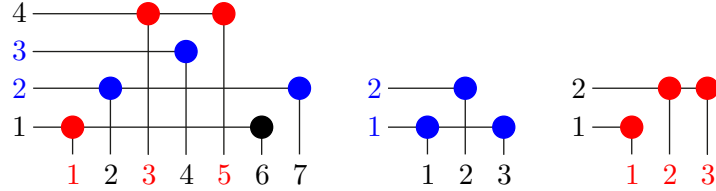


FIGURE 41. The tables of the ordered partitions $\mu = 16|27|4|35$ (left) and of its restrictions $\mu|_{\{2,3\}}$ (middle) and $\mu^{[1,3,5]}$ (right).

We define the *shifted concatenation* $\lambda\bar{\lambda}'$, the *shifted shuffle product* $\lambda\bar{\sqcup}\lambda'$, and the *convolution product* $\lambda\star\lambda'$ of two (unsigned) ordered partitions λ of $[n]$ with k parts and λ' of $[n']$ with k' parts as

$$\lambda\bar{\lambda}' := \lambda_1 | \cdots | \lambda_k | n + \lambda'_1 | \cdots | n + \lambda'_{k'}, \quad \text{where } n + \lambda'_i := \{n + j \mid j \in \lambda'_i\}$$

$$\lambda\bar{\sqcup}\lambda' := \left\{ \mu \in \mathfrak{P}_{n+n'} \mid \mu|_{\{1,\dots,n\}} = \lambda \text{ and } \mu|_{\{n+1,\dots,n+n'\}} = \lambda' \right\},$$

$$\text{and } \lambda\star\lambda' := \left\{ \mu \in \mathfrak{P}_{n+n'} \mid \mu|_{\{1,\dots,k\}} = \lambda \text{ and } \mu|_{\{k+1,\dots,k+k'\}} = \lambda' \right\}.$$

For example,

$$1|2\bar{\sqcup}2|13 = \{1|2|4|35, 1|24|35, 1|4|2|35, 1|4|235, 1|4|35|2, 14|2|35, 14|235, 14|35|2, 4|1|2|35, 4|1|235, 4|1|35|2, 4|135|2, 4|35|1|2\},$$

$$1|2\star 2|13 = \{1|2|4|35, 1|3|4|25, 1|4|3|25, 1|5|3|24, 2|3|4|15, 2|4|3|15, 2|5|3|14, 3|4|2|15, 3|5|2|14, 4|5|2|13\}.$$

Graphically, the table of the shifted concatenation $\lambda\bar{\lambda}'$ contains the table of λ as the bottom left block and the table of λ' as the top right block. The tables in the shifted shuffle product $\lambda\bar{\sqcup}\lambda'$ (resp. in the convolution product $\lambda\star\lambda'$) are obtained by shuffling the rows (resp. columns) of the table of $\lambda\bar{\lambda}'$. See Figure 42.

Remark 111. (i) Note that the shifted shuffle and convolution products are compatible with the filtration $(\mathfrak{P}_n^{\geq p})_{p \in [n]}$:

$$\mathfrak{P}_n^{\geq p} \bar{\sqcup} \mathfrak{P}_{n'}^{\geq p'} \subseteq \mathfrak{P}_{n+n'}^{\geq p+p'} \quad \text{and} \quad \mathfrak{P}_n^{\geq p} \star \mathfrak{P}_{n'}^{\geq p'} \subseteq \mathfrak{P}_{n+n'}^{\geq p+p'}.$$

(ii) By projection on the quotient $\mathfrak{P}/\mathfrak{P}^{\geq 1} \simeq \mathfrak{S}$, the (signed) shifted shuffle and convolution products coincide with the description of Section 1.2.1.

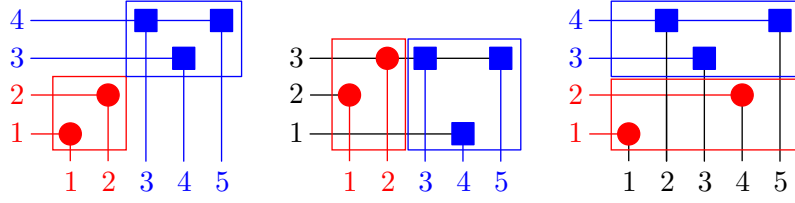


FIGURE 42. The table of the shifted concatenation $\lambda\bar{\lambda}'$ (left) has two blocks containing the tables of the ordered partitions $\lambda = 1|2$ and $\lambda' = 2|31$. Elements of the shifted shuffle product $\lambda\bar{\sqcup}\lambda'$ (middle) and of the convolution product $\lambda\star\lambda'$ (right) are obtained by shuffling respectively the rows and columns of the table of $\lambda\bar{\lambda}'$.

(iii) The shifted product of ordered partitions preserves intervals of the weak order. Namely,

$$[\lambda, \mu] \bar{\sqcup} [\lambda', \mu'] = [\lambda\bar{\lambda}', \bar{\mu}'\mu].$$

These definitions extend to signed ordered partitions: signs travel with their values in the signed shifted shuffle product, and stay at their positions in the signed convolution product.

3.2.2. Subalgebra of OrdPart_{\pm} . We denote by OrdPart_{\pm} the Hopf algebra with basis $(\mathbb{F}_{\lambda})_{\lambda \in \mathfrak{P}_{\pm}}$ and whose product and coproduct are defined by

$$\mathbb{F}_{\lambda} \cdot \mathbb{F}_{\lambda'} = \sum_{\mu \in \lambda \bar{\sqcup} \lambda'} \mathbb{F}_{\mu} \quad \text{and} \quad \Delta \mathbb{F}_{\mu} = \sum_{\lambda \star \lambda' = \mu} \mathbb{F}_{\lambda} \otimes \mathbb{F}_{\lambda'}.$$

Note that the Hopf algebra FQSym_{\pm} is isomorphic to the quotient $\text{OrdPart}_{\pm}/\text{OrdPart}_{\pm}^{\geq 1}$. Note also that the unsigned version of OrdPart_{\pm} is the dual of the algebra WQSym of word quasi-symmetric functions (also denoted NCQSym for non-commutative quasi-symmetric functions), see [BZ09, NT06].

Remark 112. The proof that OrdPart_{\pm} is indeed a Hopf algebra is left to the reader: it consists in translating F. Chapoton’s proof [Cha00] from surjections to signed ordered partitions. In fact, F. Chapoton’s Hopf algebras on faces of the permutahedra, associahedra, and cubes could be decorated by an arbitrary group, similar to the constructions in [NT10, BH08, BH06]. Once again the main point here is that the Schröder-congruence relations depend on the decoration.

We denote by SchrCamb the vector subspace of OrdPart_{\pm} generated by the elements

$$\mathbb{P}_{\mathbb{T}} := \sum_{\substack{\lambda \in \mathfrak{P}_{\pm} \\ \mathbf{P}^*(\lambda) = \mathbb{T}}} \mathbb{F}_{\lambda}$$

for all Schröder-Cambrian trees \mathbb{T} . For example, for the Schröder-Cambrian tree of Figure 33 (left), we have

$$\mathbb{P}_{\mathbb{T}} = \mathbb{F}_{\underline{12}|\underline{57}|\underline{34}|\bar{6}} + \mathbb{F}_{\underline{12}\underline{57}|\underline{34}|\bar{6}} + \mathbb{F}_{\underline{57}|\underline{12}|\underline{34}|\bar{6}}.$$

Note that the Hopf algebra Camb is isomorphic to the quotient $\text{SchrCamb}_{\pm}/\text{SchrCamb}_{\pm}^{\geq 1}$.

Theorem 113. *SchrCamb is a Hopf subalgebra of OrdPart_{\pm} .*

Proof. Similar to the proof of Theorem 24. □

As for the Cambrian algebra, the product and coproduct of \mathbb{P} -basis elements of the Schröder-Cambrian algebra SchrCamb can be described directly in terms of combinatorial operations on Schröder-Cambrian trees.

PRODUCT The product in the Schröder Cambrian algebra SchrCamb can again be described in terms of intervals in the Schröder-Cambrian lattice. Given two Schröder-Cambrian trees \mathbb{T}, \mathbb{T}' , we denote by $\mathbb{T} \nearrow \mathbb{T}'$ the Schröder $\varepsilon(\mathbb{T})\varepsilon(\mathbb{T}')$ -Cambrian tree obtained by grafting the rightmost

outgoing leaf of T on the leftmost incoming leaf of T' and shifting all labels of T' . We define similarly $T \searrow \bar{T}'$.

Proposition 114. *For any Schröder-Cambrian trees T, T' , the product $\mathbb{P}_T \cdot \mathbb{P}_{T'}$ is given by*

$$\mathbb{P}_T \cdot \mathbb{P}_{T'} = \sum_S \mathbb{P}_S,$$

where S runs over the interval between $T \nearrow \bar{T}'$ and $T \searrow \bar{T}'$ in the Schröder $\varepsilon(T)\varepsilon(T')$ -Cambrian lattice.

Proof. Similar to that of Proposition 25. \square

For example, we can compute the product

$$\begin{aligned} \mathbb{P}_{\begin{array}{c} \text{---} \\ \diagup \quad \diagdown \\ \text{---} \end{array}} \cdot \mathbb{P}_{\begin{array}{c} \text{---} \\ \diagdown \quad \diagup \\ \text{---} \end{array}} &= \mathbb{F}_{\bar{1}\bar{2}} \cdot (\mathbb{F}_{\bar{1}\bar{3}|\bar{2}\bar{4}} + \mathbb{F}_{\bar{1}\bar{3}|\bar{2}\bar{4}} + \mathbb{F}_{\bar{3}|\bar{1}\bar{2}\bar{4}}) \\ &= \left(\begin{array}{c} \mathbb{F}_{\bar{1}\bar{2}|\bar{3}|\bar{5}|\bar{4}\bar{6}} + \mathbb{F}_{\bar{1}\bar{2}|\bar{3}\bar{5}|\bar{4}\bar{6}} \\ + \mathbb{F}_{\bar{1}\bar{2}|\bar{5}|\bar{3}|\bar{4}\bar{6}} + \mathbb{F}_{\bar{1}\bar{2}\bar{5}|\bar{3}|\bar{4}\bar{6}} \\ + \mathbb{F}_{\bar{5}|\bar{1}\bar{2}|\bar{3}|\bar{4}\bar{6}} \end{array} \right) + \left(\begin{array}{c} \mathbb{F}_{\bar{1}\bar{2}\bar{3}|\bar{5}|\bar{4}\bar{6}} \\ + \mathbb{F}_{\bar{1}\bar{2}\bar{3}\bar{5}|\bar{4}\bar{6}} \\ + \mathbb{F}_{\bar{5}|\bar{1}\bar{2}\bar{3}|\bar{4}\bar{6}} \end{array} \right) + \left(\begin{array}{c} \mathbb{F}_{\bar{3}|\bar{1}\bar{2}|\bar{5}|\bar{4}\bar{6}} + \mathbb{F}_{\bar{3}|\bar{1}\bar{2}\bar{5}|\bar{4}\bar{6}} + \mathbb{F}_{\bar{3}|\bar{5}|\bar{1}\bar{2}|\bar{4}\bar{6}} \\ + \mathbb{F}_{\bar{3}\bar{5}|\bar{1}\bar{2}|\bar{4}\bar{6}} + \mathbb{F}_{\bar{5}|\bar{3}|\bar{1}\bar{2}|\bar{4}\bar{6}} + \mathbb{F}_{\bar{3}|\bar{5}|\bar{1}\bar{2}\bar{4}\bar{6}} \\ + \mathbb{F}_{\bar{3}\bar{5}|\bar{1}\bar{2}\bar{4}\bar{6}} + \mathbb{F}_{\bar{5}|\bar{3}|\bar{1}\bar{2}\bar{4}\bar{6}} + \mathbb{F}_{\bar{3}|\bar{5}|\bar{4}\bar{6}|\bar{1}\bar{2}} \\ + \mathbb{F}_{\bar{3}\bar{5}|\bar{4}\bar{6}|\bar{1}\bar{2}} + \mathbb{F}_{\bar{5}|\bar{3}|\bar{4}\bar{6}|\bar{1}\bar{2}} \end{array} \right) \\ &= \mathbb{P}_{\begin{array}{c} \text{---} \\ \diagup \quad \diagdown \\ \text{---} \end{array}} \otimes \mathbb{P}_{\begin{array}{c} \text{---} \\ \diagdown \quad \diagup \\ \text{---} \end{array}} + \mathbb{P}_{\begin{array}{c} \text{---} \\ \diagdown \quad \diagup \\ \text{---} \end{array}} \otimes \mathbb{P}_{\begin{array}{c} \text{---} \\ \diagdown \quad \diagup \\ \text{---} \end{array}} + \mathbb{P}_{\begin{array}{c} \text{---} \\ \diagdown \quad \diagup \\ \text{---} \end{array}} \otimes \mathbb{P}_{\begin{array}{c} \text{---} \\ \diagdown \quad \diagup \\ \text{---} \end{array}}. \end{aligned}$$

COPRODUCT The coproduct in the Schröder Cambrian algebra SchrCamb can again be described in terms of cuts. A *cut* of a Schröder-Cambrian tree S is a set γ of edges such that any geodesic vertical path in S from a down leaf to an up leaf contains precisely one edge of γ . We denote again by $A(S, \gamma)$ and $B(S, \gamma)$ the two Schröder-Cambrian forests above and below γ in S .

Proposition 115. *For any Schröder-Cambrian tree S , the coproduct $\Delta \mathbb{P}_S$ is given by*

$$\Delta \mathbb{P}_S = \sum_{\gamma} \left(\prod_{T \in B(S, \gamma)} \mathbb{P}_T \right) \otimes \left(\prod_{T' \in A(S, \gamma)} \mathbb{P}_{T'} \right),$$

where γ runs over all cuts of S .

Proof. Similar to that of Proposition 26. \square

For example, we can compute the coproduct

$$\begin{aligned} \Delta \mathbb{P}_{\begin{array}{c} \text{---} \\ \diagup \quad \diagdown \\ \text{---} \end{array}} &= \Delta (\mathbb{F}_{\bar{1}\bar{3}|\bar{2}\bar{4}} + \mathbb{F}_{\bar{1}\bar{3}|\bar{2}\bar{4}} + \mathbb{F}_{\bar{3}|\bar{1}\bar{2}\bar{4}}) \\ &= 1 \otimes \left(\begin{array}{c} \mathbb{F}_{\bar{1}\bar{3}|\bar{2}\bar{4}} \\ + \mathbb{F}_{\bar{1}\bar{3}|\bar{2}\bar{4}} \\ + \mathbb{F}_{\bar{3}|\bar{1}\bar{2}\bar{4}} \end{array} \right) + \mathbb{F}_{\bar{1}} \otimes \mathbb{F}_{\bar{2}|\bar{1}\bar{3}} + \mathbb{F}_{\bar{1}} \otimes \mathbb{F}_{\bar{1}\bar{2}\bar{3}} + \left(\begin{array}{c} \mathbb{F}_{\bar{1}\bar{2}} \\ + \mathbb{F}_{\bar{1}\bar{2}} \\ + \mathbb{F}_{\bar{2}|\bar{1}} \end{array} \right) \otimes \mathbb{F}_{\bar{1}\bar{2}} + \left(\begin{array}{c} \mathbb{F}_{\bar{1}\bar{3}|\bar{2}\bar{4}} \\ + \mathbb{F}_{\bar{1}\bar{3}|\bar{2}\bar{4}} \\ + \mathbb{F}_{\bar{3}|\bar{1}\bar{2}\bar{4}} \end{array} \right) \otimes 1 \\ &= 1 \otimes \mathbb{P}_{\begin{array}{c} \text{---} \\ \diagup \quad \diagdown \\ \text{---} \end{array}} + \mathbb{P}_{\begin{array}{c} \text{---} \\ \diagdown \quad \diagup \\ \text{---} \end{array}} \otimes \mathbb{P}_{\begin{array}{c} \text{---} \\ \diagdown \quad \diagup \\ \text{---} \end{array}} + \mathbb{P}_{\begin{array}{c} \text{---} \\ \diagdown \quad \diagup \\ \text{---} \end{array}} \otimes \mathbb{P}_{\begin{array}{c} \text{---} \\ \diagdown \quad \diagup \\ \text{---} \end{array}} + (\mathbb{P}_{\begin{array}{c} \text{---} \\ \diagdown \quad \diagup \\ \text{---} \end{array}} \cdot \mathbb{P}_{\begin{array}{c} \text{---} \\ \diagdown \quad \diagup \\ \text{---} \end{array}}) \otimes \mathbb{P}_{\begin{array}{c} \text{---} \\ \diagdown \quad \diagup \\ \text{---} \end{array}} + \mathbb{P}_{\begin{array}{c} \text{---} \\ \diagdown \quad \diagup \\ \text{---} \end{array}} \otimes 1. \end{aligned}$$

MATRIOCHKA ALGEBRAS To conclude, we connect the Schröder-Cambrian algebra to F. Chapoton's algebra on faces of the cubes defined in [Cha00]. We call trilean Hopf algebra the Hopf subalgebra Tril of OrdPart_{\pm} generated by the elements

$$\mathbb{X}_{\chi} := \sum_{\substack{\lambda \in \mathfrak{P}_{\pm} \\ \text{rec}^*(\lambda) = \chi}} \mathbb{F}_{\lambda}$$

for all $\chi \in \{-, 0, +\}^{n-1}$. The commutative diagram of Proposition 110 ensures that

$$\mathbb{X}_{\chi} = \sum_{\substack{T \in \text{SchrCamb} \\ \text{can}^*(T) = \chi}} \mathbb{P}_T,$$

and thus that Tril is a subalgebra of SchrCamb . In other words, the Schröder-Cambrian algebra is sandwiched between the signed ordered partitions algebra and the trilean algebra $\text{Tril} \subset \text{SchrCamb} \subset \text{OrdPart}_{\pm}$.

3.2.3. Quotient algebra of OrdPart_{\pm}^* . We switch to the dual Hopf algebra OrdPart_{\pm}^* with basis $(\mathbb{G}_{\lambda})_{\lambda \in \mathfrak{P}_{\pm}}$ and whose product and coproduct are defined by

$$\mathbb{G}_{\lambda} \cdot \mathbb{G}_{\lambda'} = \sum_{\mu \in \lambda \star \lambda'} \mathbb{G}_{\mu} \quad \text{and} \quad \Delta \mathbb{G}_{\mu} = \sum_{\mu \in \lambda \boxplus \lambda'} \mathbb{G}_{\lambda} \otimes \mathbb{G}_{\lambda'}.$$

Note that the unsigned version of OrdPart_{\pm}^* is the algebra WQSym of word quasi-symmetric functions (also denoted NCQSym for non-commutative quasi-symmetric functions), see [BZ09, NT06]. The following statement is automatic from Theorem 113.

Theorem 116. *The graded dual SchrCamb^* of the Schröder-Cambrian algebra is isomorphic to the image of OrdPart_{\pm}^* under the canonical projection*

$$\pi : \mathbb{C}\langle A \rangle \longrightarrow \mathbb{C}\langle A \rangle / \equiv,$$

where \equiv denotes the Schröder-Cambrian congruence. The dual basis $\mathbb{Q}_{\mathbb{T}}$ of $\mathbb{P}_{\mathbb{T}}$ is expressed as $\mathbb{Q}_{\mathbb{T}} = \pi(\mathbb{G}_{\lambda})$, where λ is any ordered partition such that $\mathbf{P}^*(\lambda) = \mathbb{T}$.

Similarly as in the previous section, we can describe combinatorially the product and coproduct of \mathbb{Q} -basis elements of SchrCamb^* in terms of operations on Schröder-Cambrian trees.

PRODUCT We define *gaps* and *laminations* of Schröder-Cambrian trees exactly as we did for Cambrian trees in Section 1.2.3. Note that laminations may or may not split the nodes of a Schröder-Cambrian tree, see Figure 43 (c) for examples. Given two Schröder-Cambrian trees \mathbb{T} and \mathbb{T}' on $[n]$ and $[n']$ respectively, and a shuffle s of their signature defining multisets Γ of gaps of $[n]$ and Γ' of gaps of $[n']$, we still denote by $\mathbb{T} \setminus_s \mathbb{T}'$ the Schröder-Cambrian tree obtained by connecting the up leaves of $\lambda(\mathbb{T}, \Gamma)$ to the down leaves of the forest defined by the lamination $\lambda(\mathbb{T}', \Gamma')$. See Figure 43.

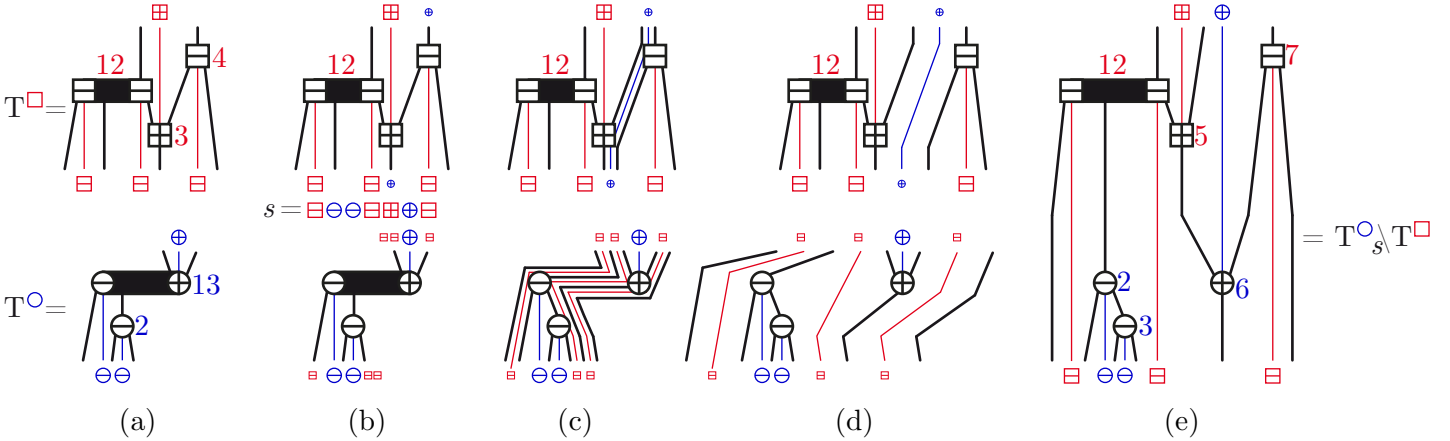


FIGURE 43. (a) Two Schröder-Cambrian trees \mathbb{T}° and \mathbb{T}^{\square} . (b) Given the shuffle $s = \square \ominus \ominus \square \square \oplus \oplus$, the positions of the \square are reported in \mathbb{T}° and the positions of the \oplus are reported in \mathbb{T}^{\square} . (c) The corresponding laminations. (d) The trees are split according to the laminations. (e) The resulting Schröder-Cambrian tree $\mathbb{T}^{\circ} \setminus_s \mathbb{T}^{\square}$.

Proposition 117. *For any Schröder-Cambrian trees \mathbb{T}, \mathbb{T}' , the product $\mathbb{Q}_{\mathbb{T}} \cdot \mathbb{Q}_{\mathbb{T}'}$ is given by*

$$\mathbb{Q}_{\mathbb{T}} \cdot \mathbb{Q}_{\mathbb{T}'} = \sum_s \mathbb{Q}_{\mathbb{T} \setminus_s \mathbb{T}'},$$

where s runs over all shuffles of the signatures of \mathbb{T} and \mathbb{T}' .

ACKNOWLEDGEMENTS

We are grateful to the participants of the *Groupe de travail de Combinatoire Algébrique de l'Université de Marne-la-Vallée* for helpful discussions and comments on preliminary stages of this work. In particular, we are indebted to J.-Y. Thibon for showing us relevant research directions and encouraging our ideas, and to J.-C. Novelli for uncountable technical suggestions and comments (leading in particular to the results presented in Proposition 15, in Section 2.1.5, and in Section 3.2). We also thank V. Pons, whose suggestions lead to the current presentation of the Cambrian correspondence Θ in Section 1.1.2, adapted from [LP13]. The second author thanks C. Hohlweg for introducing him to this algebraic combinatorics crowd. Finally, we are grateful to M. Bousquet-Mélou, C. Hohlweg and N. Reading for pointing out to us various relevant references.

REFERENCES

- [BBMF11] Nicolas Bonichon, Mireille Bousquet-Mélou, and Éric Fusy. Baxter permutations and plane bipolar orientations. *Sém. Lothar. Combin.*, 61A:Art. B61Ah, 29, 2009/11.
- [BH06] Nantel Bergeron and Christophe Hohlweg. Coloured peak algebras and Hopf algebras. *J. Algebraic Combin.*, 24(3):299–330, 2006.
- [BH08] Pierre Baumann and Christophe Hohlweg. A Solomon descent theory for the wreath products $G \wr \mathfrak{S}_n$. *Trans. Amer. Math. Soc.*, 360(3):1475–1538 (electronic), 2008.
- [BHKNO1] François Boulier, Florent Hivert, Daniel Krob, and Jean-Christophe Novelli. Pseudo-permutations. II. Geometry and representation theory. In *Discrete models: combinatorics, computation, and geometry (Paris, 2001)*, Discrete Math. Theor. Comput. Sci. Proc., AA, pages 123–132 (electronic). Maison Inform. Math. Discrèt. (MIMD), Paris, 2001.
- [BMCPR13] Mireille Bousquet-Mélou, Guillaume Chapuy, and Louis-François Préville-Ratelle. The representation of the symmetric group on m -Tamari intervals. *Adv. Math.*, 247:309–342, 2013.
- [BMFPR11] Mireille Bousquet-Mélou, Éric Fusy, and Louis-François Préville-Ratelle. The number of intervals in the m -Tamari lattices. *Electron. J. Combin.*, 18(2):Paper 31, 26, 2011.
- [BPR12] François Bergeron and Louis-François Préville-Ratelle. Higher trivariate diagonal harmonics via generalized Tamari posets. *J. Comb.*, 3(3):317–341, 2012.
- [BZ09] Nantel Bergeron and Mike Zabrocki. The Hopf algebras of symmetric functions and quasi-symmetric functions in non-commutative variables are free and co-free. *J. Algebra Appl.*, 8(4):581–600, 2009.
- [CD06] Michael P. Carr and Satyan L. Devadoss. Coxeter complexes and graph-associahedra. *Topology Appl.*, 153(12):2155–2168, 2006.
- [CGHK78] Fan R. K. Chung, Ronald L. Graham, Verner E. Hoggatt, Jr., and Mark Kleiman. The number of Baxter permutations. *J. Combin. Theory Ser. A*, 24(3):382–394, 1978.
- [Cha00] Frédéric Chapoton. Algèbres de Hopf des permutahédres, associahédres et hypercubes. *Adv. Math.*, 150(2):264–275, 2000.
- [Dev09] Satyan L. Devadoss. A realization of graph associahedra. *Discrete Math.*, 309(1):271–276, 2009.
- [DG96] Serge Dulucq and Olivier Guibert. Stack words, standard tableaux and Baxter permutations. In *Proceedings of the 6th Conference on Formal Power Series and Algebraic Combinatorics (New Brunswick, NJ, 1994)*, volume 157, pages 91–106, 1996.
- [DG98] Serge Dulucq and Olivier Guibert. Baxter permutations. In *Proceedings of the 7th Conference on Formal Power Series and Algebraic Combinatorics (Noisy-le-Grand, 1995)*, volume 180, pages 143–156, 1998.
- [FFNO11] Stefan Felsner, Éric Fusy, Marc Noy, and David Orden. Bijections for Baxter families and related objects. *J. Combin. Theory Ser. A*, 118(3):993–1020, 2011.
- [FS05] Eva Maria Feichtner and Bernd Sturmfels. Matroid polytopes, nested sets and Bergman fans. *Port. Math. (N.S.)*, 62(4):437–468, 2005.
- [Gir12] Samuele Giraud. Algebraic and combinatorial structures on pairs of twin binary trees. *J. Algebra*, 360:115–157, 2012.
- [GV85] Ira Gessel and Gérard Viennot. Binomial determinants, paths, and hook length formulae. *Adv. in Math.*, 58(3):300–321, 1985.
- [HL07] Christophe Hohlweg and Carsten Lange. Realizations of the associahedron and cyclohedron. *Discrete Comput. Geom.*, 37(4):517–543, 2007.
- [HLT11] Christophe Hohlweg, Carsten Lange, and Hugh Thomas. Permutahedra and generalized associahedra. *Adv. Math.*, 226(1):608–640, 2011.
- [HNT05] Florent Hivert, Jean-Christophe Novelli, and Jean-Yves Thibon. The algebra of binary search trees. *Theoret. Comput. Sci.*, 339(1):129–165, 2005.
- [IO13] Kiyoshi Igusa and Jonah Ostroff. Mixed cobinary trees. Preprint, [arXiv:1307.3587](https://arxiv.org/abs/1307.3587), 2013.
- [KLN⁺01] Daniel Krob, Matthieu Latapy, Jean-Christophe Novelli, Ha-Duong Phan, and Sylviane Schwer. Pseudo-Permutations I: First Combinatorial and Lattice Properties. 13th International Conference on Formal Power Series and Algebraic Combinatorics (FPSAC 2001), 2001.
- [Lod04] Jean-Louis Loday. Realization of the Stasheff polytope. *Arch. Math. (Basel)*, 83(3):267–278, 2004.

- [LP13] Carsten Lange and Vincent Pilaud. Associahedra via spines. Preprint, [arXiv:1307.4391](https://arxiv.org/abs/1307.4391), to appear in *Combinatorica*, 2013.
- [LR98] Jean-Louis Loday and María O. Ronco. Hopf algebra of the planar binary trees. *Adv. Math.*, 139(2):293–309, 1998.
- [LR12] Shirley Law and Nathan Reading. The Hopf algebra of diagonal rectangulations. *J. Combin. Theory Ser. A*, 119(3):788–824, 2012.
- [Mal79] Colin L. Mallows. Baxter permutations rise again. *J. Combin. Theory Ser. A*, 27(3):394–396, 1979.
- [MHPS12] Folkert Müller-Hoissen, Jean Marcel Pallo, and Jim Stasheff, editors. *Associahedra, Tamari Lattices and Related Structures. Tamari Memorial Festschrift*, volume 299 of *Progress in Mathematics*. Springer, New York, 2012.
- [MR95] Claudia Malvenuto and Christophe Reutenauer. Duality between quasi-symmetric functions and the Solomon descent algebra. *J. Algebra*, 177(3):967–982, 1995.
- [Nov14] Jean-Christophe Novelli. m -dendriform algebras. Preprint, [arXiv:1406.1616](https://arxiv.org/abs/1406.1616), 2014.
- [NT06] Jean-Christophe Novelli and Jean-Yves Thibon. Construction de trigèbres dendriformes. *C. R. Math. Acad. Sci. Paris*, 342(6):365–369, 2006.
- [NT10] Jean-Christophe Novelli and Jean-Yves Thibon. Free quasi-symmetric functions and descent algebras for wreath products, and noncommutative multi-symmetric functions. *Discrete Math.*, 310(24):3584–3606, 2010.
- [NT14] Jean-Christophe Novelli and Jean-Yves Thibon. Hopf algebras of m -permutations, $(m + 1)$ -ary trees, and m -parking functions. Preprint, [arXiv:1403.5962](https://arxiv.org/abs/1403.5962), 2014.
- [OEIS] The On-Line Encyclopedia of Integer Sequences. Published electronically at <http://oeis.org>, 2010.
- [Pos09] Alexander Postnikov. Permutohedra, associahedra, and beyond. *Int. Math. Res. Not. IMRN*, (6):1026–1106, 2009.
- [PR06] Patricia Palacios and María O. Ronco. Weak Bruhat order on the set of faces of the permutohedron and the associahedron. *J. Algebra*, 299(2):648–678, 2006.
- [Pri13] Jean-Baptiste Priez. A lattice of combinatorial Hopf algebras, Application to binary trees with multiplicities. Preprint [arXiv:1303.5538](https://arxiv.org/abs/1303.5538), 2013.
- [PRW08] Alexander Postnikov, Victor Reiner, and Lauren K. Williams. Faces of generalized permutohedra. *Doc. Math.*, 13:207–273, 2008.
- [Rea05] Nathan Reading. Lattice congruences, fans and Hopf algebras. *J. Combin. Theory Ser. A*, 110(2):237–273, 2005.
- [Rea06] Nathan Reading. Cambrian lattices. *Adv. Math.*, 205(2):313–353, 2006.
- [RS09] Nathan Reading and David E. Speyer. Cambrian fans. *J. Eur. Math. Soc.*, 11(2):407–447, 2009.
- [Sch61] Craige Schensted. Longest increasing and decreasing subsequences. *Canad. J. Math.*, 13:179–191, 1961.
- [Sol76] Louis Solomon. A Mackey formula in the group ring of a Coxeter group. *J. Algebra*, 41(2):255–264, 1976.
- [Vie81] Gérard Viennot. A bijective proof for the number of baxter permutations. 3rd Seminaire Lotharingien de Combinatoire, Le Klebach, 1981.
- [Vie07] Xavier Viennot. Catalan tableaux and the asymmetric exclusion process. In *19th International Conference on Formal Power Series and Algebraic Combinatorics (FPSAC 2007)*. 2007.
- [YCCG03] Bo Yao, Hongyu Chen, Chung-Kuan Cheng, and Ronald Graham. Floorplan Representations: Complexity and connections. *ACM Transactions on Design Automation of Electronic Systems*, 8(1):55–80, 2003.
- [Zel06] Andrei Zelevinsky. Nested complexes and their polyhedral realizations. *Pure Appl. Math. Q.*, 2(3):655–671, 2006.

(GC) LIGM, UNIV. PARIS-EST MARNE-LA-VALLÉE
E-mail address: gregory.chatel@univ-paris-est.fr

(VP) CNRS & LIX, ÉCOLE POLYTECHNIQUE, PALAISEAU
E-mail address: vincent.pilaud@lix.polytechnique.fr
URL: <http://www.lix.polytechnique.fr/~pilaud/>